mTOR signaling controls microglia activation and survival via 4E-BP-dependent translational regulation

Sara Bermudez
Integrated Program in Neuroscience
McGill University, Montreal
May 2023

A thesis submitted to McGill University in partial fulfillment of the requirements of the degree of Doctor of Philosophy

© Sara Bermudez, 2023

To my father With the utmost gratitude and eternal love!

List of Figures

	Figure 1. A simplified overview of the central dogma of molecular biology17
	Figure 2.The posttranscriptional operon (PTO) model19
	Figure 3. Schematic representation of mTOR signaling to the translational machinery21
	Figure 4. Schematic representation of the model of mTOR stimulated mRNA25
	Figure 5. Schematic representation of the proposed modes of gene expression regulation
	27
	Figure 6. Timing of Major AD Pathophysiological Events in Relation to Clinical Course30
	Figure 7. Terms used to describe Aβ deposits and senile plaques35
	Figure 8. Depiction of microglial cellular activities related to β -amyloid pathology37
	Figure 9. Graphical representation of the thesis research question. (Created with
Bioreno	der.com)44
	Figure 10. A β aggregates induce 4E-BP1 phosphorylation
	Figure 11. Chronic exposure to $Aeta$ induces tolerance and decrease in 4E-BP1
phosph	orylation59
	Figure 12. TREM2 signaling inhibition strongly decreases 4E-BP1 phosphorylation.)61
	Figure 13. Deletion of 4E-BP1 and 2 in microglia results in a decreased pro-inflammatory
phenot	ype64
	Figure 14. Depletion of the 4E-BPs changes the metabolic profile in microglia66
	Figure 15. Depletion of 4E-BPs mitigates microglia apoptosis related to A eta .
	Figure 16. In-vivo model optimization
	Figure 17 Translatome enrichment in vivo

Figure 18. Microglia depletion of the 4E-BPs leads to changes in the ti	ssue transcriptomic
output in response to Aβ	79

Table of Contents

Sur	iummary		
Res	sume		12
Ack	knowled	Igments	14
1.	Introd	duction	16
	1.1 Ger	ne expression	16
	1.1.	The central dogma of molecular biology	16
	1.1.2.	Gene expression in eukaryotes, a primer	17
	1.1.3.	The posttranscriptional operon	18
	1.1.4.	The mTOR pathway	19
	1.1.5.	Translation regulation, an overview	22
	1.1.6.	mTOR regulation of mRNA translation	22
	1.1.7.	The eukaryotic initiation factor 4F binding proteins (4E-BPs)	23
	1.1.8.	Intrinsic features of the mRNA affect translation	24
	1.1.9.	translation regulation effect on the proteome	27
1	L.2. A	Alzheimer's Disease	29
	1.2.1.	Alzheimer's Disease Prevalence	29
	1.2.2.	Alzheimer's Disease Pathology	29
	1.2.3.	Amyloid and Tau Pathogenesis	31
	1.2.4.	The amyloid cascade hypothesis	32
1	L.3. N	Microglia	33
	1.3.1.	Error! Reference source not found. Unveiling Microglia Involvement in Alz	heimer's Disease
		34	
	1.3.2.	Roles of microglia during AD	34
	1.3.3.	Microglia distinct phenotypes	38
	1.3.4.	Linking the mTOR pathway, translation, and microglia in AD	39
2.	Ratio	nale	42
3	Hypot	thesis	44

4.	Metho	ods	45
	4.1. Ir	n vitro methods	45
	4.1.1.	Cell line generation	45
	4.1.2.	A eta aggregation	45
	4.1.3.	pHrodo™ Aβ labeling	46
	4.1.4.	In vitro treatments	46
	4.1.5.	Western blotting	46
	4.1.6.	Live-Cell Incucyte imaging	47
	4.1.7.	Immunocytochemistry	47
	4.1.8.	Cytokine measurement	48
	4.1.9.	Lactate measurement	48
	4.1.10.	Measurement of Real-Time OCR	48
	4.2. A	nimals and environment	49
	4.2.1.	Mouse lines	49
	4.2.2.	Genotyping	49
	4.2.3.	Immunohistochemistry	50
	4.2.4.	Intracerebroventricular Injections	50
	4.2.5.	Ribosome pulldown	51
	4.2.6.	RNA Sequencing	51
	4.2.7.	Differentially expressed genes analysis.	52
	4.2.8.	Quantification and statistical analysis	52
4	4.3. T	ables	53
5.	Resea	rch Findings	55
	5.1. R	esearch findings by aim	55
	5.1.1.	Aim 1. Characterize the signal transduction alterations in mTOR-4E-BP pathway in	
		microglia responding to A eta	55
	5.1.2.	A eta aggregates induce acute microglial inflammation accompanied by phosphorylation of	:
		4E-BP1	56
	5.1.3.	Chronic exposure to A eta induces tolerance and downregulates 4E-BP1 phosphorylation	57
	5.1.4.	SYK inhibition, downstream of TREM2, strongly downregulates 4E-BP1 phosphorylation.	59
	5.1.5.	Aim 1 conclusion.	61
	5.2.	Aim 2 Characterize the functional implications of de-repressing 4E-BP-regulated translat	ion
		in microglia responding to Aβ.	62

	5.2.1.	Deleting 4E-BP1 and 4E-BP2 decreases microglia pro-inflammatory output upon stimuli.	63	
	5.2.2.	Deletion of 4E-BP1 and 4E-BP2 in microglia results in an increased mitochondrial respira	ition	
		capacity and decreased glycolysis induction upon A eta exposure	_ 65	
	5.2.3.	Depletion of 4E-BP1 and 4E-BP2 mitigates microglia apoptosis related to A eta phagocytos	is.	
		67		
	5.2.4.	Assessment of functional consequences of 4E-BP depletion in microglial response to $\ensuremath{A\beta}$	in-	
		vivo	_ 70	
	5.2.5.	Aim 2 conclusions.	_ 73	
	5.1.	Aim 3. Identify the response mediators controlled by the mTOR-4E-BP axis that allows		
		microglia to retain their cellular viability during their response to A eta	_ 74	
	5.1.1.	Translatome enrichment in-vivo	_ 74	
	5.1.2.	Microglia-specific depletion of the 4E-BPs leads to changes in the tissue transcriptomic		
		response to Aβ	_ 77	
5.	Discus	sion	80	
7.	. Conclusion			
Bib	liograph	y	87	

Summary

Microglia dystrophy is a common neuropathological finding in brains with AD pathology. Clinical and experimental data suggest that microglia dysfunction is associated with disease onset and progression. Remarkably, rare loss-of-function variants in triggering receptor expressed in myeloid cells 2 (TREM 2), preferentially expressed in microglia in the brain, are associated with an increased risk of AD with an odds ratio comparable to APOE &4. Moreover, clinical and experimental data suggest that TREM2 loss of function not only increases the risk of AD, but increased function may be beneficial in AD. Although there are ongoing efforts to therapeutically boost TREM2 signaling, the cell-autonomous and intracellular mechanisms coordinating microglia neuroprotective functions are not fully understood.

TREM2 intracellular signaling maintains metabolic fitness through the activation of mechanistic target of rapamycin (mTOR), allowing microglia to sustain a response to amyloidosis. In addition, decreased mTOR activation has been described in microglia in AD models, independent of TREM2 impairment, and leads to microglia metabolic dysfunction and worsened pathology. Besides its direct metabolic effects, the mTOR pathway controls mRNA translation by acting upstream of the eukaryotic translation initiation factor 4E (eIF4E). mTOR inhibits the eIF4E binding proteins (4E-BPs) via phosphorylation, thus releasing eIF4E and allowing mRNA translation to initiate. Crucially, previously published work from our lab has shown that mTOR boosts mitochondrial metabolism via 4E-BP-Dependent mRNA translation regulation. Yet, 4E-BP-regulated mRNA translation has not been studied in microglia in AD. Therefore, I aimed to define the dysregulated mechanisms at the intersection of the mTOR-4E-BP-dependent translation regulation and energetic metabolism in microglia responding to AD pathology.

We planned a careful and direct manipulation of the intricate mTOR pathway by knocking out the downstream effectors, the 4E-BPs, in microglia *in vitro* and *in vivo*. The results presented in this thesis show that depletion of 4E-BP in microglia, *in vitro*, leads to a decrease in proinflammatory mediators' expression and an increase in reliance on oxidative phosphorylation upon exposure to $A\beta$, ultimately mitigating microglia apoptosis while conserving phagocytosis of $A\beta$. We used a microglia-specific conditional knock-out mouse model of the 4E-BPs, to release the

brake on mRNA translation, and crossed it with a RiboTag mouse to immunoprecipitate microglial ribosome-bound mRNAs. Consistent with the *in vitro* results, in the absence of the 4E-BPs, the *in vivo* microglial translatome shows a decrease in the translation of several mediators of the inflammatory response, displaying a downregulated network centered in *apoe*. This is reflected in the transcriptomic output of the brain tissue upon microglial deletion of the 4E-BPs, as a decreased pro-inflammatory transcriptomic output of the brain after A β infusion was detected. The results outlined in this thesis suggest that the activation of the mTOR-4E-BP axis signaling may act as a mechanism of microglia self-regulation necessary for inflammatory resolution and cell survival on an on-and-off basis. The activation of this axis in microglia might represent a pivotal protective mechanism during the decade of amyloidosis that precedes disease onset. In conclusion, mTOR signaling exerts key effects on microglia function, metabolism, and survival via 4E-BP-dependent mRNA translation regulation.

Resume

La signalisation de mTOR contrôle l'activation et la survie de la microglie via une régulation de la traduction dépendante de 4E-BP.

La dystrophie de la microglie est une neuropathologie courante retrouvée dans les cerveaux atteints de la maladie d'Alzheimer (MA). Les données cliniques et expérimentales suggèrent que le dysfonctionnement de la microglie est associé à l'apparition et à la progression de la maladie. Remarquablement, de rares variantes de perte de fonction du récepteur déclencheur exprimé dans les cellules myéloïdes 2 (TREM 2), préférentiellement exprimées dans la microglie du cerveau, sont associées à un risque accru de MA avec un facteur de risques comparable à l'APOE ɛ4. De plus, les données cliniques et expérimentales suggèrent que la perte de fonction de TREM2 augmente non seulement le risque de MA, mais qu'une fonction accrue pourrait être bénéfique dans la MA. Bien que des efforts soient en cours pour stimuler thérapeutiquement la signalisation TREM2, les mécanismes cellulaires autonomes et intracellulaires coordonnant les fonctions neuroprotectrices de la microglie ne sont pas entièrement compris.

La signalisation intracellulaire TREM2 soutient le métabolisme grâce à l'activation de la cible de la rapamycine chez les mammifères (mTOR), permettant à la microglie de maintenir une réponse à l'amylose. En outre, une diminution de l'activation de mTOR a été décrite dans des modèles de MA, indépendamment de la déficience en TREM2, et mène à un dysfonctionnement métabolique de la microglie et à une aggravation de la pathologie. Outre ses effets métaboliques directs, la voie de mTOR contrôle la traduction de l'ARNm en agissant en amont du facteur d'initiation de la traduction eucaryote 4E (eIF4E). mTOR inhibe les protéines de liaison eIF4E (4E-BP) via la phosphorylation, libérant ainsi eIF4E et permettant l'initiation de la traduction de l'ARNm. De manière cruciale, des travaux précédemment publiés par notre laboratoire ont montré que mTOR stimule le métabolisme mitochondrial grâce à la régulation de la traduction de l'ARNm dépendante de 4E-BP. Pourtant, la traduction de l'ARNm régulée par 4E-BP n'a pas été étudiée dans la microglie dans la MA. Par conséquent, j'ai cherché à définir les mécanismes

dérégulés à l'intersection de la régulation de la traduction mTOR-4E-BP et du métabolisme énergétique dans la microglie répondant à la pathologie de la MA.

Nous avons planifié une manipulation minutieuse et directe de la voie de signalisation de mTOR en supprimant les effecteurs en aval, les 4E-BP, dans la microglie *in vitro* et *in vivo*. Nous avons utilisé un modèle conditionnel de souris knock-out spécifique à la microglie des 4E-BP, pour enlever le frein de la traduction de l'ARNm, et l'avons croisé avec une souris RiboTag pour immunoprécipiter les ARNm liés au ribosome microglial. Les résultats présentés dans cette thèse montrent que la suppression des 4E-BP dans la microglie entraîne une diminution de l'expression des médiateurs pro-inflammatoires et une augmentation du recours à la phosphorylation oxydative dans la microglie exposée à la pathologie MA, augmentant finalement la résilience de la microglie *in vitro* et *in vivo*. La signalisation de l'axe mTOR-4E-BP peut agir en tant que mécanisme d'autorégulation de la microglie essentiel à la résolution inflammatoire et à la survie cellulaire sur une base intermittente nécessaire au cours de la décennie qui précède l'apparition de la maladie. En conclusion, mTOR extrait des effets clés sur la fonction, le métabolisme et la survie de la microglie via la régulation de la traduction de l'ARNm dépendante de 4E-BP.

Acknowledgments

First off, I would like to thank my supervisor Dr. Sonenberg for his guidance, trust, and patience throughout my Ph.D. studies. It has been a great honor to work under your supervision and witness your incredible scientific insight.

I am eternally grateful to Dr. Healy and Dr. Aguilar-Valles. Thank you for your contributions to the design of the experiments outlined in this thesis. But mostly I am grateful for your continued support, time, and remarkable patience. This would not have been possible without your help and friendship.

I would also like to thank Dr. Ruthazer as part of my committee, and as the heart of the IPN, making the program a structure that holds us students through our struggles. You are an inspiration and essential to all of us.

I am so very thankful to my wonderful co-workers and friends. Junghyun, Sunghoon, and Niaz, thank you so much for your help. Without your help, wonderful experiments and good advice, I wouldn't have been able to tell this story. Shane, Ziying, and Laura thank you so much for your help with the mice experiments. Mehdi, thank you very much for all your help with any RNA-related experiments and for always sharing your buffers. Michael, thank you so much for all your help with the Riboseq experiment.

I would like to thank the wonderful Annie Sylvestre and Annik Lafrance for their tireless work with the mouse breedings and for dealing so kindly with all our requests.

I would also like to thank the wonderful staff of the lab: Isabelle Harvey, Eva Migon, Meena Vipparti, and Anamaria Kiss for making the lab run, so we can continue our research.

My immense gratitude to my mother and sister to whom I owe everything and who have been my rock through many waves. I would like to also thank my dear husband, who worked so tirelessly with me and walked with me through this journey.

Last but not least, I would like to thank my reviewers for their time and willingness to read this thesis. I really appreciate it!

This thesis marks the end of a long journey through resilience and dedication that taught me immensely about science but also about myself.

1. Introduction

1.1 Gene expression

1.1.1. The central dogma of molecular biology

The hereditary information is stored in the cell nucleus as Deoxyribonucleic Acid (DNA). A double helix is formed by two independent DNA strands running opposite to each other, while four different bases (adenine, thymine, cytosine, and guanine) bind facing towards the opposite strand[1]. The sequence of these bases, or nucleotides, make up the genetic "code," a unique sequence that then leads to an organism's individuality while containing the instructions for the organism's building blocks, namely proteins [2]. The spatial occurrence of DNA in the nuclei would indicate that DNA didn't directly participate in the cytosolic protein synthesis; therefore, a messenger molecule was necessary. Ribonucleic acid (RNA) was then described as the messenger of genetic information outside of the nuclei to synthesize proteins in the cytosol[3].

The classical view of the central dogma of the molecular biology states that "the coded genetic information hard-wired into DNA is transcribed into individual transportable cassettes, composed of mRNA; each mRNA cassette contains the program for the synthesis of a particular protein (or a small number of proteins)" (Figure 1) [2, 4]. The central dogma of molecular biology has remained a tenet of molecular biology; however, the standard view of a gene as a unit of hereditary information aligned along a chromosome, each coding for what would then be one protein, has changed dramatically over time [5]. Additions and modifications to the dogma have been propelled by the study of eukaryotes and complex multicellular organisms in which the cells that make it up contain identical genetic information. Yet, functionally different cells within tissues and organs in an organism use different sets of genetic information to express different combinations and subsets of proteins to accomplish differential cell function. In addition, with the development of molecular techniques and increased knowledge of gene control, it became increasingly clear that gene expression relied on many more levels of regulation [6].

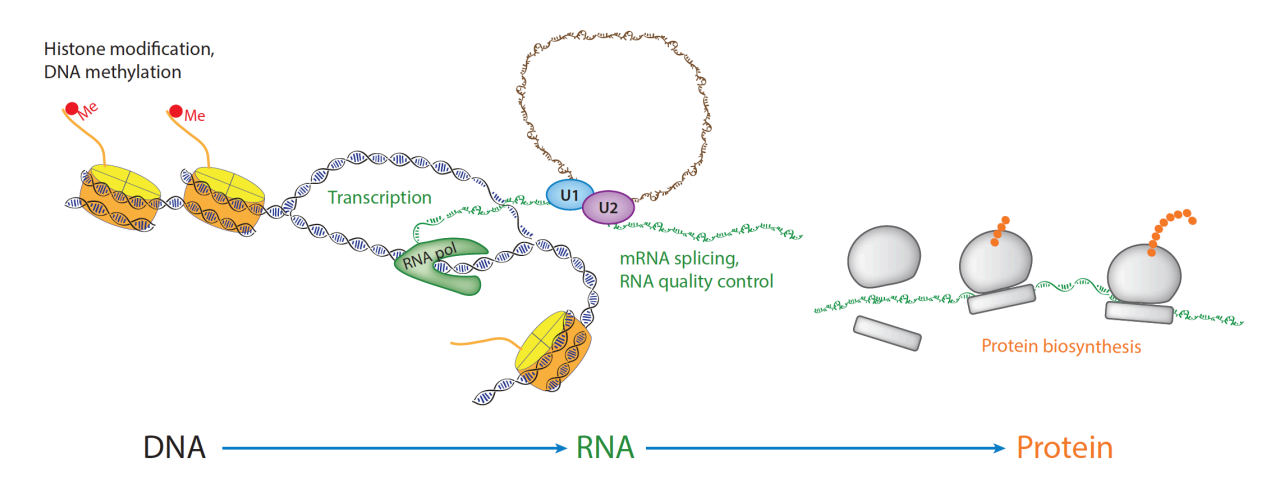


Figure 1. A simplified overview of the central dogma of molecular biology. Information contained in the DNA sequence is transcribed into RNA. The RNA message, after modification, including capping, splicing, and poly-A tailing, is exported into the cytoplasm, where the RNA sequence is translated into the sequence of a polypeptide by the ribosome. Abbreviations: mRNA, messenger RNA; RNA pol, RNA polymerase; U1, U2, small ribonuclear proteins of the spliceosome.

Reprinted with permission from Along the Central Dogma—Controlling Gene Expression with Small Molecules by Schneider-Poetsch, T. and M. Yoshida, 2018. Annual Review of Biochemistry. Copyright 2018 by Annual Reviews.

1.1.2. Gene expression in eukaryotes, a primer

In higher eukaryotes, the coordinated expression of multiple genes is needed to accomplish complex functions. For example, cells holding the same genetic information differentiate into specific cell populations carrying out specialized functions such as nervous, metabolic, or immune responses while also carrying out housekeeping functions. These differential and cue-specific responses require the spatiotemporal coordination of gene-expression programs which rely on the orchestration of different layers of gene expression, such as at the DNA, mRNA, and protein level. This coordination results in a cell type and stimulus-dependent repertoire of expressed proteins, namely, the proteome [7].

With the progress and increased availability of sequencing technology, studies of gene expression as an indication of cell function have focused on mRNA abundance and are based upon the tenet that gene expression networks are the result of collaborating transcription factors [8].

Therefore, mRNA abundance has been conventionally used as a proxy for protein abundance; however, this assumes that changes in mRNA abundance are proportionally reflected in protein synthesis. Although mRNA abundance and its coordination pathways has a significant contribution to gene expression, this same level of coordination exists as well at the mRNA translation level and has a higher correlation with the proteome [9, 10]. Furthermore, there is a temporal delay in the availability of the mature mRNA transcript in the cytosol to be translated, therefore, changes in mRNA transcript abundance can only affect the expression level of a protein after temporal delay [10]. It is then efficient for the cell to modulate the proteome through posttranscriptional mechanisms as it allows the cell to generate acute changes in the proteome without *de novo* transcription.

1.1.3. The posttranscriptional operon

In 2002, Keene and colleagues proposed the posttranscriptional operon (PTO) model by which subsets of mRNA transcripts can be collectively modulated to coordinate the expression of protein networks needed in spatiotemporal conjunction for a biological function [11]. Post-transcriptional regulation can occur at several steps through splicing regulation, mRNA export from the nucleus to the cytosol, mRNA stability and decay in the cytosol, and mRNA translation to synthesize a protein (figure 2) [8]. Additionally, this modulation can be global by affecting most transcripts, selective to a subset of transcripts, or specific to a particular transcript, allowing for the rapid fine-tuning of the specific pathways or functional responses in the cell [8]. All these factors explain a poor correlation between mRNA levels and protein levels, particularly during transitional states [10].

On the other hand, the study of gene expression at the protein level has depended on antibodies allowing for just relatively few targets at a time and adding high variability between studies. In contrast, mass spectrometry-based proteomics has become a particularly important analytical method for protein research, specifically for protein identification and quantification with a high throughput accuracy and reproducibility [12]. However, compared to nucleotide sequencing it lags behind in sensitivity and depth [12]. Hence, the study of translational control

can leverage nucleotide sequencing technology on actively translating transcripts, namely translatome, which has a higher correlation to the proteome than the transcriptome.

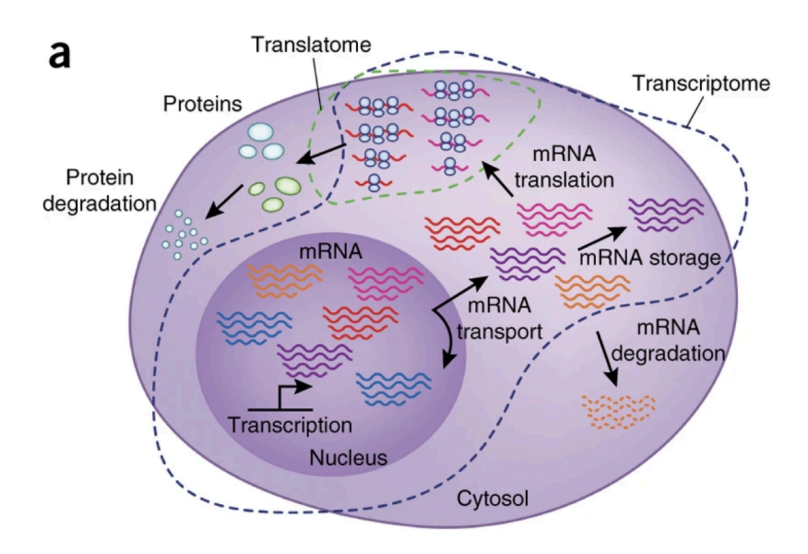


Figure 2.The posttranscriptional operon (PTO) model. The gene expression pathway consists of multiple levels that can be regulated individually and in concert. Following transcription, mRNA is transported to the cytosol, where it can be degraded, stored or used for protein synthesis. Each of these steps enables the selective regulation of subsets of mRNAs. According to the PTO model, these subsets share similar functions and are identified by 'zip codes' (distinguished here by mRNA color) that enable binding and regulation by RNA binding proteins (RBPs). Because each of these steps can be regulated for each mRNA subset separately, gene-expression mechanisms can act together to orchestrate expression patterns in response to different stimuli. Labels along top (perimeter) indicate mRNA populations studied by 'translatomics' and 'transcriptomics'.

Reprinted with permission from Translational control of immune responses: from transcripts to translatomes by Piccirillo, C.A., et al., 2014. Nature Immunolog, volume 15, pages 503–511. Copyright 2014 by Springer Nature

1.1.4. The mTOR pathway

The mechanistic target of rapamycin (mTOR) is a conserved protein Serine/Threonine kinase that acts as a rheostat coordinating numerous regulatory pathways and cellular functions (depicted in Figure 3). Depending on different cues, mTOR stimulates cell anabolic processes via the regulation

of protein synthesis [13]. Through upstream components of the signaling pathway, usually receptors, transducing different signals, the mTOR pathway integrates extracellular stimuli such as growth factors, cytokines, and hormones, with cellular energy status, nutrient and oxygen availability, ultimately modulating proliferation and cell growth. mTOR exists as the catalytic subunit in two structurally and functionally different complexes: mTOR complexes 1 and 2 (mTORC1 and mTORC1). mTORC1 components include, besides mTOR, the scaffolding protein raptor, (regulatory-associated protein of TOR), the mLST8 (mammalian lethal with Sec13 protein 8), and Deptor (DEP domain containing mTOR interacting protein). Whereas mTORC2, characterized by its insensitivity to acute rapamycin treatment, is composed of mLST8, Deptor as well, but also includes Rictor (rapamycin-insensitive companion of TOR), mSIN1 (mammalian stress-activated protein kinase [SAPK]-interacting protein), and Protor (proline-rich protein 5, also known as PRR5). Protein synthesis or mRNA translation is a major downstream target of regulation by the mTOR pathway [14]. mTORC1 regulates several components of the translation machinery through phosphorylation[13]. The activation of mTORC1 is associated with an increase in protein synthesis or mRNA translation through the phosphorylation of the p70-S6 kinase and the eukaryotic initiation factor 4E binding proteins (4E-BPs). p70-S6 kinases play an important role, downstream of mTORC1, by regulating cellular size and phosphorylate ribosomal protein S6, involved in ribosome biogenesis [15, 16]. However, this thesis focuses mainly on the mTOR-4E-BP axis of translational control.

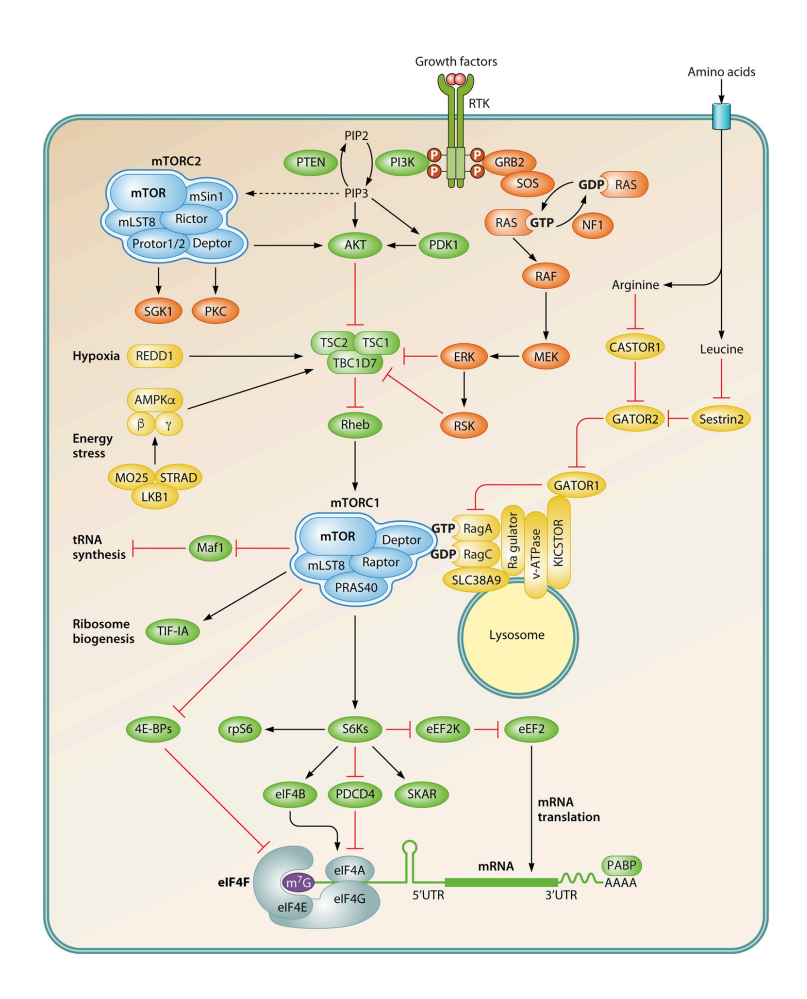


Figure 3. Schematic representation of mTOR signaling to the translational machinery. Growth factors stimulate mTORC1 signaling by activating receptor tyrosine kinases (RTKs) at the plasma membrane. Various adaptor proteins convert these extracellular signals by stimulating the PI3K/AKT and Ras/ERK pathways. Many additional cues promote mTORC1 activation, including glucose and amino acids via small Rag GTPases, which help translocate mTORC1 to the surface of lysosomes. In turn, insufficient energy resources (energy stress) and hypoxia inactivate mTORC1 via the LKB1/AMPK pathway and REDD1, respectively. mTORC2 also responds to agonists that stimulate the production of phosphatidylinositol-3,4,5-triphosphate (PIP3) and promotes the activity of AGC kinase family members (PKC, AKT, and SGK) by phosphorylating residues located in their hydrophobic motifs. mTORC1 modulates mRNA translation by promoting the phosphorylation of downstream substrates, including the 4E-BPs and S6Ks, the latter having phosphorylation substrates of their own. Red T-bars represent inhibitory signals, whereas black arrows indicate stimulatory signals. P denotes phosphorylation

Reprinted with permission from Signaling Pathways Involved in the Regulation of mRNA Translation by Roux, P.P. and I. Topisirovic. Molecular and Cellular Biology, 2018. 38(12): p. e00070-18 Published. Copyright 2018 by Roux and Topisirovic.

1.1.5. Translation regulation, an overview

The messenger RNA (mRNA) molecule is an intermediary carrier of genetic information from the nucleus to the cytoplasm where it is translated into a sequence of amino acids that makes up a polypeptide, which is then folded in a 3D structure as a protein or a part of a protein complex. mRNA possesses similarities to the DNA molecule. However, mRNA is a single-stranded nucleotide sequence template, of a stretch of DNA, typically a gene or a few genes, and it uses the base uracil instead of thymine[17]. The mRNA sequence can be dived into three distinct regions: the 5' untranslated region (5'UTR), the open reading frame (ORF), and the 3' untranslated region (3'UTR). In addition, pre-mRNAs maturation includes the attachment of a 5' cap structure m7GpppN (where N is any nucleotide), intron excision and exon ligation, and formation of a 3' end by cleavage and addition of a poly(A) tail [18-20]. Maturation stabilizes the mRNA and prevent degradation after export to the cytosol and play a pivotal role during the initiation step of mRNA translation. These and other sequence features can impact the translation efficiency of the specific mRNA molecule [21].

The translation of mRNA or protein synthesis is an energetically demanding and complex process and therefore is subject to sophisticated regulation [22, 23]. The high cost of protein synthesis constrains translation to a cost-benefit optimization restraining the use of the translational machinery to subsets of the mRNAs available in the cytoplasm at a time [10]. This process is connected to extracellular and intracellular nutritional cues through several pathways including the mTOR pathway.

1.1.6. mTOR regulation of mRNA translation

mRNA translation can be divided into four phases: initiation, elongation, termination, and ribosome recycling. In eukaryotes, translation initiation is the most intricate of all phases and is

generally rate-limiting. During canonical mRNA translation, at the initiation step, the eukaryotic initiation factor 4F (eIF4F) complex directs the recruitment of the 43S preinitiation complex (PIC) (GTP-bound eukaryotic initiation factor 2 (eIF2) loaded with a methionyl-initiator tRNA (MettRNA_i) as a ternary complex (TC) and the 40s ribosomal subunit) to bind to the mRNA near the 5'end and scan the 5' untranslated region (5'UTR) until it encounters an initiation codon [24]. The eIF4F complex consists of three eukaryotic initiation factors (eIF) subunits: the cap-binding protein eIF4E, ATP-dependent DEAD-box RNA helicase eIF4A, and scaffold protein eIF4G. The least abundant and limiting protein in the eIF4F complex is eIF4E, the mRNA 5'cap binding protein whose activity is regulated by the mTOR pathway [13]. The formation of eIF4F is suppressed by the eIF4E-binding proteins (4E-BPs); when unphosphorylated, the latter binds eIF4E and prevents its interaction with eIF4G to form the eIF4F complex, resulting in the limitation of cap-dependent mRNA translation [13]. mTORC1 phosphorylates and inactivates the translational repressors, the 4E-BPs. Phosphorylated 4E-BPs release eIF4E, allowing the latter to associate and form the eIF4F complex, thus promoting cap-dependent translation initiation[24]. This means of initiation is referred to as "cap dependent" or "eIF4E dependent" translation [25] (figure 3).

1.1.7. The eukaryotic initiation factor 4F binding proteins (4E-BPs)

The regulation of the 4E-BPs is a central mechanism for the activity regulation of eIF4E. This protein family of three —4E-BP1, 4E-BP2 and 4E-BP3— shares a 55% amino acid sequence identity. The 4E-BPs competitively bind eIF4E, thereby preventing its interaction with eIF4G [26]. Due to the increased expression of 4E-BP1 compared to 4E-BP2 and negligible expression of 4E-BP3 in microglia, 4E-BP1 was the isoform characterized in this thesis [27, 28]. mTORC1 activation results in hierarchical phosphorylation of 4E-BP1, in which phosphorylation of Thr37 and Thr46 precedes the phosphorylation of Thr70 and the last site to be phosphorylated is Ser65 ultimately resulting in the release of 4E-BP1 from eIF4E [29].

1.1.8. Intrinsic features of the mRNA affect translation

mRNAs exhibit different translation regulation properties based on their intrinsic features; these features render the transcript's translation efficiency dependent, or sensitive, to the availability of various translation machinery components. Particularly the 5' UTR features provide sensitivity to changes in the availability of different components of the translational machinery, which in turn are controlled by signal transduction pathways such as the mTOR pathway[23]. An array of mechanisms linking cell-autonomous pathways to the translational machinery allow for the selective induction of translation of a subset of mRNAs in different intra- and extracellular contexts.

The mTOR-sensitive mRNAs are a particularly relevant mechanism of cost-benefit optimization of translation to maintain proteostasis and energy homeostasis in the cell. A set of particularly abundant and stable mRNAs contain a specific cis-regulatory RNA element in their 5′ UTR, termed the terminal oligo pyrimidine tract (TOP); this set of transcripts is called TOP-mRNAs. The TOP motive is characterized by a cytosine immediately following the cap, followed by 4 to 15 uninterrupted pyrimidines[30]. TOP mRNAs almost exclusively encode components of the translational machinery itself. Therefore, a decrease in mTOR signaling leads to a reduction in the translation of TOP mRNAs, encoding for translation machinery, thereby reducing the overall protein synthesis level in the cell [31]. Thus, mTOR controls the availability of the translational machinery's components by regulating the translation rate of the mRNAs encoding for the components of the translation machinery itself. More specifically, La-related protein 1 (LARP1) is a key repressor of TOP mRNA translation, mTORC1-mediated LARP1 phosphorylation leads to translation de-repression of TOP mRNAs [32]. This mechanism allows the mTOR pathway to directly impact the availability and stoichiometry of the elF4F components and translation machinery in the cell, thereby affecting the overall rate of protein synthesis.

In addition, alterations in mTOR activity impact transcripts other than the TOP-mRNAs, the so-called mTOR-sensitive non-TOP mRNAs (figure 4). These transcripts lack the 5' TOP motif and possess other 5' UTR features. Two functionally and translationally distinct subsets of mTOR-sensitive non-TOP mRNAs have been described. First, mRNAs with short 5' UTRs, enriched for mRNAs encoding for mitochondrial functions, which require eIF4E but are less sensitive to

changes in the availability of the DEAD-box helicase that unwinds secondary RNA structure, the eIF4A. Second, long 5' UTR mRNAs which encode proliferation- and survival-promoting proteins, which are both eIF4E- and eIF4A-sensitive [33]. A large proportion of cellular mRNAs, mainly encoding housekeeping proteins, have relatively short, unstructured 5' UTRs that enable efficient ribosome recruitment and translation initiation even when eIF4F complex levels are limiting, therefore exhibiting minimal sensitivity to changes in the availability of eIF4E. The mRNA subsets mentioned above, transcripts enriched for mitochondrial functions, proliferation, and pro-survival proteins, are preferentially and disproportionately affected by eIF4E availability and, therefore, particularly responsive to mTOR activity.

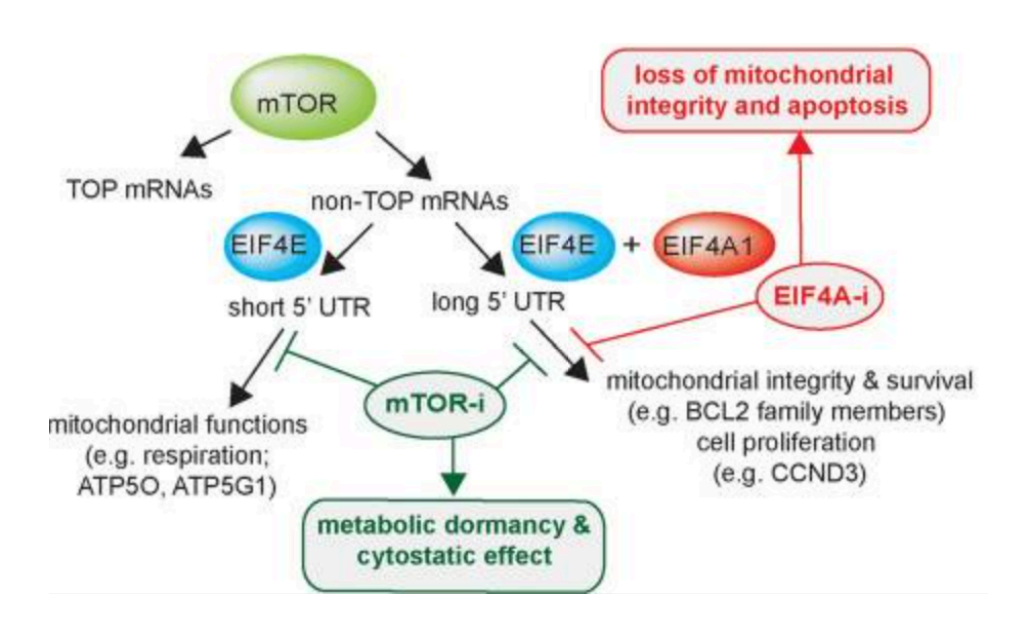


Figure 4. Schematic representation of the model of mTOR stimulated mRNA. In addition to 5' TOP motif (TOP mRNAs), 5' UTR features define two distinct subsets of non-TOP mRNAs whose translation is stimulated by MTOR (mTOR; green): (1) mRNAs with long 5' UTRs whose translation is sensitive to both EIF4E (blue) and EIF4A1 (red), which encode pro-survival- (e.g., BCL2) and proliferation-promoting (e.g., CCND3) proteins, and (2) mRNAs with short 5' UTRs whose translation is sensitive to EIF4E (blue), but not EIF4A1 (red), which encode proteins with mitochondrial functions (e.g., ATP5O). Whereas MTOR-I (mTOR-I; green) suppresses translation of both subsets of mRNAs (1 and 2) leading to metabolic dormancy and cytostatic effect, EIF4A-I (red) selectively inhibits translation of mRNAs with long 5' UTRs (1), leading to apoptosis.

nanoCAGE reveals 5' UTR features that define specific modes of translation of functionally related MTOR-sensitive mRNAs. Genome Res, 2016. 26(5): p. 636-48. Gandin, V., et al., Published by Cold Spring Harbor Laboratory Press. Used under a Creative Commons License as described at http://creativecommons.org/licenses/by/4.0/.

Specialized mechanisms have evolved that allow specific mRNAs to be translated under stress conditions where the global translation is decreased and the availability of initiation factors is limiting. Subsets of eukaryotic mRNAs can bypass the limitation of the initiation factors by leveraging specialized sequences, called internal ribosome entry sites (IRESs), that recruit the PIC to the start codon in a cap-independent manner [34].

In parallel to the mTOR pathway, the integrated stress response (ISR) is a conserved adaptive pathway that allows cells to respond to different stress contexts. In the ISR, several kinases converge in the phosphorylation of $elF2\alpha$ subunit thereby inhibiting elF2's ability to deliver the ternary complex to the ribosomes [35]. This results in the downregulation of global mRNA translation initiation. However, it promotes the translation of mRNAs containing upstream open reading frames (uORFs)[21]. A prime example is Activating Transcription Factor 4 (ATF4), ATF4 transcript has two uORFs, the second of which overlaps the start codon of the main ORF [36]. During normal conditions, after translation of the uORF1, the 40S ribosomal subunit resumes scanning [37]. If ternary complex is abundant, re-initiation at uORF2 is efficient, and the peptide encoded by the uORF2 will be translated with high efficiency, preventing *ATF4* from being translated. The slow rate of reloading of ternary complexes results in some ribosomes that have completed the translation of uORF1 scanning past the start codon of uORF2 before they have acquired a new TC. Past that point, if a TC loads between the start codons of uORF2 and the coding sequence, *ATF4* can be translated.

1.1.9. translation regulation effect on the proteome

Transcripts exhibit different rates of translation depending on cellular context. This rate is termed translation efficiency (TE), commonly measured by the number of ribosomes per RNA molecule, which drives alterations in the levels of encoded proteins[38]. Changes in the levels of a given mRNA transcript and/or its TE can alter the relative composition of the translatome, and consequently the proteome [39]. Thus, changes in the translatome can be representative of fluctuations in the mRNA abundance or can occur independently of fluctuations in mRNA levels, and represent actual changes in translational efficiency [40]. Although it is a developing field, several mechanisms have emerged in the literature. The traditional view is that changes in mRNA abundance drive changes in the encoded protein levels as a product of changing mRNA levels, which are always translated at the same efficiency [41]. However, changes in TE can modulate levels of encoded proteins under conditions where corresponding mRNA levels are relatively stable. In addition, the opposite can be true, where the changes in the TE buffers changes in mRNA levels (Figure 5)[42].

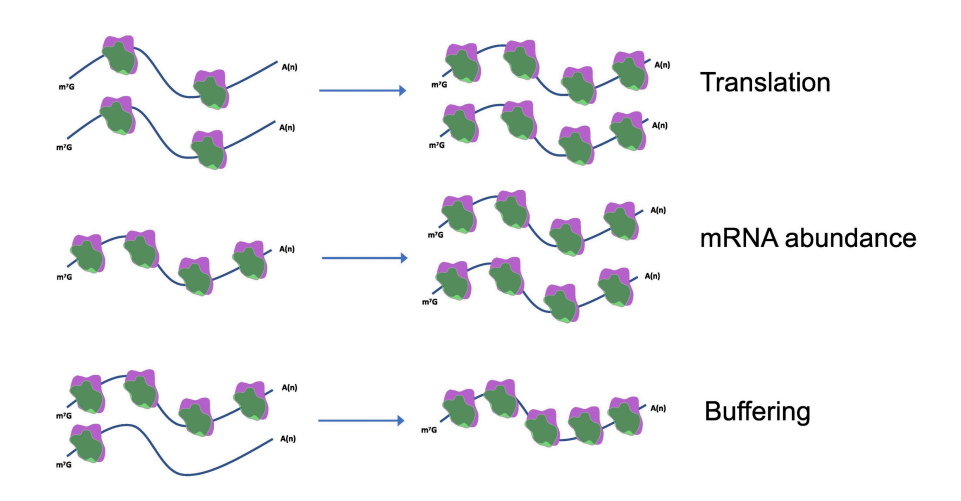


Figure 5. Schematic representation of the proposed modes of gene expression regulation. Top panel: changes in translational efficiency (TE) that drive alterations in protein synthesis; middle panel: changes in mRNA abundance; lower panel: translational buffering during which ribosome-association of mRNA is maintained despite changes in corresponding mRNA levels. To this end, translational buffering prevents alteration in protein synthesis upon perturbations in corresponding mRNA levels. Specifically, top panel illustrates increase in TE, whereby ribosome-

association of mRNA is increased without changes in mRNA abundance. Middle panel shows increase in total mRNA levels that is accompanied by congruent upregulation in ribosome association. Lower panel indicates the example of translational buffering whereby the number of ribosomes associated with mRNA remains constant notwithstanding decrease in mRNA levels.

Reprinted with permission from Regulation of gene expression via translational buffering by Kusnadi E.P., et al, 2022. Biochimica et Biophysica Acta (BBA) - Molecular Cell Research, 2022. 1869(1): p. 119140. Copyright 2022 by Elsevier.

Deep sequencing of ribosome-protected mRNA fragments can be leveraged to map genome-wide translation at nucleotide resolution. Using this approach, a recent report profiled the translational landscape of the developing and adult human brain [43]. Several modes of translational regulation were observed in the developing and adult human brain, significantly shaping the brain proteome. Translation modulation mechanisms were classified as buffered, intensified (change in TE that amplifies the change in RNA level), mRNA Abundance, or exclusively translationally regulated. Furthermore, in accordance with the PTO model, proteins enriched in distinct biological processes were shown to be preferentially modulated in concert by one of the mechanisms. This report highlighted the determining importance and significant input of translation regulation in shaping, in a very dynamic manner, the complex proteome necessary for proper brain function.

Due to neurons' long and multicompartmental morphology, these cells rely on the transportation of cellular components and machinery to carry out specific functions in distant cellular compartments such as the synapse. Particularly synapses, responsible for interneuronal connections, require *de novo* protein synthesis for long-lasting synaptic plasticity in a cuedependent manner [44]. Considering the speed necessary to procure structural changes to assure plasticity, translation of mRNA encoding proteins necessary to these structural changes occurs locally, at the synapse [44]. This fascinating mechanism of local mRNA translation, primordial for successfully carrying out higher cognitive tasks such as memory, is affected in neurodegenerative diseases [45]. However, this thesis focuses only on mRNA translation control associated with the mTOR-4E-BP axis in microglia, in the whole cell, and in the context of amyloidosis. Therefore,

shouldn't be confused with the control of local mRNA translation associated with memory formation.

1.2. Alzheimer's Disease

1.2.1. Alzheimer's Disease Prevalence

According to the World Health Organization, currently, more than 55 million people have dementia worldwide, over 60% of whom live in low-and middle-income countries. Every year, there are nearly 10 million new cases of dementia worldwide. Alzheimer's disease (AD) is the most common cause of dementia. Most AD cases occur after age 65, constituting late-onset AD (LOAD). In contrast, familial cases show clinical manifestation earlier than age 65, constituting less than 5% of all cases, and are termed early-onset AD (EOAD)[46]. Age is the predominant risk factor for AD development, and its worldwide prevalence is expected to increase along with the aging population [47, 48]. In the United States, the largest ever demographic generation of the American population — the baby-boom generation — started reaching age 65 in 2011 [49]. Today in the United States, 6.7 million people 65 and older are estimated to suffer from AD. By 2025, the number of people aged 65 and older with AD is projected to reach 7.2 million, and by 2060, this number is projected to reach 13.8 million [49].

1.2.2. Alzheimer's Disease Pathology

AD is a progressive neurodegenerative disorder. The histopathology of AD is characterized by amyloid plaques composed of extracellular deposits of amyloid beta (Aβ) peptides, intracellular neurofibrillary tangles primarily composed of tau protein, dystrophic neurites and loss of neurons and synapses resulting in brain atrophy [50, 51]. In addition, chronic activation of brain innate immunity is a prominent feature in the histopathology of AD [52]. The development of AD biomarkers using cerebrospinal fluid, positron emission tomography (PET) imaging, or plasma has allowed to reasonably monitor pathology and diagnose AD antemortem. Longitudinal studies show that the pathological processes underlying AD start years, if not decades, before clinical

onset [53]. The current paradigm suggests that the deposition of $A\beta$ in the precuneus is the first detectable pathological event of the disease. There is a subsequent activation of glia followed by accumulation of tau pathology, and synaptic and neuronal loss in the entorhinal cortex (Figure 6)[53]. Importantly, these pathologies progress in a neuroanatomical and temporally heterogeneous fashion. Among all the different pathological processes, tau pathology and synaptic and neuronal loss best correlate to the onset of cognitive impairment, whereas amyloid pathology has a poor correlation.

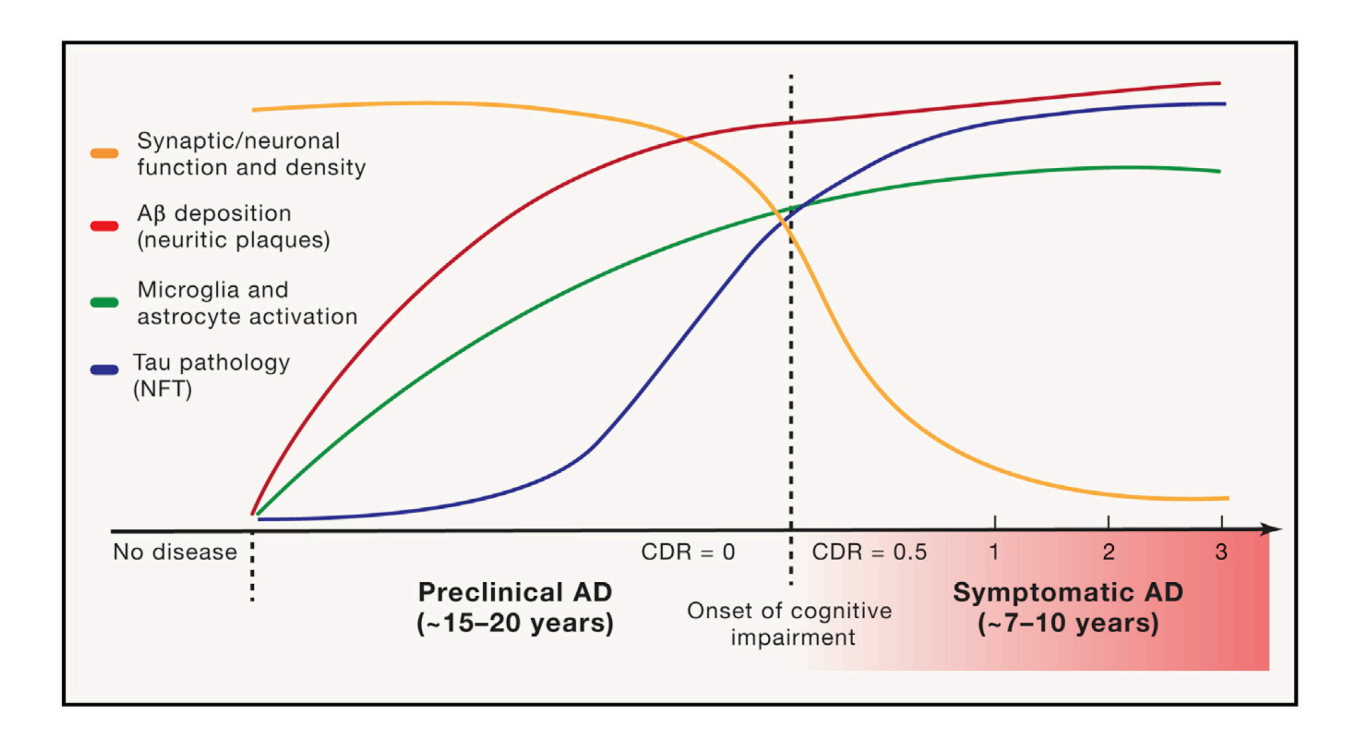


Figure 6. Timing of Major AD Pathophysiological Events in Relation to Clinical Course. A protracted preclinical phase of disease is characterized by the early onset of amyloid deposition. This is detected by a reduction in CSF and plasma levels of Ab42 or increased global signal on amyloid PET imaging. Concurrently, there are early neuroinflammatory changes (such as microglial activation). Microgliosis can be detected longitudinally via use of PK11195 PET imaging, though better agents are needed. This is followed by the spread of neurofibrillary tangle (NFT) tau pathology from the medial temporal lobes into neocortex. Increased signal on tau PET imaging and increased CSF phospho-tau levels mark this change in patients. Synaptic dysfunction, synapse loss, and neurodegeneration accumulate with pathologic spread of tau aggregates. Imaging analysis of hippocampal and cortical volumes allows for longitudinal tracking of neurodegenerative changes. Onset and progression of cognitive impairment correlates with accumulation of tau and hippocampal volume loss but not amyloid deposition. Onset and severity of clinical symptoms in AD can be staged by use of the Clinical Dementia Rating (CDR) scale, where

a score of 0 indicates normal cognition and scores of 0.5, 1, 2, and 3 indicate questionable, mild, moderate, and severe dementia, respectively.

Reprinted with permission from An Update on Pathobiology and Treatment Strategies by Long, J.M. and D.M. Holtzman, 2019. Cell, 2019. 179(2): p.312-339. Copyright 2019 by Elsevier.

1.2.3. Amyloid and Tau Pathogenesis

Amyloid beta is an ancient neuropeptide highly conserved across vertebrates[54]. The A β peptide is generated through the sequential cleavage of the amyloid precursor protein (APP) by β - and γ -secretases. This cleavage usually happens in the endosome in neurons, and through a mechanism modulated by synaptic activity, the peptide is released into the interstitial fluid as a soluble monomer of A β [54]. APP and its secretion as A β monomers exert critical physiological roles in maintaining neuronal function and is essential for proper synaptic activity [55]. The levels of A β monomers in the brain critically affect the structural properties of A β [56]. Consequently, the concentration of A β in the brain needs to be tightly controlled; therefore, the processing, secretion, degradation, and removal from brain parenchyma are all highly regulated processes [57]. If the concentration of A β monomers increase in the brain interstitial fluid, A β is prone to aggregate into insoluble β sheet-containing oligomers, protofibrils, and fibrils, which are detectable in the AD brain.

After the appearance of amyloid deposits, the other determining hallmark of Alzheimer's disease is tau pathology. Tau protein is encoded by the MAPT gene and primarily expressed by neurons in the brain [58]. Although the physiological role of tau protein is not completely elucidated, it exerts important functions under normal physiological conditions. Tau is a microtubule-associated protein that stabilizes neuronal cytoskeleton microtubules and is preferentially localized in axons [58]. Tau undergoes post-translational modifications such as phosphorylation. Tau modifications, particularly phosphorylation, seem to be associated with tau pathology [59]. Aberrant phosphorylation decreases tau binding affinity for microtubules resulting in an increased cytosolic tau [60]. Although tau is generally a soluble protein in its natively unfolded form, it can aggregate into insoluble β -sheet oligomers and fibrils known as

paired helical filaments (PHFs)[59]. Furthermore, tau fibrils have a prion-like ability to self-propagate and propagate transsynaptically to connected distant brain regions where endogenous tau in the recipient neuron also becomes misfolded through a seeding mechanism of templated misfolding [61]. These intracellular tau fibrils aggregate into neurofibrillary tangles (NFTs) and along amyloid- β (A β) plaques are the cornerstone of the current National Institute of Aging criteria for the post-mortem diagnosis of AD [62].

1.2.4. The amyloid cascade hypothesis

To explain the pathogenesis of AD, Hardy and Higgins in 1992 proposed the amyloid cascade hypothesis. This hypothesis states that the deposition of $A\beta$ in the brain is the initiating step of AD pathogenesis, leading to subsequent tau deposition, neuron and synaptic loss, and finally cognitive decline [63]. The amyloid cascade hypothesis was propelled by genetic evidence showing that APP gene mutations cause AD and that in autosomal dominant forms of AD, an increase in the total A β production, or A β aggregation properties is sufficient to induce typical AD pathology. Furthermore, while the familial cases of AD are caused by mutations in the genes encoding APP and its metabolism, the vast majority of AD cases, late-onset, are thought to arise from impaired A β clearance mechanisms [64]. However, the reasons why the clearance mechanisms are insufficient are not completely elucidated and can implicate defective microglia response to A β or comorbidities such as vascular pathology. The amyloid cascade hypothesis has been the leading model of AD pathogenesis since its proposal. However, given that A β deposition doesn't correlate to cognitive decline and anti-amyloid therapies failed for a long time to slow cognitive decline, it has been re-evaluated over time. While amyloid accumulation may be key in initiating the pathological cascade, other downstream events, such as neuroinflammation and tau accumulation, may be the main drivers of neurodegeneration [56].

Several genetic and environmental factors can increase the risk of LOAD development. In this sense Genome-wide association studies (GWAS) have identified many loci that influence the risk of developing AD later in life [65]. The ϵ 4 allele of *APOE*, remains by far the most critical genetic variant affecting the risk of LOAD because of its prevalence and the size of its effect on

risk. The *APOE* gene has three common alleles encoding variants of the protein (APOE2, APOE3, and APOE4). One copy of *APOE* $\varepsilon 4$ allele increases risk of developing late onset AD by ~ 3 - to 4-fold, whereas two copies increases risk by ~ 12 -fold [53]. APOE primary function in the brain is to transport cholesterol, APOE is a component of lipoprotein particles in the cerebrospinal fluid and in the interstitial fluid of the brain parenchyma, as well as in the plasma in the periphery [66]. APOE mediates the binding of lipoproteins or lipid complexes in the plasma or interstitial fluids to specific cell-surface receptors. These receptors internalize APOE-containing lipoprotein particles; thus, APOE transports lipids in the brain heterocellular environment.

1.3. Microglia

In the central nervous system, microglia are the resident immune cell population and a primary mediator of the immune response in the brain; However, their role expands well beyond immune functions[67]. Microglia are established in the Central Nervous System (CNS) early during embryogenesis, well before other glial cells arise, and therefore have several developmental functions[68]. Microglia are critically involved in the establishment of the neuronal architecture of the CNS by modulating neuronal fate, neuronal numbers, and synaptic connections [67, 69]. During adulthood, microglia also perform physiological, homeostatic functions in the CNS [70, 71]. Although the microglial cell body is relatively static and seemingly resting, microglia processes continuously probe their surrounding area and have close interactions with neighboring cells mediated by various receptors including purinergic receptors, ion channels, and neurotransmitters [71]. These constant interactions allow microglia to survey their surroundings and perform functions including clearing dead and surplus cells in neurogenic regions, and actively contribute to the restructuring of neuronal circuits by phagocytizing synaptic elements and remodeling perisynaptic areas [71].

As part of the innate immune system, microglia display a wide array of functional states in health and disease [72]. Pathological stimuli promote an inflammatory response that serves to further engage the immune system and clear out pathogens or debris; however, this response is usually self-limiting once the insult has been resolved [73]. During neurodegeneration, protein

aggregates can be perceived by the immune system as pathological stimuli, and under this chronic stimulation, microglia acquire a phenotype characterized by exacerbated and self-perpetuating responses leading to detrimental effects [68]. These microglia phenotypes have been described in both aging and neurodegenerative diseases such as AD [73].

1.3.1. Unveiling Microglia Involvement in Alzheimer's Disease

Ample genetic evidence has pointed toward the crucial role of neuroinflammation in AD pathology. The vast majority of AD cases are late-onset AD, which appears to result mainly from a mixture of genetic and environmental factors, including aging, that impair the brain's ability to clear A β peptides[74]. Many AD-risk loci have been identified; However, the molecular mechanisms of many of these loci remain to be fully elucidated. Yet, a striking feature of the identified risk genes in large-scale genome-wide association studies is that the majority of these genes are expressed selectively or preferentially in microglia relative to other cell types in the brain [75]. Furthermore, AD risk-associated noncoding genetic variants were found to be regulatory regions of genes expressed mostly in microglia in the brain [76]. This general trend suggests that microglia dysfunction may constitute a driving force for disease progression, more so than an associated feature. Mediation models examining post-mortem brain tissues from LOAD patients support an upstream role of microglial activation in cognitive decline during Alzheimer's disease [77]. A recent report states that the co-occurrence of A β and tau with activated microglia was the strongest predictor of cognitive impairment [78]. Although extensively studied, the roles of microglia in AD remain to be fully elucidated due to their dynamic and heterogeneous nature.

1.3.2. Roles of microglia during AD

Mounting genetic and experimental evidence suggests that proper microglia function protects against the onset of AD [79]. A central aspect of microglia physiological functions is the engulfment and clearing of misfolded proteins and debris, including A β aggregates and apoptotic cells or cell debris, maintaining a healthy environment for neuronal function [80]. Notably, these protective microglial functions are highly dependent on strong AD risk factors such as apolipoprotein E (APOE) and triggering receptor expressed in myeloid cells 2 (TREM2)[81]. A β uptake is diminished in TREM2 deficient microglia and more efficient when A β is complexed with

lipoproteins such as APOE [82]. In the same fashion, the uptake of cell debris, damaged cells, and APOE-bound apoptotic neurons is also facilitated by TREM2 [83, 84]. Microglial processes become static around A β aggregates, showing a stable association with A β plaques and increased proliferation around the aggregates [85]. This corralling mechanism is reliant on APOE and promoted by TREM2 [86, 87]. Furthermore, strong evidence suggests that dense-core A β or focal A β deposits do not form spontaneously but require microglia functions. Microglia phagocytosis of A β can be routed to the lysosomal pathway, and A β aggregation and compaction can occur in the low pH of the microglia lysosome into a dense-core material that is 'indigestible' and therefore deposited via exocytosis or microglial cell death [88, 89]. In the AD brain histopathology, activated microglia nearly always accompany the dense core A β deposits [90]. The presence of dystrophic neuronal processes surrounding the plaque core would then constitute a neuritic plaque, commonly found in the AD brain (figure 7).

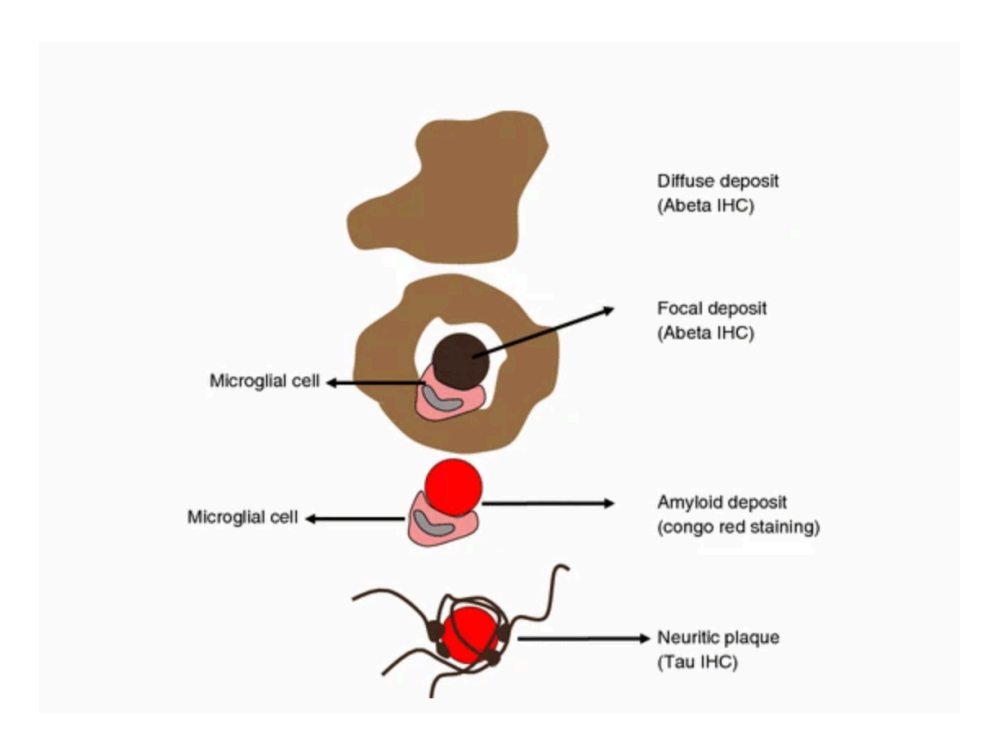


Figure 7. Terms used to describe A6 deposits and senile plaques. Various aspects of A6 deposition, as seen with A6 and tau immunohistochemistry (IHC), and Congo red staining are illustrated. Care has been taken to distinguish diffuse from focal deposits, the former ones being poorly correlated with the symptoms. The terms applied to qualify the focal deposits depend on the technique used to reveal them, for instance the amyloid deposit is Congo red or thioflavin S

positive. Tau IHC only reveals neuritic plaques. The vertical position of the drawing tentatively represents the sequence of events leading to the neuritic plaque. Stellate deposits have not been represented here.

Reprinted with permission from Classification and basic pathology of Alzheimer disease by Duyckaerts, C., B. Delatour, and M.-C. Potier, 2009. Acta Neuropathologica, 2009. 118(1): p. 5-36. Copyright 2009 by Springer Nature.

On the other hand, there is also abundant evidence suggesting a detrimental role of activated microglia during AD. Microglia, as part of the innate immune system, express pattern recognition receptors including damage-associated molecular patterns (DAMPs). DAMPs are often found under neurodegenerative conditions, including age-related debris, misfolded proteins, aggregated peptides, and released nucleic acids to which microglia respond [73]. These represent a chronic stimulation to microglia. In addition, Microglia can release inflammatory mediators and toxic substances such as reactive oxygen species and nitric oxide that are meant to exert an anti-infectious, and antitumor immunity and generate a proteolytic cascade; however, it can directly damage neurons[91]. Inflammatory stress can also induce stressed neurons to express signals to be phagocytosed by activated microglia via a process called phagoptosis [92]. Moreover, activated microglia also induce astrocytes to acquire a reactive phenotype, which secrete neurotoxic factors and lose neurotrophic functions causing rapid neuronal dead [93].

Even though amyloid pathology may initiate decades before the symptom's onset, synapse loss and tau pathology correlate best with cognitive decline [94]. During brain development, microglia prune synapsis, thereby sculpting synaptic connections, this involves direct engulfment of synapses via the classical complement pathway [95]. Several lines of evidence point toward the active role of microglia in complement-mediated synapse loss in AD. Components of the complement pathway show increased activation in the AD brain tissue [96]. Although there are conflicting results, in amyloidosis mouse models of AD, depletion of microglia or components of the complement pathway can prevent synapse loss and preserve cognitive function even with high amyloid burden [97] (for a diagram of microglia myriad of states and roles in amyloidosis see Figure 8) [80].

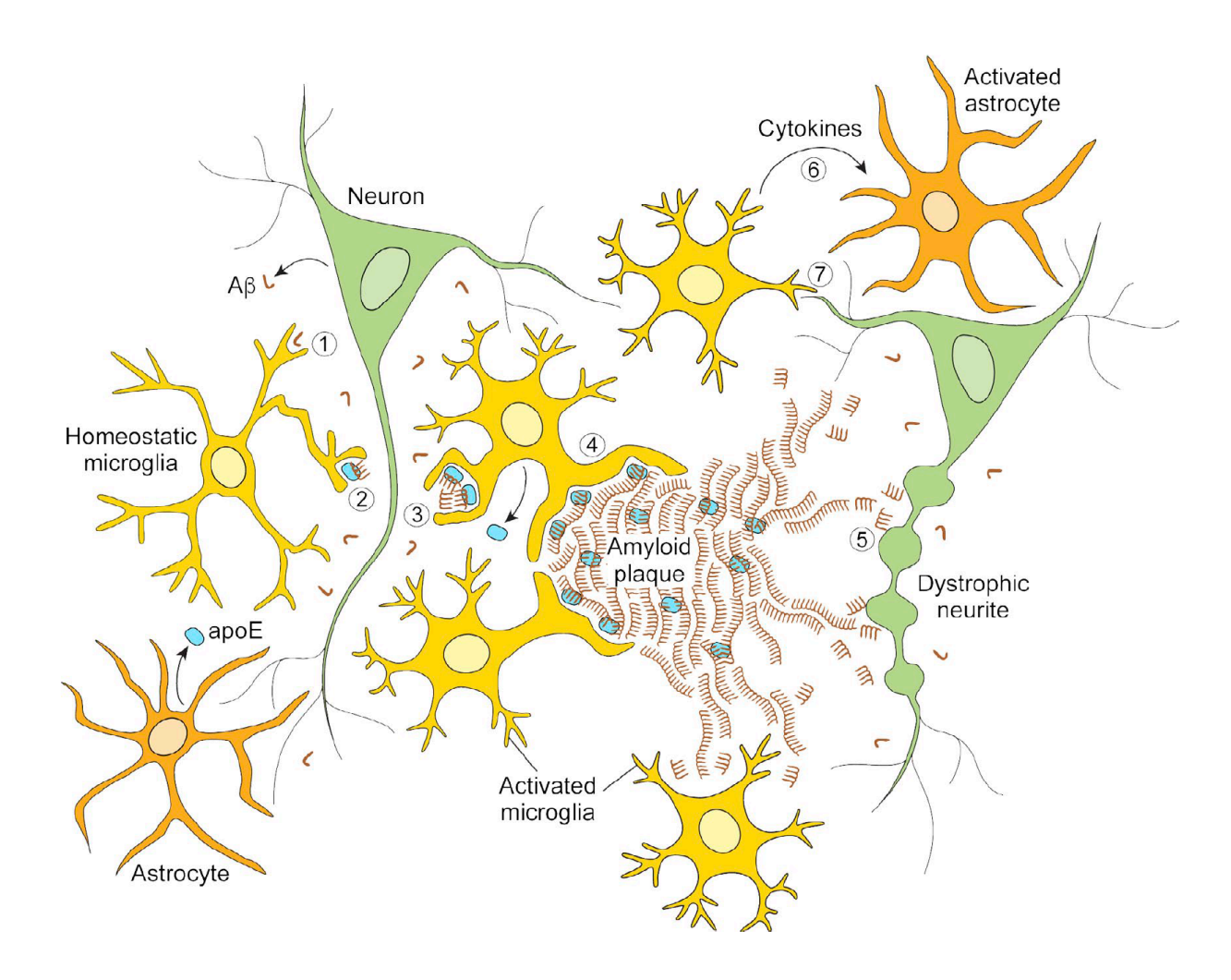


Figure 8. Depiction of microglial cellular activities related to β-amyloid pathology. The left side illustrates protective microglial activities that limit disease progression. Microglia may clear Aβ peptides via macropinocytosis of soluble Aβ (1; Mandrekar et al., 2009), uptake of lipoprotein-associated Aβ (2), or phagocytosis of fibrillar Aβ aggregates (3). Microglia also help corral larger deposits of Aβ in plaques (4), minimizing damage to the adjacent neuropil. The right side illustrates disease states when microglial containment mechanisms are defective or outstripped. Aβ fibrils on the outskirts of plaque act as substrate for additional Aβ fibrillization and a reservoir of toxic Aβ species that induce neuritic dystrophy (5). Microglia can secrete factors that activate astrocytes (6) and participate in amyloid-dependent synapse loss (7).

Reprinted with permission from Microglia in Alzheimer's disease by Hansen, D.V., J.E. Hanson, and M. Sheng, 2018. 217(2): p. 459.Copyright 2018 by Rockefeller University Press.

Microglia seem to also have an active role in tau pathology which has begun to be uncovered. Activated microglia release cytokines that can trigger tau phosphorylation in neurons [98]. In a mouse model of tauopathy, microglia depletion halted phospho-tau pathology

progression [99]. In addition, the $\epsilon 4$ allele of apoE (apoE4) was shown to significantly exacerbate neurodegeneration in a mouse model of tauopathy. However, microglia depletion eliminated apoe4's effect on neurodegeneration[100]. Furthermore, using PET tracers for microglia activation, amyloid, and tau pathology, it was reported that the extent of microglial activation, in the presence of amyloid pathology, paralleled and predicted tau propagation in patients with AD pathology [78]. This and other studies have suggested microglia activation as a mediator of the progression of neurodegeneration after the appearance of amyloid pathology [77].

1.3.3. Microglia distinct phenotypes

Microglia are a distinct cell population in the brain; However, microglia exhibit remarkable plasticity in the functional states they can adopt [72]. Microglia exist in the healthy brain in a homeostatic yet dynamic state, carrying out roles both during development and adulthood, as described above. With the advance of isolation techniques and single-cell RNA sequencing, heterogeneous subpopulations of microglia have been described both in health a disease [72, 101]. During the pathogenesis of neurodegenerative diseases, microglia lose their homeostatic signature and functions and acquire heterogeneous phenotypes with associated gene expression and functions [102]. These states or phenotypes have been cataloged by their transcriptomic 'signature'. In the context of AD pathology, microglia show a shift in which their homeostatic signature is suppressed, and an inflammatory phenotype is induced [102]. However, these heterogeneous states co-exist and depend on microglia immediate surroundings (see figure 8). Of note, a reactive signature present in Aβ-plaque-associated microglia has been described in both mice and humans and termed Disease Associated Microglia (DAM microglia)[103]. These studies demonstrated that cellular reprogramming of microglia occurs in response to neurodegeneration and is reflected in unique underlying transcriptional programs detected as transcriptomic signatures.

1.3.4. Linking the mTOR pathway, translation, and microglia in AD.

Genome-wide association studies (GWAS) have identified many loci that influence the risk of developing AD later in life [65]. The ε4 allele of APOE, remains by far the most critical genetic variant affecting the risk of LOAD because of its prevalence and the size of its effect on risk. However, over the years AD risk GWAS have identified a set of genes enriched in inflammatory processes, including variants of immune receptors expressed on microglia [65, 104]. Of note, TREM2 risk variants, although rare, confer an AD risk with a reported odds ratio between 2.9-4.5 [105, 106]. Considering these findings, researchers aimed to understand the roles of TREM2 in AD pathogenesis.

Several studies have shown that TREM2 is a receptor with many ligands and functions in AD, it recognizes phospholipids, apoptotic cells, lipoproteins such as APOE, and A β in different conformations [107, 108]. This receptor is preferentially expressed in microglia cells in the brain [109]. TREM2 loss-of-function variants or haplodeficiency affect microglial proliferation, survival, and clustering around A β deposits, rendering microglia unable to isolate A β pathology from neurons[108]. To mediate all these functions, this receptor transmits intracellular signals to coordinate microglia functions. The signaling pathway was initially described in osteoclasts and macrophages; TREM2 transmits intracellular signals through two adapters proteins, DAP12 and DAP10, which recruit protein tyrosine kinase (SYK) and phosphatidylinositol 3-kinase (PI3-K), respectively, leading to the activation of Akt/mTOR and ERK1/2 pathways [110]. However, the effect of the risk variants, haplodeficiency, or AD pathology in the TREM2-related intracellular signaling and cell-autonomous processes is not fully elucidated.

In 2017, Ulland and colleagues at the Colonna lab aimed to investigate how the AD risk gene TREM2 affected microglia biology [111]. Initially, they found that microglia in AD patients carrying TREM2 risk variants and TREM2-deficient AD mouse model have abundant autophagic vesicles. After these observations, given the mTOR signaling effect on autophagy, investigators examined this pathway and showed that this anomalous autophagy reflected defective activation of mTOR signaling in microglia. TREM2-deficient macrophages confirmed the impairment of mTOR activation, which leads to derailed energetic pathways decreasing ATP levels and

biosynthetic pathways, including ribosomal proteins, ultimately leading to microglia cell death. Overall, this decrease in mTOR signaling led to a deficient microglial response to amyloidosis, resulting in microglia cell death and worsening of pathological outcome in an amyloidosis mouse model. The authors concluded that during amyloidosis, TREM2 sustains microglial cell anabolic and energetic metabolism through mTOR signaling.

In 2019, Baik and colleagues at the Mook-Jung laboratory showed that mTOR activation is decreased in microglia during amyloidosis independent of TREM2 loss-of-function [112]. They found that A β triggers acute microglial inflammation, which requires metabolic reprogramming from oxidative phosphorylation to glycolysis, also known as the Warburg effect. This switch requires the activation of the mTOR-hypoxia-inducible factor-1a (HIF-1a) pathway. However, upon chronic exposure to A β oligomers and during amyloidosis in the 5XFAD mouse, microglia reach a tolerant state in which they enter a lethargic state, exhibiting defects in both glycolysis and OXPHOS metabolism. This tolerant state is associated with decreased mTOR signaling and decreased phagocytosis and mobility upon immune stimuli both *in vitro* and *in vivo*. Although tolerance may be protective in the context of chronic inflammation, activated microglial phenotypes are necessary during amyloidosis to surround and phagocytize A β , thereby preventing the spread of A β pathology.

Both studies employed approaches to rescue microglia energetic deficits finding beneficial results in mouse models of amyloidosis. However, although mRNA translation is a major downstream target of the mTOR pathway, the alterations in mRNA translation control were not studied. Furthermore, published work from our laboratory has shown a feed-forward mechanism by which mTOR stimulates 4E-BP-regulated mRNA translation of nuclearly encoded mitochondrial genes, boosting mitochondrial biogenesis and increasing ATP production capacity in the cell [113]. Therefore, linking mTOR controlled energetic metabolism through mRNA translation.

This sets several questions that I aimed to answer in the thesis. First, what are the signal transduction alterations in the mTOR/4E-BP pathway in the absence of TREM2 signaling or chronic A β stimulation? Second, what are the functional implications of de-repressing 4E-BP-controlled

translation in these contexts? Finally, what are the specific mediators controlled via mTOR/4E-BP axis that allow microglia to sustain a protective phenotype and cell viability in AD?

2. Rationale

During the years or even decades of amyloid aggregation that precedes cognitive decline in AD, microglia seem to undergo a switch from a neuroprotective to a detrimental functional state [114]. This might represent a progressive state of dysfunction induced by chronic activation, possibly associated with the non-resolving immune stimulation from A β aggregation and debris characteristic of neurodegeneration. Consequently, it is a common neuropathological finding to encounter dystrophic microglia, characterized by fragmented cytoplasmic processes, in the Alzheimer's brain [114]. The ability of microglia to exercise their function in health and disease is contingent on coupling various extracellular signals, usually through receptors, to major downstream signaling networks. Many identified AD risk genes enriched in microglia are immune receptors, and deletion or hypofunction worsens disease outcomes in animal models. Considering this enrichment in immune receptors, there are ongoing efforts to boost microglia neuroprotective functions by targeting microglia receptors that elicit TREM2-like functions and intracellular signals, including activating the mTOR pathway [115, 116]. Furthermore, anti-amyloid therapies rely on microglia as effectors of phagocytosis. However, the intracellular pathways and cell-autonomous mechanisms to generate the necessary energy and coordinate gene expression to carry out these functions are not fully defined. Understanding major shared intracellular signaling pathways and mechanisms may provide more effective ways to instruct microglia neuroprotective responses.

Additionally, the transcriptomic profiling commonly used to characterize microglia gene expression is missing crucial aspects of microglial biology, failing to provide a higher resolution repertoire of expressed proteins and their levels. There is a gap in our understanding of the concomitant translational regulation of the transcriptional output in different microglia states. Translational control is a critical layer of gene expression regulation and is not reflected in transcriptomic profiling, particularly during cellular activated or stressed states[10]. The divergence between the transcriptome and proteome may be even wider in microglia in AD because of the dysregulation of the mTOR pathway, which controls mRNA translation. Therefore, I aimed to understand the dysregulated mechanisms at the intersection of mTOR-regulated mRNA translation and metabolism in microglia response to A β . Outlining these mechanisms and

identifying mediators should unveil novel therapeutic avenues to enable microglia to sustain an efficient response to restrict AD pathology.

3. Hypothesis

Amyloid pathology or AD genetic susceptibility leads to aberrant mTOR signaling in microglia. I hypothesized that 4E-BP-regulated translation is repressed in microglia, rendering these cells metabolically exhausted, immunologically detrimental, and ultimately apoptotic. Therefore, restoring translation control in microglia may return their ability to halt AD pathology.

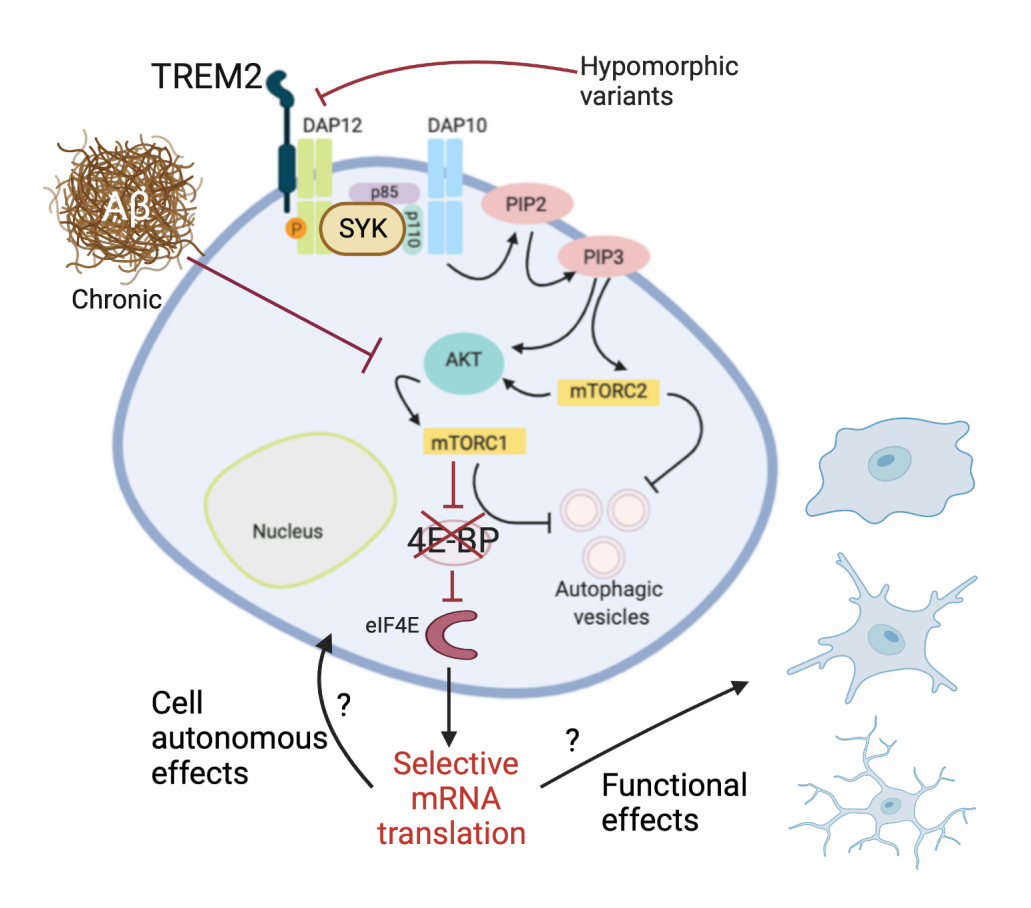


Figure 9. Graphical representation of the thesis research question. (Created with Biorender.com).

4. Methods

4.1. In vitro methods

4.1.1. Cell line generation

Cell lines were generated from BV2 microglia at passage 13, a kind gift from Dr. Carol Anne Colton at Duke University. Gene editing was performed using CRISPR synthetic single guide RNAs (sgRNAs, Synthego) as per manufacturers protocol. Briefly, cells were transfected with the Lipofectamine™ CRISPRMAX™ Cas9 Transfection Kit (Thermo) with ribonucleoprotein (RNP) complexes of synthetic sgRNAs and S.pyogenes Cas9 nuclease. RNPs were constructed with a sgRNA:Cas9 ratio of 3.91:3 as per the manufacturer's suggestion. Two guides were used per gene and transfection was performed simultaneously for eIF4E-BP1 and eIF4E-BP2 in a 1:1 ratio (see Table 1. for guides). After transfection, cells were incubated for 3 days in a humidified 37°C/5% CO₂ incubator. Following incubation cells were sorted into single cells per well in a 96-well plate. A total of 18 colonies were picked, expanded in duplicate, and examined by Western blot. Double knockouts (DKO) and non-edited cells (WT) were picked as controls from the same plate and were expanded and used further for the remainder of the investigation. Mycoplasma contamination was assessed by PCR routinely.

4.1.2. $A\beta$ aggregation

A β 1–42 peptides, HFIP (A-1163-2, r-peptide) were dissolved to 2.5mM in anhydrous dimethyl sulfoxide (Hybri-Max D-2650 DMSO, Sigma-Aldrich) to obtain a 2.5mM A β stock solution, which was then incubated in a bath sonicator for 10 minutes at room temperature. The peptide stock was then diluted to a concentration of 100 μM with 10 mM Tris-HCl, pH 7.4, and incubated for 48 hours at 22°C to facilitate the formation of higher molecular weight oligomers. These preparations were stored at –80°C or used in experiments immediately. Individual A β aggregate stocks were never thawed and re-frozen. To confirm oligomer formation, the preparation was resolved on a 4-20% TGX precast gel (Biorad) and immunoblotted with anti- β -Amyloid 1-16 (clone 6E10; Biolegend).

4.1.3. pHrodo™ Aβ labeling

For phagocytosis determination, Aβ was labeled as described by FUJIFILM Cellular Dynamics International, iCell® Microglia Application Protocol, Labeling Amyloid Beta with pHrodo Red https://www.fujifilmcdi.com/assets/iCell_MGL_ABeta_phago_AP.pdf

4.1.4. *In vitro* treatments

Bv2 cell lines were used between passages 13 and 20. Cells were maintained in Dulbecco's Modified Eagle Medium (DMEM) (Wisent) supplemented with 10% fetal bovine serum (FBS) (Wisent) heat-inactivated (30 minutes at 60° C) and 1% streptomycin-penicillin (Wisent) in a humidified atmosphere containing 5% CO_2 at 37°C. Cell culture treatments were performed in 24 or 96 well plates, at least in triplicate. Bv2 microglia cells were plated at 2.5x10^4 cells/ml overnight in 10% FBS-supplemented DMEM and changed to treatment media (2% FBS DMEM) before treatment. All drugs were dissolved in treatment media, and cells were incubated with Syk inhibitor (R406, 1uM, MedChemExpress), VEH or A β (2 uM) in treatment media for the indicated times. Syk inhibitor (R406, 1uM) was added 15 minutes before VEH or A β .

4.1.5. Western blotting

Cell culture plates were washed twice with ice-cold PBS. The cells were incubated in ice-cold RIPA lysis buffer (Thermo) supplemented with EDTA-free protease inhibitor cocktail and phosphatase inhibitor. Plates were placed in a rocking platform in the cold room for 20 minutes and scraped. After lysis, the samples were centrifuged at 12,000 g for 10 minutes at 4°C to remove insoluble material. The protein concentration was determined by the Bradford protein assay (Bio-Rad) using a BSA curve. Protein was equalized to be loaded 15ug of protein per well, with ddH₂O mixed with a volume of Laemmli sample buffer. Proteins were resolved in 12 or 15% SDS-PAGE gels at 100V until the gel bottom was reached by loading buffer. The gels were transferred to 0.2 uM nitrocellulose membranes (25V overnight at 4°C) and equal protein loading was confirmed

using Ponceau Red staining. The membranes were blocked for 1 hour with 5% BSA at room temperature in a rocking platform. After blocking, membranes were incubated overnight with primary antibody diluted in 5% BSA at 4°C. After 3x TBS-T washes, the membranes were incubated with peroxidase-coupled secondary antibody (1 hour at room temperature) and washed 3x on TBST. Enhanced chemiluminescence (Western Lighting® Plus ECL, PerkinElmer) was added to membranes for 1 minute (see Table 2. for antibodies). Membranes were visualized on film.

4.1.6. Live-Cell Incucyte imaging

Microglia were plated into a 96-well plate at 2.5×10^4 cells/ml (4 to 5 wells per line/condition). At time 0, all wells were treated with Caspase-3/7 (CellEventTM Caspase-3/7 Green, Invitrogen) 1:1000 in treatment media with A β , pHrodoTM (Thermo) labeled A β or VEH. Four 20X images per well were collected every hour. Using Incucyte® S3 Live-Cell Analysis System software, 2019A image masks for phase confluence, caspase 3/7 signal (green), and pHrodoTM labeled A β (red) were generated. Graphs display caspase normalized to phase confluence.

4.1.7. Immunocytochemistry

Cells were seeded on poly-L-lysine (Sigma) coated coverslips. After indicated treatments, cells were washed in PBS and fixed in 4% paraformaldehyde (PFA) for 15 minutes on a rocking platform at room temperature. After washing 3X with PBS, cells were permeabilized with PBS containing 0.05% Triton X-100 for 15 minutes at room temperature and blocked with blocking solution (PBS containing 10% BSA). Fixed cells were incubated with the primary antibody in blocking solution overnight at 4°C and thereafter incubated with Alexa Fluor (Thermo)-conjugated secondary antibodies (1:1000 in blocking solution) for 1 h at room temperature protected from light (see Table 2. for antibodies). Coverslips were mounted onto a glass slide using the ProLong Diamond Antifade Mountant with DAPI (Thermo). For Mitotracker (Thermo) staining, live imaging was used and no fixing was performed. Mitotracker Green was dissolved into a final concentration of 100 nM in phenol red-free FBS-free DMEM medium, and cells were incubated

for 30 min at 37°C. Samples were imaged with a ZEISS confocal microscope (LSM 800). Image processing was performed with FIJI (NIH).

4.1.8. Cytokine measurement

Cell media was obtained from treated cells as indicated, centrifuged at 10,000 rpm for 5 minutes at 4°C aliquoted, and frozen. Samples were shipped in dry ice to Eve Technologies Corporation (Calgary, Canada). The cytokines GM-CSF, IFN γ , IL-1 β , IL-2, IL-4, IL-6, IL-10, IL-12p70, MCP-1 and TNF α were evaluated in a Mouse Cytokine Proinflammatory Focused 10-Plex Discovery Assay® Array (MDF10).

4.1.9. Lactate measurement

Cells were plated on 96-well cell culture plates and treated as indicated with A β or VEH. Thereafter, lactate secreted into the cultured medium was quantified using a Lactate Lactate-GloTM (Promega) according to the manufacturer's instructions.

4.1.10. Measurement of Real-Time OCR

Real-time oxygen consumption rate (OCR) was measured using XFe96 plate (Seahorse Bioscience) according to the manufacturer's instructions, with minor modifications. Briefly, cells were plated on the XFe96 cell culture microplate and treated for 4 hours with A β or VEH. The cartridge plate was hydrated with XF calibrant buffer and incubated overnight (37°C, CO₂-free). The assay medium (XF base medium containing 1 mM pyruvate, 4 mM glutamine, and 25 mM glucose) was prepared immediately before the assay. XF sensor cartridges were loaded with test compounds. OCR was measured every 6 minutes in response to the ATPase inhibitor oligomycin (2.5 uM), the uncoupling agent FCCP (1 uM), and the electron-transport-chain inhibitors rotenone (2 uM), and Antimycin A (1 uM).

4.2. Animals and environment

Mice were housed in standard laboratory cages with 4–5 mice in each cage. Mice were given water and standard rodent chow ad libitum. Cages were maintained in ventilated racks in temperature- (20–21°C) and humidity-(~50%) controlled rooms, on a 12 h light/dark cycle. Standard corncob bedding was used for housing (Harlan Laboratories, Inc). Mice were maintained under standard conditions at the Goodman Cancer Research Centre (GCRC) animal facility. All procedures followed the Canadian Council on Animal Care guidelines and were approved by the McGill University Animal Care Committee.

4.2.1. Mouse lines

Eif4ebp1^{f/f} and Eif4ebp2^{f/f} mice are an established mouse line in the laboratory. Mice were generated by Ozgene Pty Ltd (Perth, Australia) by targeting a construct containing a neomycin selection cassette flanked by two short flippase recognition target (FRT) sites was used to generate a conditional allele [28]. The targeting construct also contained two loxP sites between exons 1 and 2 and between exons 2 and 3 for both Eif4ebp1 and Eif4ebp2 genes. The neomycin selection cassette was removed after the generation of the 'floxed' lines. Conditional microglial knockouts were generated by crossing Eif4ebp1^{f/f} Eif4ebp2^{f/f} with the B6.129P2(Cg)-Cx3cr1tm2.1(cre/ERT2) Litt/WganJ mouse line (Cx3cr1^{creERT2}, Jackson laboratories) and then further crossed with (JAX stock # 011029 B6N.129-Rpl22^{tm1.1Psam}/J). The presented data translatomic and transcriptomic data was generated with animals homozygote for the Rpl22^{HA} allele and heterozygote for the Cx3cr1^{creERT2} alleles.

4.2.2. Genotyping

During weaning, ear punches were collected from 3-week-old pups to determine the genotype. The DNA was prepared by boiling tissue in 50 uL of Solution 1 (25mM NaOH, 0.2mM EDTA, pH 12.0) for 20 minutes at 100°C. Next, 50uL of Solution 2 (40mM HCL, pH 5.0) was added and the tube was vortexed. The PCR reactions were performed using AccuStart™ II PCR SuperMix

(Avantor) following the manufacturer's instructions (see Table 3. for primers) The reactions were carried out and the PCR products were visualized on a 1.5% TAE-Agarose gel with ethidium bromide.

4.2.3. Immunohistochemistry

For immunohistochemistry, mice were placed under isoflurane anesthetics until loss of pain reflex and transcardially perfused with filtered ice-cold PBS then 4% paraformaldehyde (PFA, Electron Microscopy Sciences). Brains were cryoprotected in 30% sucrose. Brains were sectioned coronally into 30µm-thick slices on a freezing microtome (Leica SM 2010R) and stored in a solution of 0.05% NaN3 PBS as free-floating slices. For immunostaining, tissue was blocked for 1h in PBS, 0.2% Triton X-100, and 10% goat serum. Immediately following blocking, brain sections were incubated in primary antibodies diluted in PBS supplemented with 1% goat serum and incubated overnight at 4°C. Samples were then incubated with Alexa Fluor (Thermo)-conjugated secondary antibodies (1:1000 in blocking solution). Sections were adhered to glass slides and coverslips were mounted onto a glass slide using DAPI Mounting Medium (VECTASHIELD). Samples were imaged with a ZEISS confocal microscope (LSM 800). Image processing was performed with FIJI (NIH).

4.2.4. Intracerebroventricular Injections

A Kopf stereotaxic frame was used for intracerebroventricular (ICV) injections. Briefly, anesthesia was induced until loss of pain reflex with 3% isoflurane and maintained with 1.5% isoflurane. Mice were mounted on a Kopf stereotaxic frame, a midline incision was made, and the skull was exposed. Then 5ul of VEH or A β aggregates (100uM) were stereotaxically infused at 0.5 ul/min into the lateral ventricle (anteroposterior -0.4mm, mediolateral 1.0mm or -1.0mm, and dorsoventral -2.5mm relative to bregma) using a microliter syringe (Hamilton) attached to a stereotactic infusion pump. The needle was removed from the brain 10 minutes after completion of the infusion.

4.2.5. Ribosome pulldown

Bilateral hippocampi were extracted from mice, flash-frozen in liquid nitrogen, and stored at – 80°C until use. Simultaneously, samples were homogenized in ice-cold homogenization buffer (50 mM Tris, pH 7.4, 100 mM KCl, 12 mM MgCl2, 1% NP-40, 1 mM DTT, 1:100 protease inhibitor, 200 units/ml RiboLock RNase Inhibitor (Thermo) and 0.1 mg/ml cycloheximide in nuclease-free H2O (Wisent) 10% w/v with a dounce homogenizer (Sigma) until a homogeneous suspension could be observed. The sample was incubated for 10 minutes on ice, and 1 ul of the lysate was transferred to a microcentrifuge tube and centrifuged at 10,000 g at 4°C for 10 minutes. Supernatants were transferred to a fresh microcentrifuge tube on ice, and then 40ul was removed for input fraction analysis. Two ug of IgG (Sigma, only for validation pilot) or anti-HA (Biolegend) were added into the lysate and incubated for at least 30 minutes at 4°C in a rotator. Meanwhile, Dynabeads (Thermo), 100 ul per sample, were equilibrated to homogenization buffer by washing 3X. At the end of the sample incubation with antibody, beads were added to each sample, followed by incubation overnight at 4°C on a rotating mixer. The next day, samples were washed 3X with high-salt buffer (50 mM Tris,300 mM KCl, 12 mM MgCl2, 1% NP-40, 1 mM DTT, 1:200 protease inhibitor, 100 units/ml RiboLock, and 0.1 mg/ml cycloheximide in nuclease-free H2O (Wisent) and magnetized. At the end of the washes, beads were magnetized, and excess buffer was removed and 700µl of Trizol was added. RNA was eluted using the Direct-zol RNA Microprep kit (Zymo Research) per manufacturer's instructions.

4.2.6. RNA Sequencing

After RNA extraction, samples were submitted to The Donnelly Centre at the University of Toronto. Two or 3 samples were pooled and libraries were constructed using the NEBNext Ultra II Directional RNA Library Prep Kit for Illumina. Sequencing was performed on an Illumina NovaSeq 6000 system for a total of 24 samples (n=3/group, 4 groups IP and 4 groups for input). Canadian Center for Computational Genomic's pipeline GenPipes [117] was used to align the raw files and quantify the read counts. Briefly, raw fastq files were aligned to the mouse genome

GRCm38 Genome Reference with default parameters and raw reads were quantified using HTseq count [118].

4.2.7. Differentially expressed genes analysis.

The pipeline for differentially expressed genes is as follows. First, genes with low read counts (<10) were filtered out, which brought the total number of genes from 47,069 to 24,557. Next, we took two steps for visual quality control of the samples. By inspecting the log2-normed sample by gene heatmap, one sample (IP DKO Veh) showed severely outlying values across all genes. As a second quality control step, we performed cell-type deconvolution of each sample to assess whether IP samples indeed showed microglia gene enrichment. We used the 'cellanneal' python package, while using the Allen Mouse Brain Atlas "Whole cortex & hippocampus with 10x-smart-seq taxonomy" atlas as the reference dataset. Three IP samples (two MG^{WT}+AB, one MG^{DKO}+AB) showed obviously aberrant deconvolution indicating compromised sample quality. The four samples identified through these two quality control procedures were removed.

The "pyDESeq2" python library was used for differential expression analysis. Briefly, this process involves fitting size factors, dispersions, and dispersion trend curves to identify log-fold change across given contrasts. The model was fit once to identify outliers, and then once again after outliers have been refit. We evaluated two different contrasts separately, based on the samples that were remaining. Given the low number of AB samples among IP samples, we instead evaluated a WT vs DKO contrast in vehicle samples only. We report genes surviving multiple comparisons correction. For the Input samples, we were interested in evaluating a contrast to identify genes that change with AB exposure where DKO rescues these changes. Therefore, we evaluated genes that differ between AB Veh and all other groups. For this contrast, no genes survived multiple comparison corrections, though we report genes that are nominally significant as well. Gene lists were annotated using StringDB.

4.2.8. Quantification and statistical analysis

Statistical analyses were performed using GraphPad Prism 9.0 (GraphPad Software). Comparisons between two groups were performed using two-tailed unpaired t test. One-way analysis of variance (ANOVA) with Tukey's post hoc test was used to compare three or more independent groups. For comparison of multiple factors, a two-way ANOVA followed by Tukey's post hoc test was used. Data are presented as means \pm standard errors of the mean (SEM). Statistical parameters are detailed in the legend for each figure. Data are presented as means \pm SEM. *p < 0.05, **p < 0.01, ***p < 0.001. Sample sizes were determined based on pilot experiments.

4.3. Tables.

sgRNA 1 eIF4E-BP1 mouse	GACUACAGCACCACUCCGGG
sgRNA 2 eIF4E-BP1 mouse	GGAGCUGCACGCCAUCGCCG
sgRNA 1 eIF4E-BP2 mouse	ACUACUGCACCACGCCCGGG
sgRNA 2 eIF4E-BP2 mouse	UGAUAGCCACGGUGCGCGUG

Table 1. CRISPR guides used for the Knockout of eIF4E-BP1 and eIF4E-BP2 in BV2 microglia cell line.

Source	Atibody	Catalogue #
CST	4E-BP1	#9644
CST	Phospho-4E-BP1 (Thr37/46)	#2855
CST	Phospho-4E-BP1 (Ser65)	#9451
CST	4E-BP2	#2845
CST	Phospho-Syk (Tyr525/526)	#2710
CST	Syk	#2712
CST	NF-κB p65	#8242
R&D Systems	IL-1b	AF-401-NA
Sigma	b-Actin	#A5441

Table 2. Antibodies used for Western blotting and immunofluorescence.

	Jackson primer	primer 5' to 3' sequence	
cx3cr1	12266	AAG ACT CAC GTG GAC CTG CT	Common
cx3cr1	14314	CGG TTA TTC AAC TTG CAC CA	Mutant Reverse
cx3cr1	16221	AGG ATG TTG ACT TCC GAG TTG	Wild type Reverse
rpl22	9508	GGG AGG CTT GCT GGA TAT G	Forward
rpl22	9509	TTT CCA GAC ACA GGC TAA GTA CAC	Reverse
4ebp1		CAC ATT TCA GGG AGA GGG TGA TG	Forward
4ebp1		GCT GGG TTC TAA GAG TGG TAC TTT	Reverse
4ebp2		GTC GGT CTT CTG TAG ATT GTG AGT	Forward
4ebp2		GGC GAT CCC TAG AAA ATA AAG CCT	Reverse

Table 3. Primers used for mouse model genotyping.

5. Research Findings

The here presented thesis work aims to describe the mechanisms and effects of 4E-BP-dependent mRNA translation regulation that might contribute to microglia dysfunction in AD. The results to be presented in this thesis dissertation indicate that de-repressing 4E-BP-regulated mRNA translation in microglia leads to a decreased expression of pro-inflammatory mediators, and increased mitochondrial respiration, both at baseline and during exposure to $A\beta$, ultimately increasing microglia resilience to AD pathology. The fine-tuning of 4E-BP-regulated mRNA translation emerges as a pivotal mechanism regulating microglia functional states and maintaining microglia fitness in neurodegeneration.

Specific aims are as follows:

- 1. Characterize the signal transduction alterations in mTOR-4E-BP pathway in microglia responding to $A\beta$.
- 2. Characterize the functional implications of de-repressing 4E-BP-regulated translation in microglia responding to $A\beta$.
- 3. Identify the specific mediators controlled via the mTOR–4E-BP axis that allows microglia to retain a protective function and their cellular viability during AD.

5.1. Research findings by aim

5.1.1. Aim 1. Characterize the signal transduction alterations in mTOR-4E-BP pathway in microglia responding to $A\beta$.

The 4E-BPs are crucial downstream mTOR effectors that control mRNA translation (protein synthesis). Under low mTOR activity, hypo-phosphorylated 4E-BPs bind to the eIF4E reducing its affinity for the 5'cap of the mRNA and other initiation factors, which together mediates the recruitment of the ribosome, thus inhibiting translation initiation and therefore protein synthesis. Whereas under increased mTOR activity, mTOR phosphorylation of the 4E-BPs

leads to their dissociation from eIF4E. Available translation initiation factor eIF4E can then bind the 5'cap structure and upon interaction with other factors allow ribosome recruitment thus promoting mRNA translation initiation.

Accordingly, a characterization of the 4E-BPs phosphorylation was performed in microglia *in-vitro*, upon different AD pathology-related conditions. There were several important considerations for relying on this characterization *in vitro*; such as microglia state variability *in-vivo* and technical issues such as changes in phosphorylation during mouse euthanasia/perfusion or cell sorting that would not have allowed for clear results. Due to the increased expression of 4E-BP1 compared to 4E-BP2 and negligible expression of 4E-BP3 in microglia, 4E-BP1 was the isoform characterized in this thesis [27, 28].

5.1.2. A β aggregates induce acute microglial inflammation accompanied by phosphorylation of 4E-BP1.

Several reports suggest that signaling through the mTOR pathway is pivotal to microglia survival and ability to sustain a response in the context of Alzheimer's disease pathology [111, 112, 119]. An mTOR-dependent metabolic defect has been proposed as a mechanism underlying microglia dysfunction, yet the role of 4E-BP-dependent mRNA translation, downstream of the mTOR pathway, has not been examined in these contexts. Thus, I aimed to first characterize the phosphorylation of the downstream effector of the mTOR pathway, 4E-BP1, in microglia exposed to A β pathology.

BV2 microglia were exposed to a mixture of soluble A β aggregates (here on, A β) for 24 hours, at that point cell lysates were extracted to be analyzed by Western Blotting (Figure 10A). The biochemical analysis showed that A β prompts an inflammatory response, observed by induction of Pro-IL-1 β . This inflammatory response was accompanied by 4E-BP1 phosphorylation. Yet, a significant increase in the phosphorylation is only detected by upward band shift or use of a specific antibody for 4E-BP1 phosphorylation at Serine 65 (*Figure 10.B*). Importantly, phosphorylation at Serine 65 happens after the phosphorylation at the priming sites, Threonine

37/46, and is necessary for 4E-BP1 release of eIF4E. Available eIF4E can then promote translation initiation. Therefore, a single exposure to A β induces an inflammatory response and releases the 4E-BP1-dependent break in translation, although the temporal or causal dynamic of this co-occurrence is unclear. It is also noticeable that 4E-BP1 itself is increased at this time point, meaning that it might overtake the phosphorylation, again repressing translation at later time points. Therefore, the 4E-BP1 phosphorylation was studied further under different paradigms.

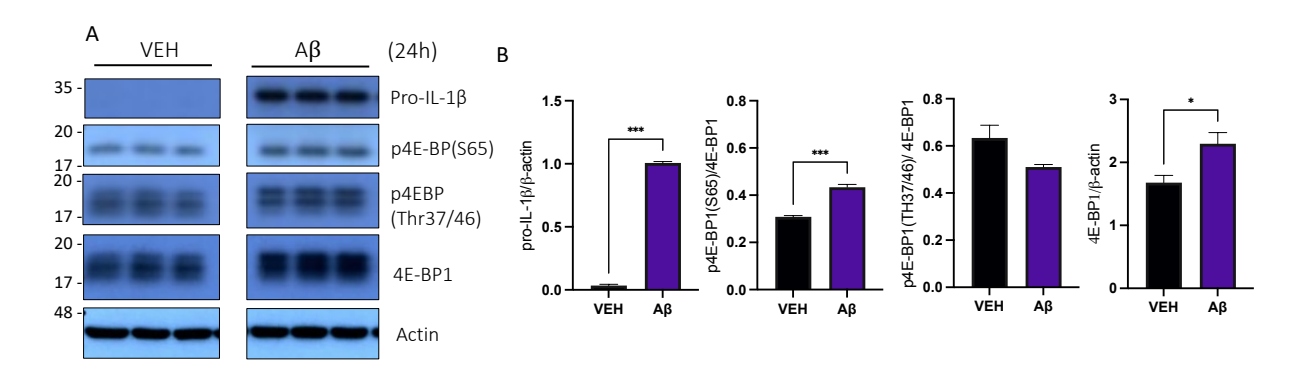


Figure 10. A β aggregates induce 4E-BP1 phosphorylation. A) immunoblot analysis of total and phosphorylation status of the indicated proteins in cell lysates from BV2 microglia treated with Vehicle or A β for 24h. β -Actin was used as loading control. B) Quantification of phosphorylation and total protein level ratio to loading control. Data are presented as means \pm SEM. *p < 0.05, ***p < 0.001 by unpaired t test.

5.1.3. Chronic exposure to $A\beta$ induces tolerance and downregulates 4E-BP1 phosphorylation.

Microglia show immune tolerance when exposed chronically to A β [112]. Although tolerance may be protective in the context of chronic inflammation, during amyloidosis, activated microglial phenotypes are necessary to surround and phagocytize A β , thereby preventing the spread of A β pathology [103]. The activation of the mTOR-HIF-1 α pathway shifts immune cells, including microglia, toward increased aerobic glycolysis and decreased oxidative phosphorylation (OXPHOS) during acute activation [120]. However, an mTOR-dependent metabolic defect has

been observed in A β tolerant microglia in which both glycolysis and OXPHOS were defective and led to functional impairment of microglia. Crucially, besides the mTOR-HIF-1 α pathway, mTOR also exerts an important control of cellular metabolism, independently of HIF-1 α , through the mTOR-4E-BP axis via 4E-BP-regulated translation of mitochondrial transcripts[113]. To better understand the effect of chronic exposure on 4E-BP-dependent translational regulation, I characterized the phosphorylation of 4E-BP1 in microglia chronically treated with A β .

A paradigm in which BV2 microglia were exposed to A β acutely or chronically, and tolerance was reached, was established (modified from Baik et al., 2019)[112]. Microglia were stimulated with vehicle or A β for 6 hours (pre-stimulation). After washing out treatment, cells were rested overnight and then re-stimulated with vehicle, A β or LPS for 6 hours and then subjected to lysis (see schematic in Figure 11A). Protein levels of Pro-IL-1 β , total and phosphorylation levels of 4E-BP1 were examined by western blotting (Figure 11B). A decrease in levels of Pro-IL-1 β in expression in the chronically exposed cells confirmed tolerance. Quantification showed that the 4E-BP1 phosphorylation at Ser65 is significantly increased in the acute lysate, whereas in the chronic exposure, it doesn't differ from baseline (Figure 11C). This indicates that during tolerance, there is an inhibition of eIF4E and therefore, repression of 4E-BP-regulated translation. Raising the question of how the repression in 4E-BP-regulated translation affects microglial physiology and response to AD pathology.

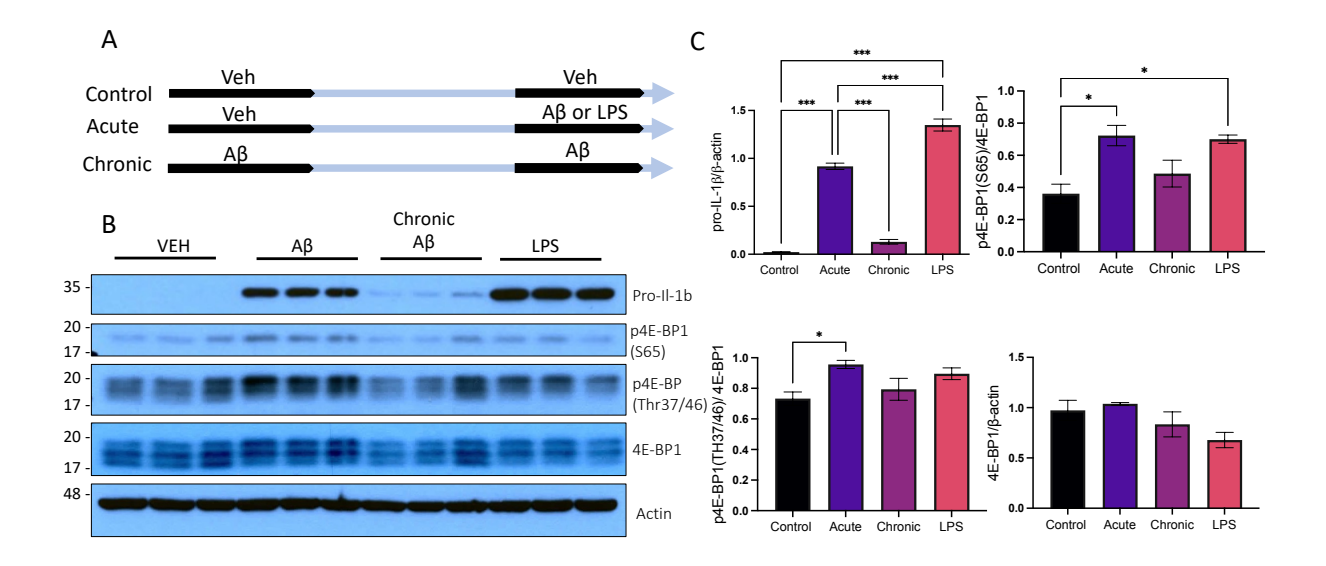


Figure 11. Chronic exposure to A β induces tolerance and decrease in 4E-BP1 phosphorylation. A) Experimental design schematic of acute or chronic treatments. B) Immunoblot analysis of total and phosphorylation status of the indicated proteins in cell lysates from the noted treatment. C) Quantification of phosphorylation and total protein level ratio to loading control. Data are presented as means \pm SEM. *p < 0.05, **p < 0.01, ***p < 0.001 (one-way ANOVA, Tukey's post-hoc test)

5.1.4. SYK inhibition, downstream of TREM2, strongly downregulates 4E-BP1 phosphorylation.

Another AD context in which a defect in mTOR signaling has been reported is in microglia lacking TREM2 or expressing TREM2 risk variants. Genetic studies have shown that TREM2 hypomorphic variants confer a high odds ratio increased risk of developing AD later in life [105]. A seminal paper in the field reported that TREM2 signaling activates the mTOR pathway in microglia during AD pathology, and mTOR signaling is defective in microglia of TREM2-deficient mouse models and AD patients carrying TREM2 risk alleles[111]. The TREM2-dependent mTOR signaling was suggested to maintain metabolic 'fitness' in microglia during AD. However, 4E-BP-dependent translation regulation downstream of the mTOR pathway has not been explored, so I aimed to characterize the phosphorylation of 4E-BP1 in the absence of TREM2 signaling as well.

I tried to establish a TREM2 KO and TREM2KO/DKO cell line. Unfortunately, this cell line was not viable in my hands. Alternatively, transduction of TREM2 signaling can be hindered by inhibiting the Spleen tyrosine kinase (SYK). SYK acts downstream of TREM2, to transduce its intracellular signal; its depletion or inhibition dampens mTOR signaling and microglia's ability to acquire a neuroprotective phenotype in-vitro and in-vivo [116]. Hence, a protocol for inhibiting the TREM2 signal transduction was established using R406 (MedChemExpress), a potent SYK inhibitor. BV2 microglia were exposed to vehicle or Aβ in the presence or absence of R406 and lysed 45 minutes after for biochemical characterization by Western blotting (Figure 12A). This timepoint was chosen due to TREM2 signaling temporal dynamic [107]. Microglia show a baseline SYK phosphorylation, and exposure to Aβ elicits a rapid increase in SYK phosphorylation. Both baseline and Aß induced SYK phosphorylation were significantly decreased in the presence of the SYK inhibitor, validating the use of this inhibitor (Figure 12B). Furthermore, the inhibition of SYK strongly decreases the phosphorylation of 4E-BP1 at both priming sites, Threonine 37/46 and Serine 65. This indicates that during the defect of TREM2/SYK signaling, there is a strong inhibition of eIF4E and, therefore repression of 4E-BP-regulated translation. These results indicate that TREM2 signal strongly modulates the mTOR pathway and 4E-BP1 phosphorylation. Again, raising the question of how repression in 4E-BP-regulated translation affects microglial physiology during the response to AD pathology.

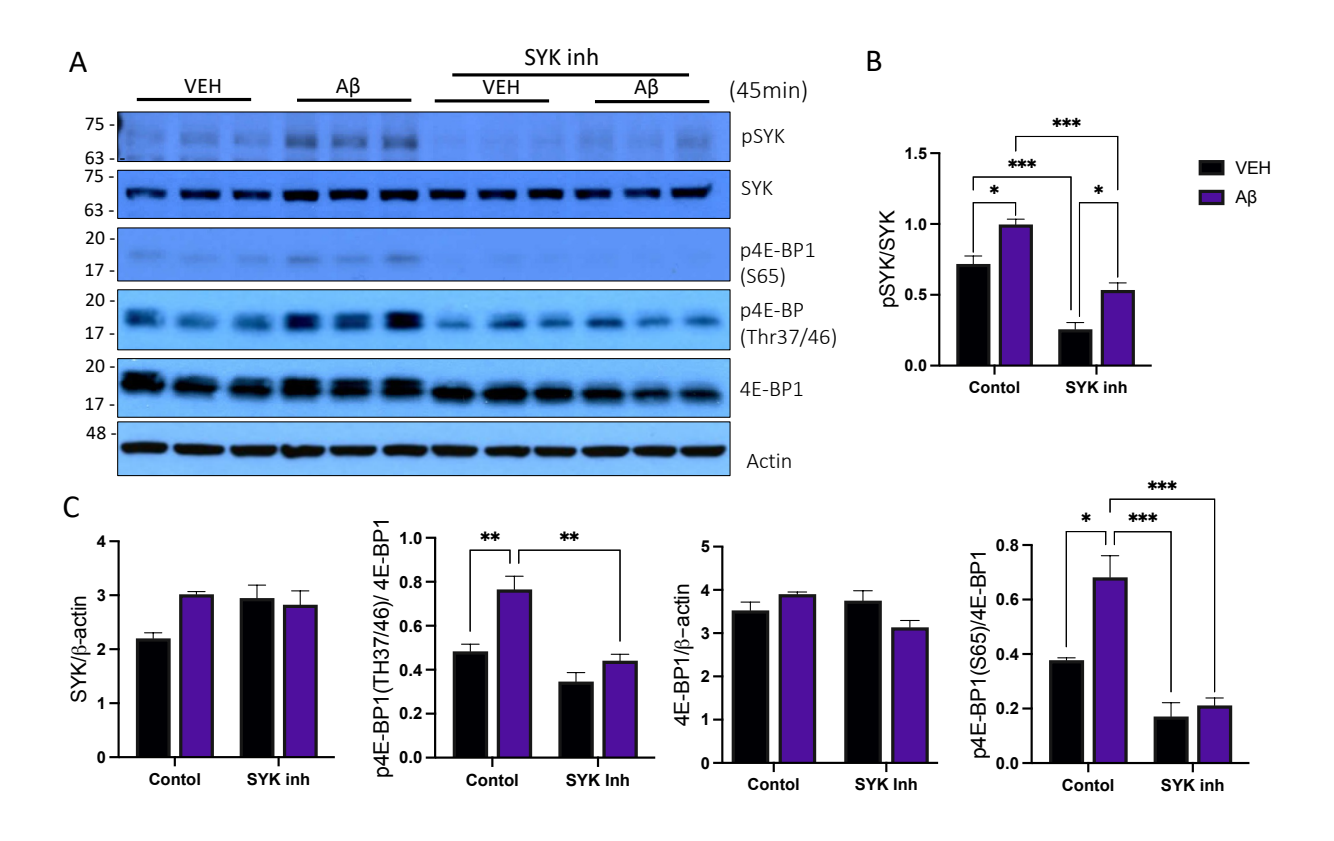


Figure 12. TREM2 signaling inhibition strongly decreases 4E-BP1 phosphorylation. A) Immunoblot analysis of total and phosphorylation status of the indicated proteins in cell lysates 45 minutes after A β exposure with or without SYK inhibition. B) and C) Quantification of phosphorylation and total protein level ratio to loading control. Data are presented as means \pm SEM. *p < 0.05, **p < 0.01, ***p < 0.001 (two-way ANOVA Tukey's post-hoc test)

5.1.5. Aim 1 conclusion.

Microglia are long-lived cells, spanning around 4 years in the adult human brain [121]. During the years or decade of amyloid aggregation that precedes cognitive decline in AD, microglia seem to undergo a switch from a neuroprotective to a maladaptive pro-inflammatory phenotype [114]. This might represent a progressive state of dysfunction induced by chronic activation. Consequently, it is a common neuropathological finding to encounter dystrophic microglia, characterized by fragmented cytoplasmic processes, in the Alzheimer's diseased brain [114]. In addition, a growing number of genetic AD risk studies pinpoint to microglia function [80].

Of note, and having a very strong effect, are TREM2 AD risk variants, which alter the functional state of microglia, particularly during chronic activation [105, 122]. In both cases, either defective TREM2/SYK signaling or chronic exposure to $A\beta$, the mTOR-related metabolism has been proposed as the underlying mechanism involved in maintaining microglia "fitness" [123]. Although the defect of the mTOR-related metabolic impairment has been explored, the role of the 4E-BP-regulated translation, downstream of the mTOR pathway, has not been studied in microglia biology in these AD-related contexts.

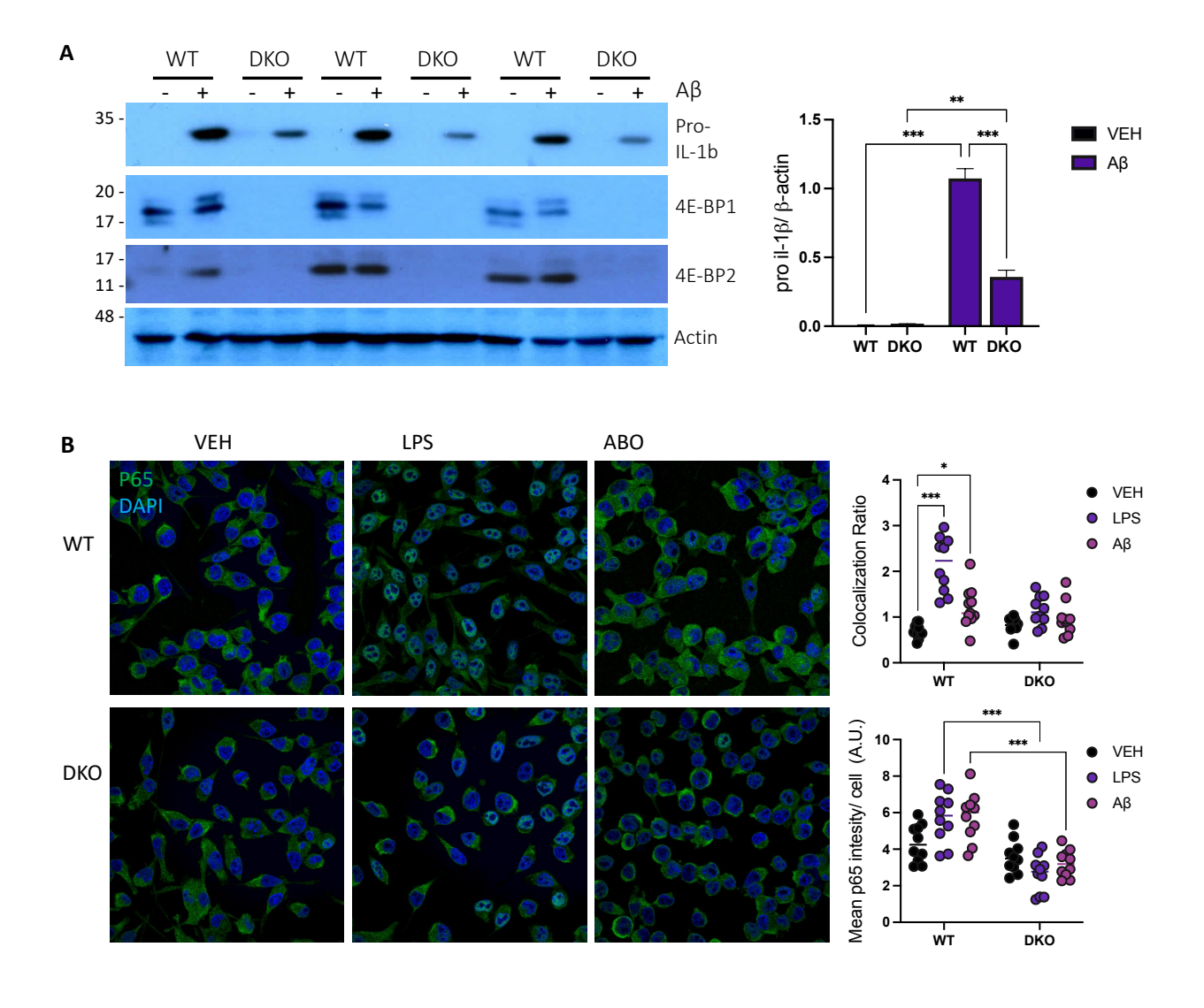
The signaling characterization of 4E-BP1 in these AD-relevant paradigms such as the exposure to Aβ acutely, chronically, and in the absence of TREM2 signaling, showed that 4E-BP1 phosphorylation at Serine 65 happened very early on, at 45 minutes (Figure 12) continues at 6 hours (Figure 11) and stays up to 24h (Figure 10). Yet, this phosphorylation is decreased both during tolerance and in the absence of TREM2 signaling. Given that phosphorylation at Serine 65 happens after the phosphorylation at the priming sites Threonine 37/46 and is necessary for 4E-BP1 release of eIF4E, allowing mRNA translation to initiate, it is possible to conclude that there is a break on 4E-BP-regulated translation in these cases. Furthermore, 4E-BP1 itself is increased at 24h, and this increase could surpass the phosphorylation and lead to translation repression at later time points. Due to cellular detachment and/or cell death, later time points could not be studied by WB. However, these findings furthered my interest, and accordingly, my Aim 2 was to describe the consequences of releasing this break on 4E-BP-regulated translation.

5.2. Aim 2 Characterize the functional implications of de-repressing 4E-BP-regulated translation in microglia responding to $A\beta$.

The mTOR pathway is a complex signaling network that integrates extra and intracellular cues to regulate many crucial cellular processes. mTOR activity positively regulates protein synthesis through the regulation of mRNA translation. In Aim 1, I established that during several AD-related conditions, a decrease in mTOR signaling in microglia results in repression of 4E-BP-regulated mRNA translation. To circumvent this repression, using CRISPR, I established a microglial cell line in which 4E-BP1 and 4E-BP2 were knocked out. Both Isoforms were knocked

out to avoid any possible compensation. The eIF4E is a rate-limiting factor for translation initiation and is carefully kept at constant numbers in the cell; the depletion of 4E-BPs allows eIF4E to be available while maintaining its numbers constant [25]. The 4E-BP depletion results then in the derepression of 4E-BP-regulated mRNA translation, simultaneously providing a single axis downstream manipulation of the mTOR pathway that avoids unintended crosstalk of upstream manipulations.

5.2.1. Deleting 4E-BP1 and 4E-BP2 decreases microglia pro-inflammatory output upon stimuli.



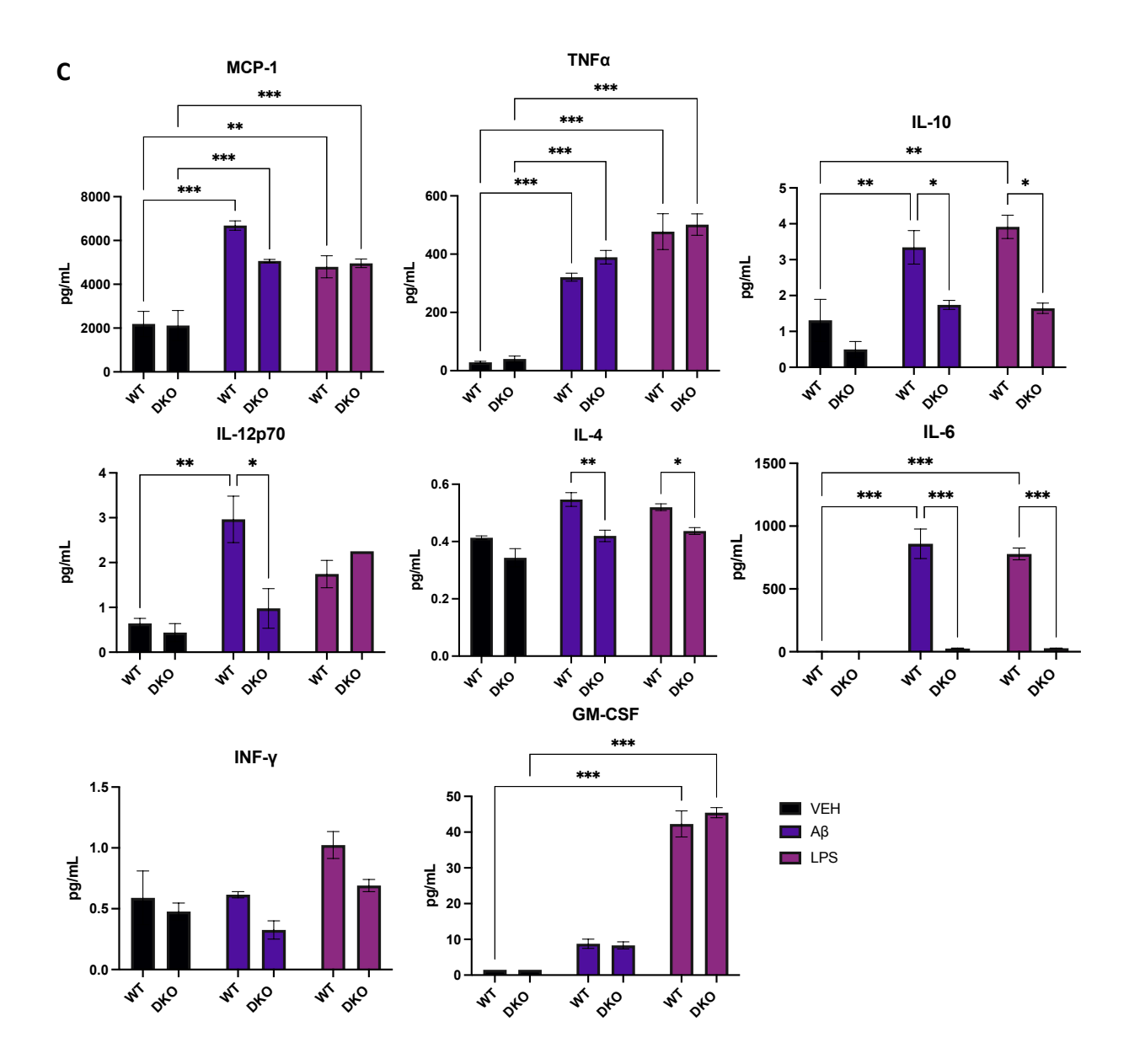


Figure 13. Deletion of 4E-BP1 and 2 in microglia results in a decreased pro-inflammatory phenotype. A) Immunoblot analysis of protein levels of 4E-BP1 and 4E-BP2 levels as KO confirmation and, Pro-Il-1 β protein levels after A β exposure for 24 h. B) Representative confocal microscopy images of p65 cellular localization and quantification of nuclear co-localization after A β (24h) or LPS (6h) stimulation. C) Determination of inflammatory cytokines in supernatant from A β (24h) or LPS (6h) treated microglia. Data are presented as means \pm SEM. *p < 0.05, **p < 0.01, ***p < 0.001 (two-way ANOVA Tukey's post-hoc test).

5.2.2. Deletion of 4E-BP1 and 4E-BP2 in microglia results in an increased mitochondrial respiration capacity and decreased glycolysis induction upon A β exposure.

Metabolic function is fundamentally linked to immune cell function. In immune cells such as macrophages, pro-inflammatory activation is linked to a glycolytic switch, which then also provides metabolites used to secrete antimicrobial compounds [124]. Whereas alternatively activated macrophages involved in inflammatory resolution and wound healing rely mostly on oxidative phosphorylation. However, the mechanisms coordinating microglial metabolism to fuel microglial protective functions in AD, such as phagocytosis, are not fully understood [120]. Previous work from our laboratory showed that mTOR controls mitochondrial activity and biogenesis by selectively promoting the translation of mitochondria-related mRNAs via inhibition of 4EBPs [113]. Furthermore, mTOR-related metabolic defect in TREM2-deficient microglia has been shown to result in a reduced mitochondrial mass [111]. Thus, I aimed to characterize the changes in microglia metabolism in the absence of the 4EBPs. Mitochondrial mass was examined at baseline in WT and DKO microglia using a mitochondrial stain (MitoTracker®) and confocal imaging (Figure 14A). Quantification of the mitochondrial area per cell showed that there is indeed an increase in mitochondrial mass in DKO microglia.

I then aimed to further investigate these cells' energetic metabolism in an AD pathology context. Metabolic reprogramming is crucial for immune cells to regulate their effector response. Accordingly, the metabolic profile of microglia was examined using the Seahorse analyzer after A β or VEH treatment (3 h). Mitochondrial function was assessed by real-time measurement of oxygen consumption rate (OCR), this analysis showed a significant increase of basal respiration in microglia exposed to A β regardless of genotype (Figure 14B). The posterior addition of Oligomycin shows that proton leak is not significantly different, meaning that the difference relies on respiration that is used to drive ATP synthesis, possibly reflecting the increase in energy demand upon exposure to A β in both cell lines.

On the other hand, maximal respiration capacity did show a genotype and treatment-dependent increase in which $A\beta$ and VEH treated cells, the maximal respiration capacity of the

DKO cells was significantly higher compared to WT. Lastly, using Lactate-Glo^m Assay (Promega), lactate secretion was measured as an indicator of glycolysis (Figure 14C). This assay showed that DKO microglia have a reduced reliance on glycolytic metabolism at baseline and reduced glycolytic switch in the presence of A β that starts at 1h and continues at 24h.

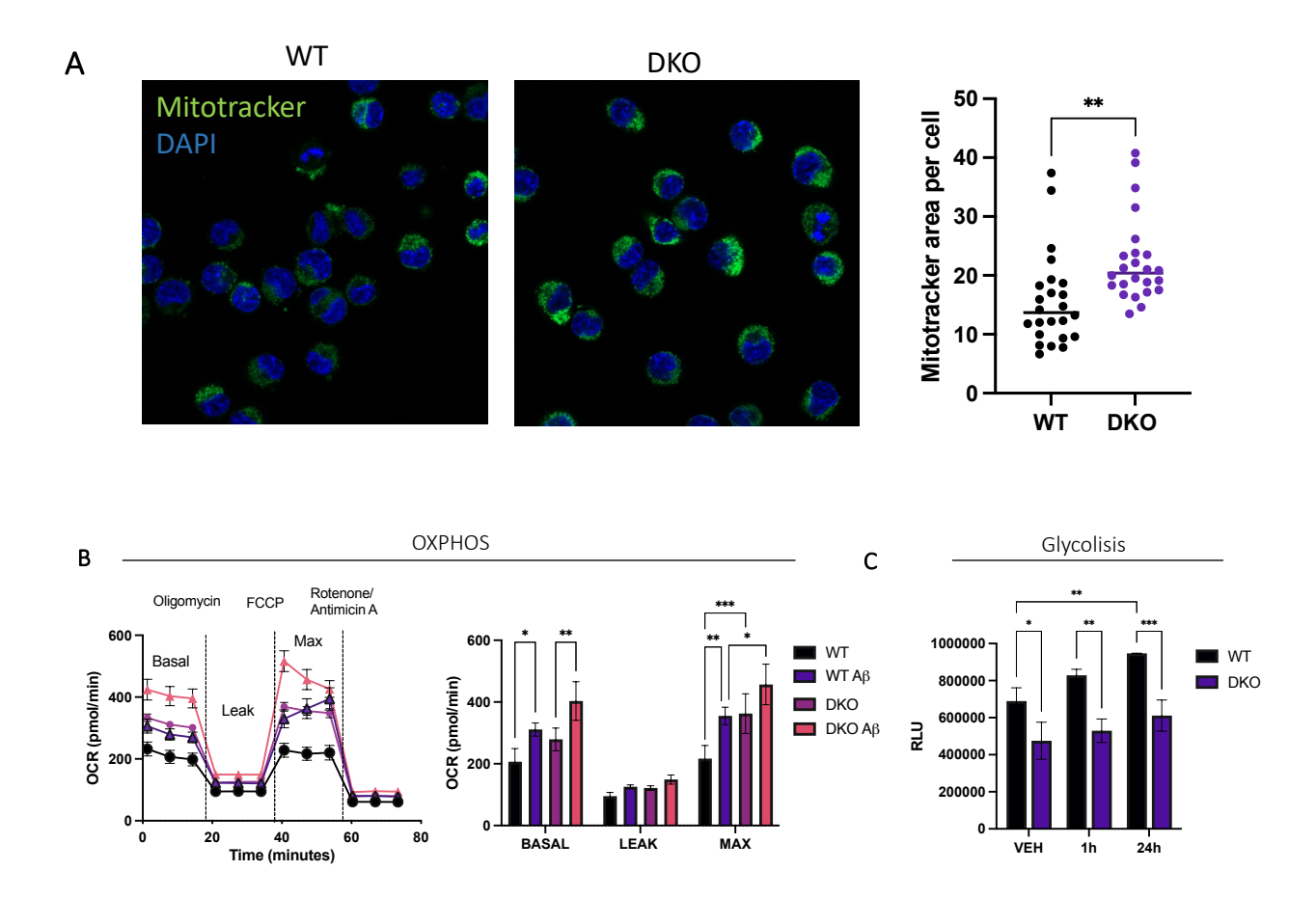


Figure 14. Depletion of the 4E-BPs changes the metabolic profile in microglia. A) Representative confocal images of microglia mitochondria labeled with mitotracker and quantification of green fluorescence area. B) Real-time measurement of oxidative oxygen phosphorylation measured by consumption rate (OCR) upon the indicated treatments. C) Glycolysis level determined by lactate secretion at 1 and 24h after A β or VEH. Data are presented as means \pm SEM. *p < 0.05, **p < 0.01, ***p < 0.001 (two-way ANOVA, Tukey's post-hoc test)

Considering the glycolytic switch associated with pro-inflammatory phenotypes in immune cells, the metabolic function characterization couples my previous findings of reduction

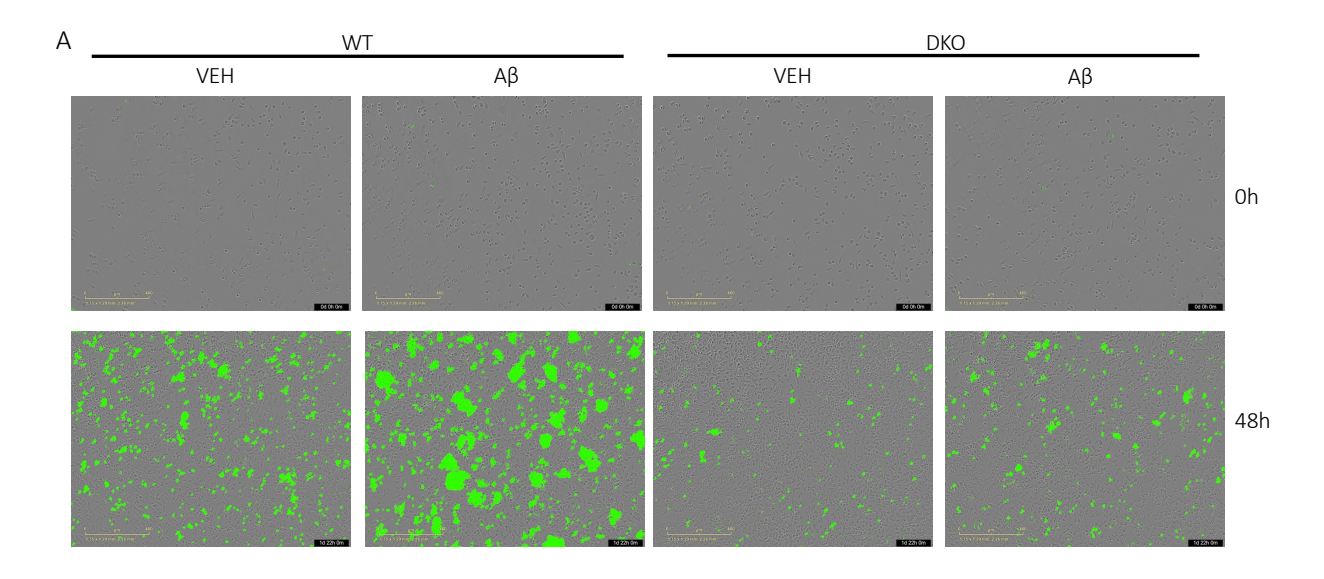
in the pro-inflammatory phenotype observed in DKO microglia with a decreased glycolytic induction upon $A\beta$ exposure. This finding prompted me to wonder if there were any changes in microglia viability.

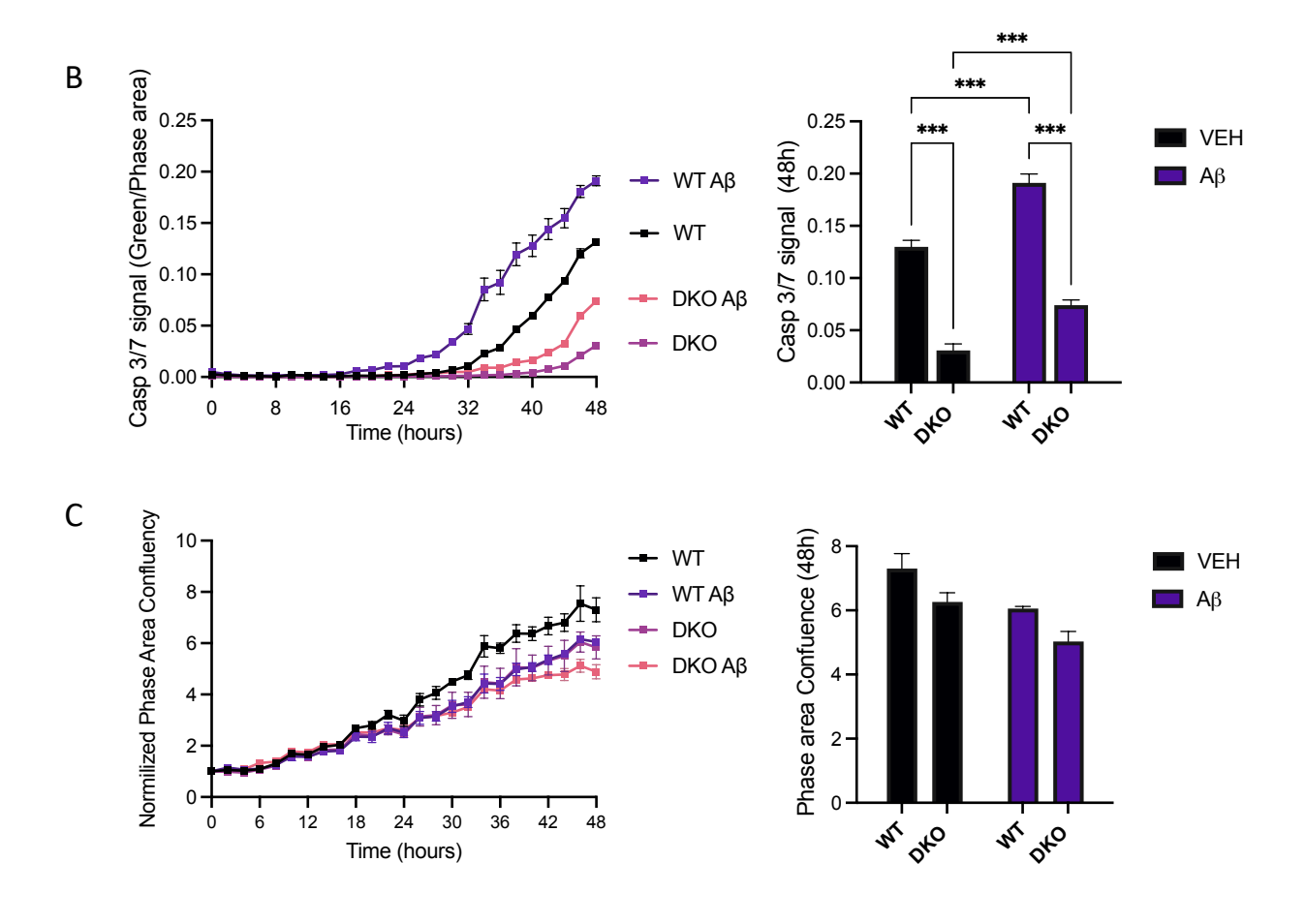
5.2.3. Depletion of 4E-BP1 and 4E-BP2 mitigates microglia apoptosis related to A β phagocytosis.

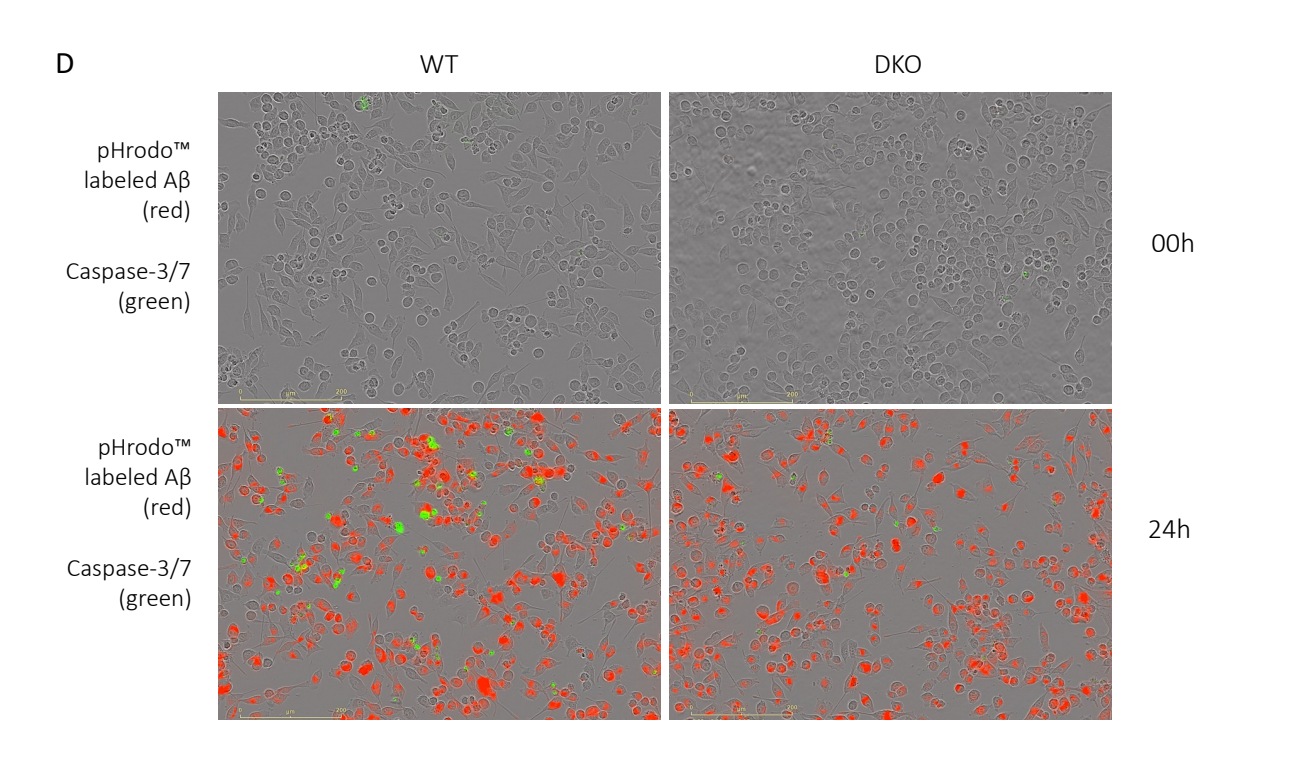
Previous reports have shown that microglia activate caspase-3 in response to AD pathology. In TREM2 deficient 5XFAD mice, microglia have increased cleaved caspase 3 when associated to A β plaques compared with TREM2 proficient 5XFAD mice [111]. Cleaved caspase-3 is as well increased in human-derived microglia from patients carrying AD risk TREM2 mutations compared to control [125]. Furthermore, in post-mortem AD brain, cleaved caspase-3, is mostly co-localized with CD68-labelled microglia [126]. Thus, I aimed to examine caspase-3 activation in WT and DKO microglia exposed to Aβ. Live cells were imaged for 48h using the Incucyte[®] Live-Cell Analysis System in the presence of CellEvent™ Caspase-3/7 (green, Invitrogen) detection reagent. This assay indicated that depletion of the 4E-BPs in microglia mitigates the induction of caspase-3/7 activation (Figure 15A). Caspase 3/7 activity is induced in WT microglia at a significant higher rate than in DKO microglia both in the presence and absence of Aβ aggregates (Figure 15B). The rate of caspase activity increases after 24 hours even in the absence of Aβ aggregates, as media is not changed during live imaging, it is possible that cells start running out of factors. Interestingly, although caspase-3/7 activity is increased the confluency of the cells was not similarly affected (Figure 15C). Although some non-apoptotic roles of caspase 3 have been suggested in microglia, the morphology observed suggests that those cells showing caspase activity have detached, shrunk, and clumped, more consistent with apoptosis. However, cells in the well continued to proliferate.

Given the low reactiveness of DKO microglia to the presence of $A\beta$ aggregates, I wondered if the DKOs were phagocytizing $A\beta$. To this end, $A\beta$ aggregates were labeled with a pHrodoTM dye (Invitrogen), this dye has no fluorescent signal at neutral pH and fluoresces bright red in acidic environments such as the lysosome. I co-incubated the pHrodoTM $A\beta$ (red) with

CellEventTM Caspase-3/7 (green) to examine if $A\beta$ phagocytosis colocalized in cells with caspase activation (Figure 15D). Indeed, both WT and DKO microglia phagocytize $A\beta$, yet the colocalization with caspase activity was significantly higher in the WT compared to the DKO microglia (Figure 15E and F). It is noticeable that WT phagocytic cells adopted a more enlarged morphology, yet it is unclear if this is related to $A\beta$ phagocytosis, lysosomal function or dysfunction related to the increased apoptosis observed in these cells.







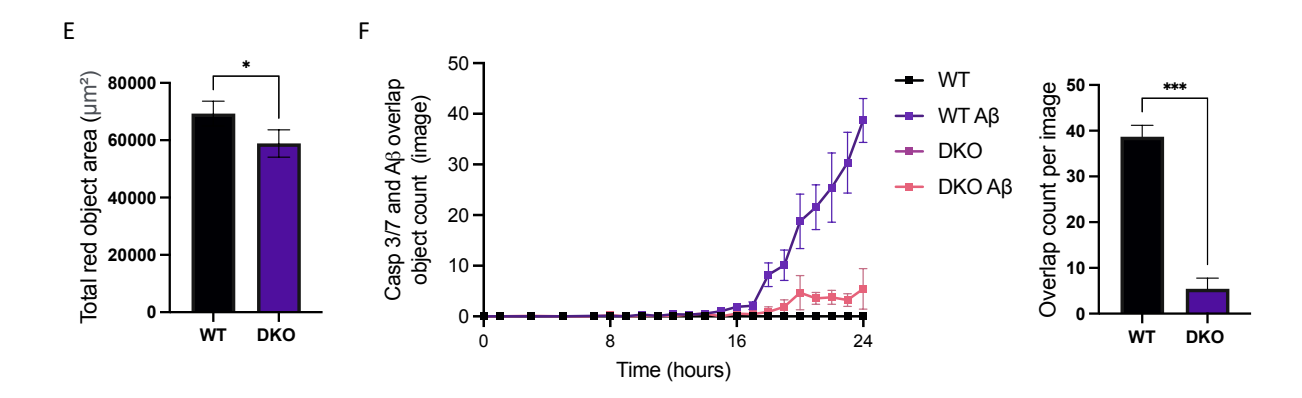


Figure 15. Depletion of 4E-BPs mitigates microglia apoptosis related to A β . A) Representative IncuCyte micrographs of microglia co-incubated with the indicated treatments and Casp3/7 cell event (green) at 0 and 48h. B) Measurement of Casp3/7 green fluorescence over phase area for 48h and quantification at 48h. C) Measurement of confluence for 48h and quantification at 48h. D) Representative images obtained at the IncuCyte of microglia co-incubated with the indicated treatments. E) Quantification of total red fluorescence area per image. F) Kinetics of overlap of Casp3/7 (green) and labeled A β (red) and quantification of co-stained cells at 24h.

5.2.4. Assessment of functional consequences of 4E-BP depletion in microglial response to $A\beta$ *in-vivo*.

The *in-vitro* results showed that 4E-BP depletion leads to a decrease in apoptotic markers as well as decreased expression of pro-inflammatory mediators. This was accompanied by a decrease in the inflammatory glycolytic switch while mitochondrial respiration is increased both at baseline and during exposure to AD pathology. Hence, I aimed to investigate the functional consequences of 4E-BP depletion in microglial response to A β *in-vivo*.

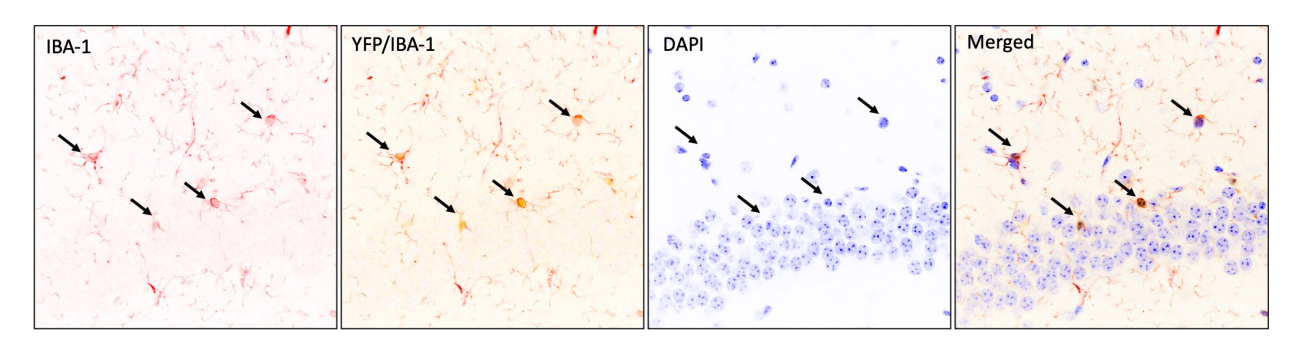
There is a transient cognitive impairment observed *in-vivo* after intracerebroventricular infusion of soluble A β [127]. This cognitive impairment is thought to result from the direct effect of soluble A β on synaptic plasticity and is indirectly prolonged through the secondary immune response [127-129]. Thus, I aimed to use the A β intracerebroventricular (ICV) infusion paradigm on inducible microglia-specific 4E-BPs DKO and WT mice (Cx3cr1^{CreER/+};4E-BP1^{f/f}/4E-BP2^{f/f} or

Cx3cr1^{CreER/+}, respectively) to examine the impact of targeting microglial translation control on $A\beta$ induced memory impairment and inflammation.

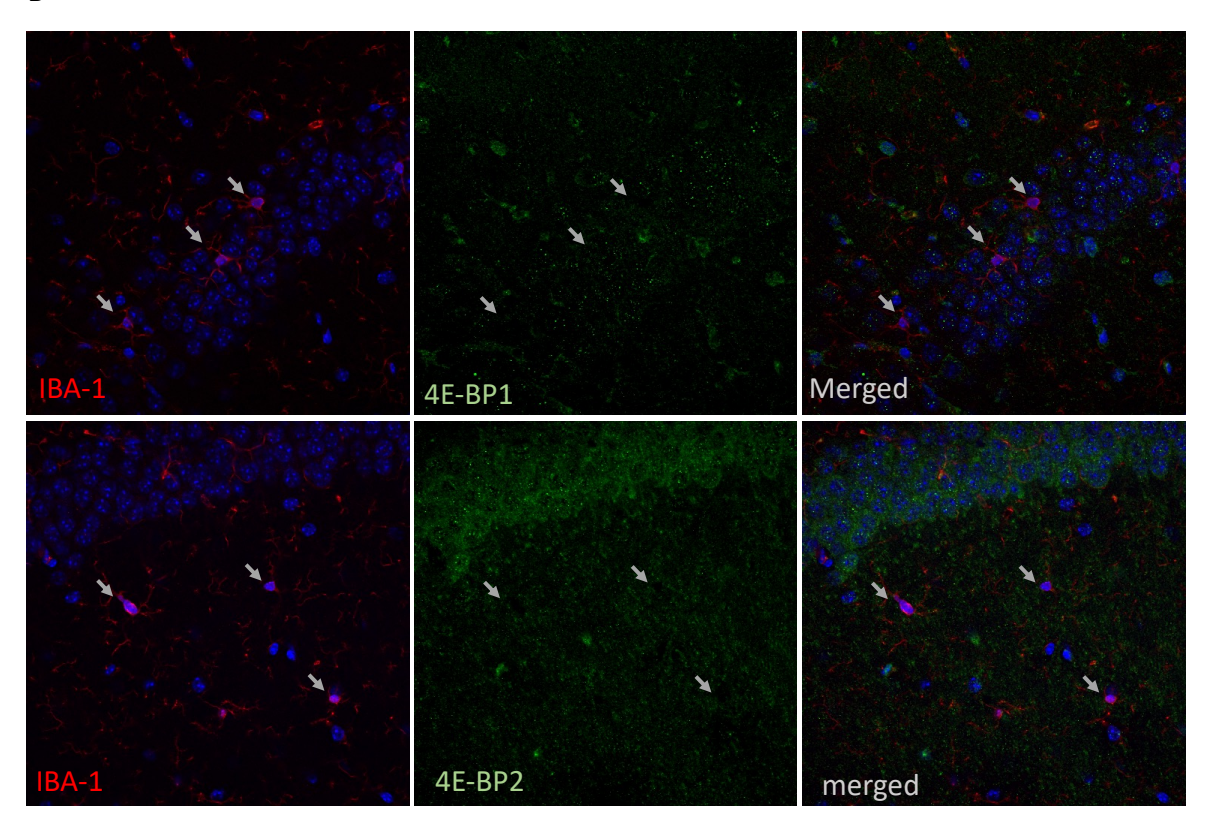
The efficiency and specificity of the Cx3cr1^{CreER/+} mouse line were examined. Yellow fluorescence protein (YFP) expression, as a marker of CRE Recombinase expression in microglia, and the tamoxifen-inducible deletion of the floxed 4E-BP1 and 4E-BP2 were confirmed (Figure 16A and B). The stereotaxic Aβ ICV infusion paradigm was optimized and western blotting examination of ipsilateral and contralateral hemibrains was performed (Figure 16C). This analysis showed an acute inflammatory response observed by pro-IL-1β induction ipsilaterally at 24 hours post-infusion, while also showing a bilateral increase in p-SYK and SYK, indicating TREM2 signaling engagement. Microglia activation was detected by Ionized calcium binding adaptor molecule 1 (IBA-1) expression. IBA-1 expression increased ipsilaterally at 24h, and then continued to be increased bilaterally at 7 days. Given the decrease in SYK phosphorylation by day 7, this timepoint would then represent a state in which microglia are activated in the absence of TREM2 signaling. As per my *in-vitro* results in AIM1, in the absence of TREM2-dependent mTOR activation, 4E-BPs are active and therefore repressing translation, providing a window to examine the effect of the depletion 4E-BPs in activated microglia *in-vivo*.

After the model confirmation and optimization of the ICV paradigm, a battery of cognitive tests such as Novel Object Recognition (NOR), Novel Object Location (NOL) and Contextual Fear Conditioning (CFC) was set to be performed seven days after ICV of A β or VEH infusion to examine changes in A β induced cognitive impairment contingent to changes in microglia (see experimental design schematic, **Figure 16**D)[130, 131]. Unfortunately, after extensive breeding, the number of animals needed to perform the behavior in the different genotypes and treatments (n>6/group, VEH vs AB) was not met. In addition, the animals meant to act as control did not learn the behaviors, possibly due to the short recovery after stereotaxic A β or VEH ICV infusion. However, A β induced cognitive impairment is transient and a longer recovery period was not possible. Therefore, it was not possible to carry out this cognitive assessment in the time range for my PhD studies.





В



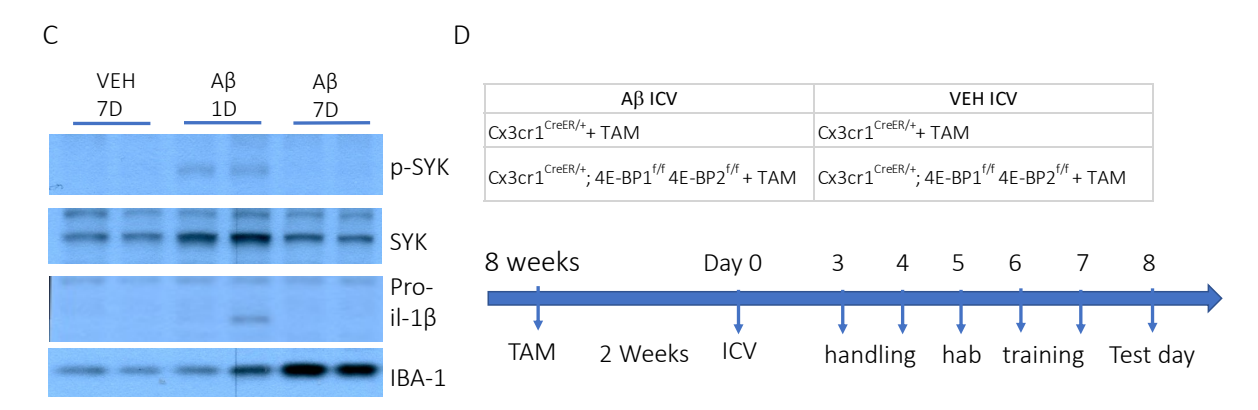


Figure 16. In-vivo model optimization. A) Representative confocal microscopy images of Cx3cr1^{CreER/+} mouse expressing YFP as a marker of CRE recombinase expression in microglia. B) Representative confocal microscopy images of DKO microglia in Cx3cr1^{CreER/+}; 4E-BP1^{f/f}/4E-BP2^{f/f} mice 2 weeks after tamoxifen induction. C) Immunoblot analysis of indicated proteins in ipsilateral and contralateral hippocampi of WT mice after ICV infusion. D) Treatment groups and schematic of experimental design.

5.2.5. Aim 2 conclusions.

The results from this aim make it clear that the beneficial cell-autonomous effects of the mTOR pathway exerted in microglia physiology rely to an important extent on the fine-tuning of 4E-BP-regulated translation. Ablation of mRNA translation repressors, the 4E-BPs, results in a decreased pro-inflammatory shift upon stimulus, increased mitochondrial respiration reducing the pro-inflammatory glycolytic switch resulting in the mitigation of microglia cell death in the presence of stressors such $A\beta$.

The ability of microglia to finely tune their physiology, including 4E-BP-dependent translation, is contingent on coupling temporal extracellular signals to major downstream signaling networks. It is not surprising then that many of the AD LOAD risk genes are enriched in microglia receptors and their signal transducers. Although there are efforts to target these receptors therapeutically, the intracellular pathways and effector mechanisms that dictate microglia responses in health or neurodegeneration are not fully understood. Furthermore, in the context of the study of microglia, the field has relied on transcriptomic profiling, yet the transcriptome is not representative of protein abundance in many cells[9]. Therefore, my Aim 3 is to identify microglia translatome (the genome-wide pool of actively translating mRNA transcripts in a cell) *in vivo*, which is a more accurate proxy of protein abundance and direct corroboration of translation control [9].

5.1. **Aim 3.** Identify the response mediators controlled by the mTOR-4E-BP axis that allows microglia to retain their cellular viability during their response to Aβ.

Translational control is a critical layer of gene expression regulation and is not reflected in transcriptomic profiling. Microglia in all contexts are and continue to be studied mainly through transcriptomic profiling, yet there is a gap in our understanding of the concomitant translation regulation to the transcriptional output of these cells. Taking advantage of the previously established A β ICV infusion paradigm, I aimed to identify the microglia-specific translatome enriched in the absence of the translation repressors, the 4E-BPs, *in vivo*.

5.1.1. Translatome enrichment *in-vivo*

The molecular mechanisms and cellular pathways underlying microglial response to $A\beta$ remain to be fully elucidated [132]. In this regard, microglia biology investigation has been challenging. Microglia functional states have conventionally been characterized by their mRNA signature. However, microglia are resident macrophages embedded in the brain parenchyma, and isolating them from tissue for cell-type specific transcriptional profiling induces significant artifact [133]. Furthermore, as mentioned, there is a poor correlation between mRNA and protein abundance in many cells [7].

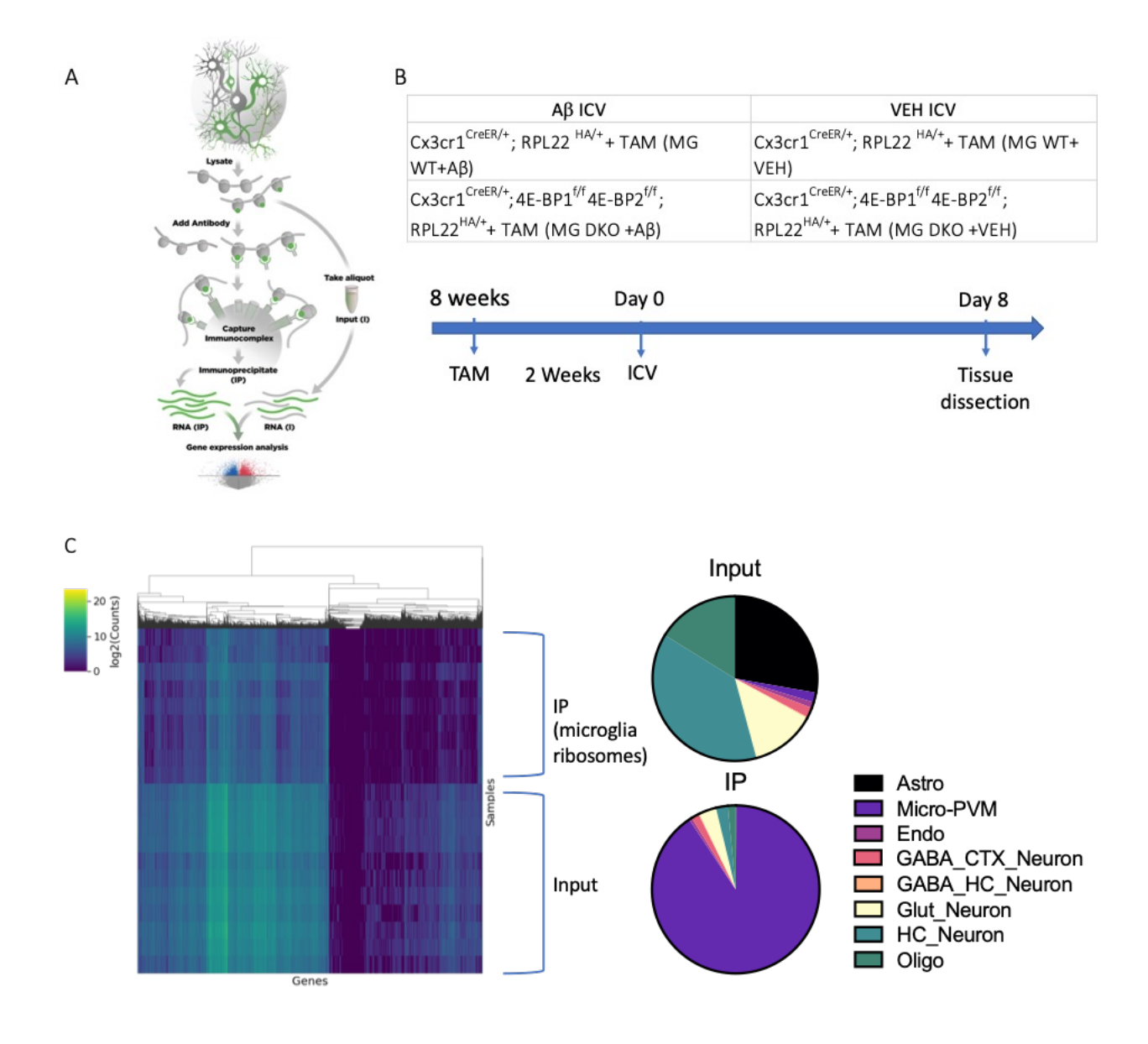
For this project, an inducible mouse model, developed to tag ribosomes 'Ribo-Tag' (RPL22^{HA/+}) for analysis of cell-type specific mRNA expression *in vivo*, was crossed with our microglia-specific mouse models [134]. The Ribo-Tag mouse model allows the immunoprecipitation of ribosome-bound mRNA transcripts upon cell-type-specific Cre recombinase, comprising the translatome (genome-wide pool of actively translating mRNA transcripts in a cell). Using this mouse model, the microglial translatome can be directly immunoprecipitated from the tissue without the need for cell-type specific isolation (see immunoprecipitation schematic (Figure 17A). It was, therefore, opportune to examine the translatome changes in our inducible microglia-specific 4E-BP WT or 4E-BP DKO (see crossings, figure 17B)

In order to identify the translatome of activated microglia responding to AD pathology \it{In} \it{vivo} , an ICV infusion of soluble A β or VEH was performed in these different mouse crossings, and the tissue was harvested at seven days post-infusion. As per the paradigm established in AIM2, at this time point after infusion, there is continued microglia activation after the decrease in TREM2 signaling and consequently, TREM2 dependent mTOR activation (Figure 16C).

The A β or VEH ICV infusions were performed as mice were available, and seven days post-surgery, hippocampal tissue was dissected and flash frozen (n=4 to 7/group). After all the tissue was harvested, frozen samples were simultaneously dissociated for RNA extraction. During RNA extraction, before immunoprecipitation (IP) of the tagged ribosomes, an initial aliquot (Input) was obtained to sample mRNAs in the tissue (all cell types), the transcriptome. Input and IP, transcriptome and microglia translatome, respectively, were obtained, sequenced and analyzed. CellAnneal, a cell-type deconvolution software, was used to confirm microglia transcript enrichment. This analysis showed that IP was effective at enriching cell-type specific transcripts, representing the microglia translatome (Figure 17C).

Possibly due to microglia cell death or proliferation in the A β infused groups, there was poor microglia enrichment in those samples, and were excluded from the analysis. However, an analysis of the translatome was performed comparing MG^{WT}+VEH and MG^{DKO}+VEH. Differentially expressed genes (DEG) were identified (p[adj]<0.05) (Figure 17D). Functional enrichment analysis was performed on both upregulated and downregulated DEG. In line with my *in vitro* findings in which WT microglia show higher reactiveness than DKO microglia, the translatome from the MG^{DKO} mice shows a downregulated expression of several mediators associated with microglial activation compared to the MG^{WT} translatome. These include several genes encoding for several apolipoproteins including apolipoprotein E (*Apoe*). Other genes associated with inflammation such as toll-like receptor 2 (Tlr2) and CC-chemokine ligand 3 (*Ccl3*) were downregulated in the DKO microglia translatome. Using the STRING database, association networks were predicted in downregulated DEGs in MG^{DKO} (Figure 17E). Apoe appears as a central node in this highly associated network. Functional enrichment showed that the depletion of 4E-BP in microglia *in vivo* led to the downregulation of several biological functions related to apolipoprotein production and regulation, as well as other inflammatory associated functions such as Il-1 β regulation and

positive regulation of immune response, consistent with a decreased pro-inflammatory phenotype on the DKO microglia, even in the absence of A β stimulation (Figure 17F). Interestingly, no significant functional enrichment was detected in the upregulated DEGs in MG^{DKO}.



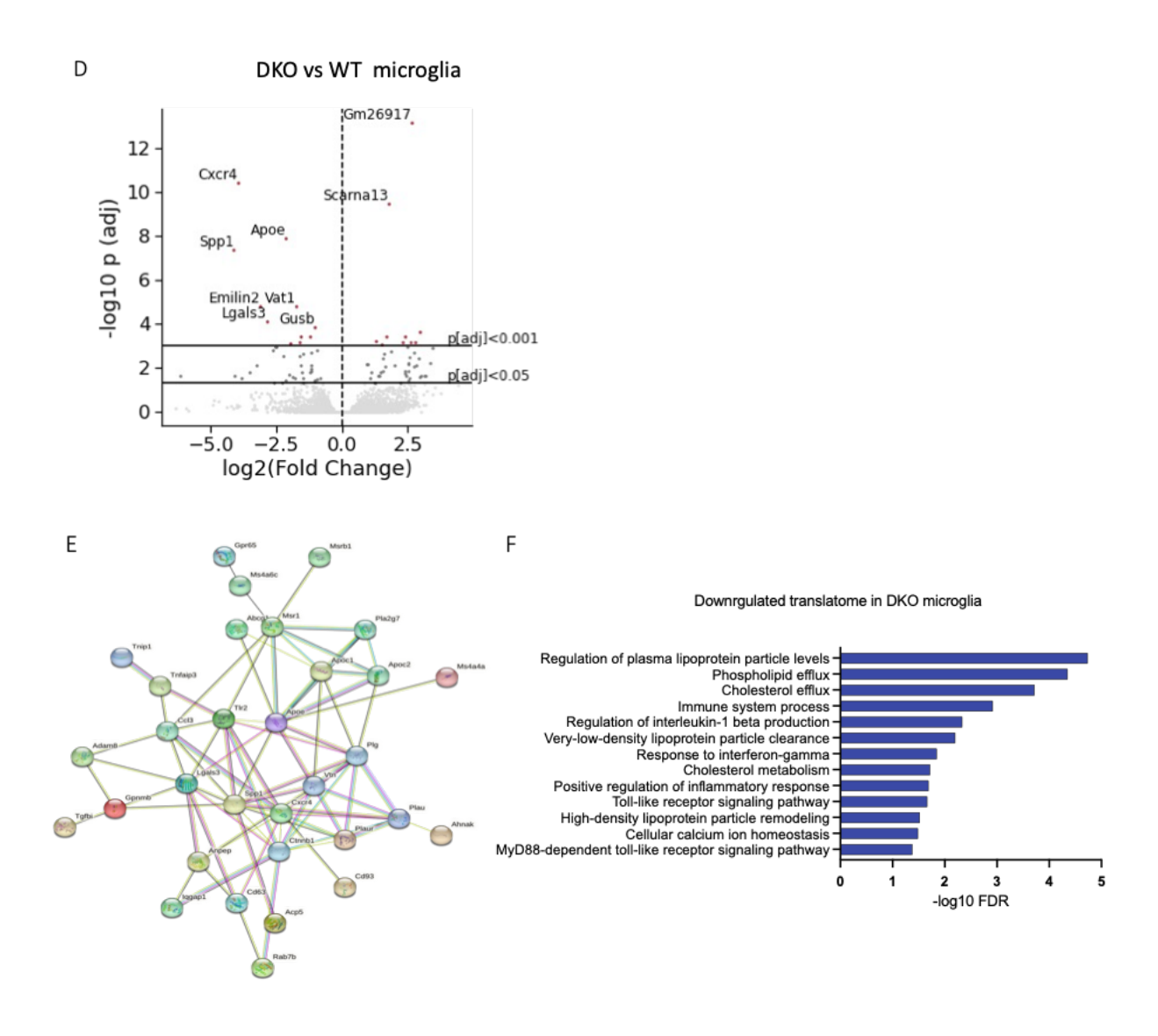
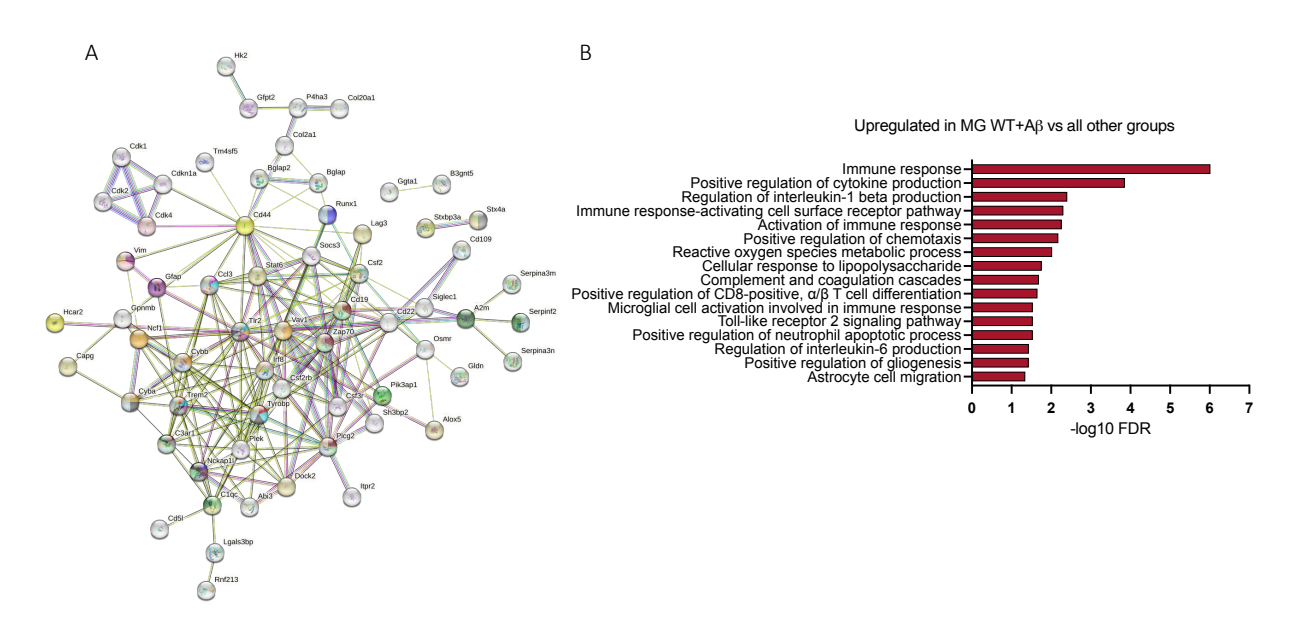


Figure 17. Translatome enrichment in vivo. A) schematic of Ribo-tag cell-type specific immunoprecipitation (IP) and input. B) treatment groups and schematic of experimental design. C) Heatmap of differentially expressed genes of IP versus Input (all samples included) and cell type enrichment pie chart. D) String database association networks from upregulated DEG in MG^{WT} vs MG^{DKO} translatome. E) Functional enrichment of downregulates MG^{DKO} translatome.

5.1.2. Microglia-specific depletion of the 4E-BPs leads to changes in the tissue transcriptomic response to $A\beta$.

The input or transcriptome, RNA from all the cells in A β or VEH-infused brain, was analyzed as well. The MG^{WT}+A β group was compared against all other groups. The DEGs were identified using a nominal p-value <0.05. Using the STRING database, association networks were predicted in upregulated DEGs (Figure 18A). Functional enrichment analysis was also performed on this gene set (Figure 18B). In line with the *in-vitro* results and the translatome enrichment, MG^{WT}+A β tissue transcriptome compared to the rest of the groups exhibits an upregulated gene set enriched in inflammatory responses, including the positive regulation of cytokine production and chemotaxis, complement and coagulation cascade, astrocyte activation and TREM2. Interestingly, positive regulation of gliogenesis was also upregulated in the WT +A β , indicating either microglial cell death, proliferation, or both.

A smaller set of DEGs were downregulated, association networks were predicted in this gene set as well as functional enrichment analysis was performed (Figure 18C and D, respectively). Interestingly the association network shows the central downregulated association node to be Fos Proto-Oncogene (Fos), regarded as a mediator of synaptic plasticity. Furthermore, genes associated with G protein-coupled receptor (Gpcr), calcium regulation, distal axon, and terminal buttons were also downregulated, indicative of synaptic plasticity loss or dysfunction.



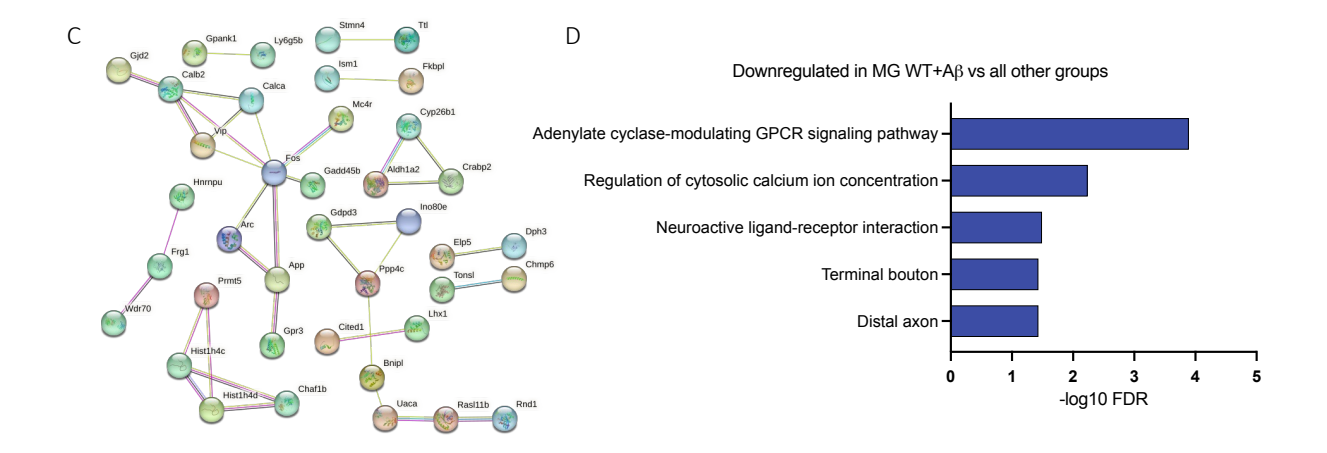


Figure 18. Microglia depletion of the 4E-BPs leads to changes in the tissue transcriptomic output in response to A β . A) STRING database association networks from upregulated DEG in MG^{WT} vs MG^{DKO} transcriptome. B) Functional enrichment of upregulated DEGs in MG^{WT} vs MG^{DKO} transcriptome. C) STRING database association networks from downregulated DEG in MG^{WT} vs MG^{DKO} transcriptome. D) Functional enrichment of downregulated DEGs in MG^{WT} vs MG^{DKO} transcriptome.

6. Discussion

Many AD risk genes are enriched in microglia, and as such, microglia manipulation in experimental settings has been extensive aiming to elucidate how AD risk genes alter disease pathology. However, less is known about the alterations in the cell-autonomous and intracellular mechanisms that coordinate neuroprotective or detrimental functions in microglia. Overall, this thesis uncovers mechanisms by which the mTOR pathway modulates key aspects of microglia biology and how the mTOR pathway links AD risk variants and AD pathology to the intracellular biology of microglia.

Control at the mRNA translational level of gene expression shapes the cell proteome in without the need of *de novo* mRNA synthesis. In immune cells, like microglia, translational control has a profound effect by adjusting the immune response through changes of translation of select mRNAs [8, 135]. Furthermore, translational control is a mechanism linking energetic metabolism to function in immune cells [8]. Published work from our laboratory has shown a feed-forward mechanism by which mTOR controlled 4E-BP-dependent translation regulation boosts mitochondrial biogenesis to maintain cellular energy homeostasis [113]. Considering the reports in which mTOR signaling is defective in microglia in AD contexts [111, 112], I thus hypothesized that in AD pathogenesis, 4E-BP-controlled mRNA translation is repressed in microglia, rendering these cells metabolically exhausted, immunologically deficient, and ultimately apoptotic. Therefore, restoring translation control in microglia should restore microglial functional phenotypes to halt AD pathology.

In Aim1, I initially went to characterize the phosphorylation of 4E-BP1 in response to A β . To be able to assess this cell-autonomous signaling, I used a monoculture of microglia. This characterization showed that 4E-BP1 is phosphorylated at Serine 65 in the presence of A β (Figure 1). This phosphorylation is decreased in microglia repeatedly or chronically exposed to A β (Figure 2), and in the absence of TREM2/SYK intracellular signaling (figure 3), indicating that there is a repression of 4E-BP-controlled mRNA translation in these cases. Furthermore, during the prolonged exposure (24h), 4E-BP1 full protein expression is significantly increased, indicating that the initial phosphorylation is probably overtaken by the increase of the total protein levels leading

to the repression of 4E-BP-controlled mRNA translation. This is consistent with previous reports in which there is an increase of 4e-bp1 expression in microglia after an inflammatory challenge in mice[27]. Overall, this characterization showed decreased mTOR signaling, decreasing 4E-BP1 phosphorylation at Serine 65 in these AD-relevant contexts. This is consistent with the literature examining the mTOR pathway in microglia and extends this finding to the mTOR-4E-BP1 axis [111, 112]. Interestingly, the effect of SYK signaling inhibition has a very strong and rapid on 4E-BP1 phosphorylation, more than chronic exposure. Two recent reports examining the role of SYK in coordinating microglia neuroprotective functions described a convergence into the mTOR pathway, however, they did not focus on 4E-BP [136, 137]. In summary, there is a repression of 4E-BP-controlled mRNA translation during chronic exposure or the absence of TREM2/SYK signaling.

With the Aim1 results in mind, I next continued to study the effect of the depletion of 4E-BPs in Aim 2. Both isoforms were depleted to avoid any kind of compensation. This downstream manipulation of the mTOR pathway avoids unintended upstream crosstalk. However, this manipulation imitates a constitutive activation of mTOR at this level, which then may have feed-forward effects on the pathway. It is worth mentioning that there are conflicting reports regarding the effect of the inhibition of the mTOR pathway and immune cells or neurodegeneration, including AD. These contradictory results are partly because there are different manipulation of this very intricate pathway and the use of Rapamycin, which potently suppresses S6K phosphorylation while having only a marginal effect on 4E-BP phosphorylation [138, 139]. As of May 2023, there is one clinical trial using Rapamycin to inhibit the mTOR pathway as a therapeutic for Alzheimer's disease. However, the pre-clinical data is mixed regarding rapamycin's beneficial or detrimental effects on AD-like pathology [119]. Considering that mTOR pathway machinery is present in all cell types in the brain, with heterogeneous activation states, dissecting the effect of the mTOR-4E-BP1 axis needs to be performed in a cell type in a context-specific manner.

In Aim 2, the depletion of 4E-BP1 and 2 *in vitro* (DKO microglia) showed an overall beneficial effect in a cell-autonomous manner. Initially, upon A β exposure, DKO cells showed a decrease in expression of IL-1 β , a major proinflammatory cytokine in the brain believed to play a key role in the progress of AD [140]. This decrease in IL-1 β prompted me to examine the NF κ B nuclear translocation and cytokine secretion upon A β or a classic LPS stimulus in culture. In DKO cells, compared to WT, NF κ B translocation into the nuclei and several cytokines were decreased, including the complete reduction of IL-6. However, some other cytokines were not affected, including TNF α , which indicated that either different pathways were active to secrete TNF α or the time point examined didn't capture any differences. Overall, deleting the 4E-BPs, simulating the activation of the mTOR-4E-BP axis, leads to reduced pro-inflammatory output in microglia.

Considering the literature regarding the mTOR pathway in microglia, in which the reduction in mTOR signaling generates a metabolic defect and that 4E-BP-dependent mRNA translation boosts mitochondrial biogenesis, I next went to examine the cell's metabolic profile [111, 112]. Initially, consistent with previous reports from our group, DKO cells showed an increase in mitochondrial mass compared to WT. This increase in mitochondrial mass translated into an increased reliance of the DKO cells on OXPHOS and a decreased switch to glycolytic metabolism upon A β exposure. Although it is hard to establish which came up first, the decrease of pro-inflammatory phenotype or a change in metabolic profile, these processes in immune cells are so intertwined that they will change in response to each other. Immune cells' inflammatory response requires metabolic reprogramming from oxidative phosphorylation to glycolysis, also known as the Warburg effect. However, a detrimental hyperglycolysis has been observed in microglia in the aging brain and is associated with defective Aβ related chemotaxis, phagocytosis, and increased secretion of pro-inflammatory cytokines [141, 142]. In contrast, a report found that myeloid cells shut down major metabolic pathways during aging [143]. Interestingly, restoring metabolism in these cells is sufficient to alleviate age-related cognitive decline in mice. Therefore, the results discussed in this thesis may suggest that microglia's ability to activate the mTOR-4E-BP axis, and thereby re-activate or sustain OXPHOS-dependent metabolism represents an important vulnerability and opportunity, both in aging and AD.

Since microglia become dysfunctional, dystrophic, and apoptotic during AD, I also examined microglia cell death during exposure to A β . The DKO cells exhibited a significant reduction in apoptosis, as observed by caspase activity after 48 hours in the presence of A β (Figure 6). Considering the decrease in pro-inflammatory mediators, continued reliance on OXPHOS, and reduced apoptosis in the presence of A β , I wondered if the DKO cells were effectively phagocytizing A β . Indeed, the DKO cells phagocytized A β to a similar extent. However, although in the images it can be observed that all the cells have phagocytized A β , the cell morphology shows a larger area of phagocytized A β (red) per cell in the WT cells. Lysosomal leakage or dysfunction may be associated with this enlargement and increased apoptosis in the WT cells. This was not studied further due to time constraints.

Considering the beneficial effects observed in DKO in microglia, it seemed opportune to examine the effect of the depletion of 4E-BPs in microglia *in vivo*. A mouse model with conditional microglia depletion of 4E-BPs was meant to be examined for changes in cognitive impairment upon intracerebroventricular infusion of A β . However, even though the stereotaxic infusion approach of A β was established for this thesis, it was not possible to perform the experiment. Mice that underwent the stereotaxic surgery, even WT controls, couldn't learn the tests. The short recovery and the stress from the stereotaxic surgery influenced the ability of mice to learn the cognitive tests. However, the induction of cognitive deficits after A β infusion is transient; therefore, it was not possible to allow for a more extended recovery period [128]. In the future, mouse crossing with an AD model or cannula implantation might be a good alternative to overcome this issue.

Although the behavioral assessment could not be performed, overall, the depletion of the 4E-BPs *in vitro* decreases the pro-inflammatory phenotype, skews microglia metabolism towards OXPHOS, and mitigates cell death associated with A β . Therefore, in Aim 3, I went on to examine how the deletion of 4E-BPs affects microglia translatome in response to A β *in vivo*. Taking advantage of the established stereotaxic infusion approach and the mouse models (CX3CR1^{crert2}; 4E-BP1/2^{fl/fl or wt/wt}), the translatomes of DKO and WT microglia were examined upon the infusion of A β or VEH. The translatome of microglia from mice treated with A β was not effectively

retrieved, and therefore was not analyzed. Nevertheless, the translatome of VEH-treated mice in both MG^{WT} and MG^{DKO} mice was analyzed.

Interestingly the translatome of MG^{DKO} showed a downregulation of the expression of a highly correlated set of genes, including *Apoe* and other Apolipoproteins. Previous reports profiling microglia have shown that *Apoe* is one of the most abundantly expressed transcripts in microglia, even at basal conditions, and is further increased in pathological conditions or aging [133, 144]. Importantly, *apoe* is a critical node of activation programs observed in microglia during neurodegenerative diseases [101]. In addition, genes such as secreted phosphoprotein 1 (*spp1*; also known as osteopontin) which has been found to be correlated with worse outcomes for tau pathology in human cerebrospinal fluid, were decreased in DKO microglia[145]. Other genes associated with microglia inflammatory response, such as galectin 3 (*Lgals3*), toll-like receptor 2 (*tlr2*), and CC-chemokine ligand 3 (*ccl3*) were downregulated in the DKO microglia translatome. This was also reflected in the functional analysis, suggesting that indeed the DKO microglia *in vivo* show a reduced basal activation reflected in the repertoire of mRNAs actively translated at the examined time point.

Although the translational profiling informs about the repertoire of mRNAs actively being translated, the translatome doesn't inform about the efficiency of translation of the different mRNAs. Changes in translational efficiency are determined as a function of the number of ribosomes associated with an mRNA molecule, which can drive significant changes in the proteome [146]. Interestingly, MG^{DKO} mice translatome didn't exhibit upregulated functional networks, however, the mTOR–4E-BP axis selectively boosts the abundance of a subset of proteins by increasing the translation efficiency of distinct mRNAs. This is actively being investigated in the DKO and WT cell lines by using a ribosome profiling approach. This approach leverages deep sequencing of ribosome-protected fragments to enable assessment of the translatome and the number of associated ribosomes at codon resolution [147]. However, the translatomic profiling presented suggests that the activation of the mTOR-4E-BP axis suppresses a translatomic program in microglia encompassing several AD risk genes and inflammatory mediators.

The hippocampal tissue transcriptome provided a window to examine some of the functional consequences of the 4E-BP depletion in microglia *in vivo* upon A β exposure. Consistent with the *in vitro* data and the translatomic profiling, this examination showed that the MG^{WT} brain tissue had an increased inflammatory profile upon A β infusion compared to MG^{DKO}. The upregulated genes comprise some disease associated microglia (DAM) signature genes including *trem2*, Transmembrane Immune Signaling Adaptor (*tyrobp*), *spp1*, and Glial Fibrillary Acidic Protein (*gfap*) as an indication of astrocyte activation as well. Considering that the upregulated genes comprise several components of the TREM2 signaling pathway but not *Syk* and that TREM2 can be cleaved without necessarily conveying the intracellular signal, a correlation to phosphorylation of the pathway in microglia would be fitting, although outside of the scope of this thesis [148]. Another very interesting gene that was upregulated in the A β -infused MG^{WT} brain tissue is Hexokinase 2 (*Hk2*). HK2 has been associated with an increase in aerobic glycolytic metabolism while decreasing OXPHOS in microglia and a worsened AD pathology outcome in a mouse model [149].

Several mediators of the complement pathway were upregulated in the A β -infused MG^{WT} brain tissue, hinting at synaptic and neuronal loss. Simultaneously, some mediators of synaptic plasticity were downregulated, including Amyloid precursor protein (app), fos (Proto-Oncogene C-Fos) and Activity-Regulated Cytoskeleton-Associated Protein (arc). The functional pathway analyses showed a decreased G protein–coupled receptor (Gpcr) signaling pathway and decreased cellular components of the distal axon and terminal bouton as well. Overall, the transcriptome analysis, in conjunction with the translatome analysis, shows that the depletion of 4E-BP in microglia reduces inflammation and synaptic loss upon the A β infusion.

7. Conclusion

During the decade-long pathological trajectory of AD, microglia develop a myriad of states and functional profiles. Microglia activation and acquisition of a DAM signature is necessary for microglia to surround and engulf A β , thereby hindering the spread of A β pathology[103]. Yet, microglia are long-lived and not only develop diverse phenotypes but also must sustain these phenotypes or resolve these states to preserve homeostasis. Overall, the results observed in this thesis suggest that activating the mTOR-4E-BP axis in microglia has a vital role in limiting microglia pro-inflammatory output and skewing the associated glycolytic metabolism towards OXPHOS-dependent metabolism. Therefore, one may suggest that the mTOR-4E-BP axis signaling may act as a mechanism of self-regulation necessary for inflammatory resolution and cell survival on an on-and-off basis.

Furthermore, the ability of microglia to target the mTOR pathway, usually by coupling extracellular signals to this intracellular pathway, may provide resilience and the inability to do so may provide vulnerability, explaining why AD risk genes enriched in microglia are surface receptors and downstream transducers. This is of particular importance considering the chronic presence of damage-associated immune activators characteristic of neurodegeneration. This thesis adds to the understanding of the intracellular pathways and mechanisms converging in the activation of mTOR signaling. It extends to the role of this pathway in controlling microglia activation, metabolism, and survival via the 4E-BP-Dependent translational regulation [116].

Bibliography

- 1. Watson, J.D. and F.H.C. Crick, *Molecular Structure of Nucleic Acids: A Structure for Deoxyribose Nucleic Acid.* Nature, 1953. **171**(4356): p. 737-738.
- 2. Crick, F.H.C., et al., *General Nature of the Genetic Code for Proteins.* Nature, 1961. **192**(4809): p. 1227-1232.
- 3. Brachet, J., *The role of nucleic acids in morphogenesis.* Progress in Biophysics and Molecular Biology, 1965. **15**: p. 97-127.
- 4. Bruce Alberts, A.J., Julian Lewis, Martin Raff, Keith Roberts, and Peter Walter., *Molecular Biology of the Cell*. Garland Science. 2002, New York.
- 5. Gerstein, M.B., et al., *What is a gene, post-ENCODE? History and updated definition.* Genome Research, 2007. **17**(6): p. 669-681.
- 6. Schneider-Poetsch, T. and M. Yoshida, *Along the Central Dogma—Controlling Gene Expression with Small Molecules*. Annual Review of Biochemistry, 2018. **87**(1): p. 391-420.
- 7. Vogel, C. and E.M. Marcotte, *Insights into the regulation of protein abundance from proteomic and transcriptomic analyses.* Nat Rev Genet, 2012. **13**(4): p. 227-32.
- 8. Piccirillo, C.A., et al., *Translational control of immune responses: from transcripts to translatomes.* 2014. **Nature immunology**(volume 15, pages 503–511).
- 9. Schwanhäusser, B., et al., *Global quantification of mammalian gene expression control.* Nature, 2011. **473**(7347): p. 337-342.
- 10. Liu, Y., A. Beyer, and R. Aebersold, *On the Dependency of Cellular Protein Levels on mRNA Abundance*. Cell, 2016. **165**(3): p. 535-550.
- 11. Keene, J.D. and S.A. Tenenbaum, *Eukaryotic mRNPs May Represent Posttranscriptional Operons*. Molecular Cell, 2002. **9**(6): p. 1161-1167.
- 12. Timp, W. and G. Timp, *Beyond mass spectrometry, the next step in proteomics.* Science Advances, 2020. **6**(2): p. eaax8978.
- 13. Hay, N. and N. Sonenberg, *Upstream and downstream of mTOR*. Genes Dev, 2004. **18**(16): p. 1926-45.
- 14. Barbet, N.C., et al., *TOR controls translation initiation and early G1 progression in yeast.* Mol Biol Cell, 1996. **7**(1): p. 25-42.
- 15. Chauvin, C., et al., *Ribosomal protein S6 kinase activity controls the ribosome biogenesis transcriptional program.* Oncogene, 2014. **33**(4): p. 474-83.
- 16. Fingar, D.C., et al., *Mammalian cell size is controlled by mTOR and its downstream targets S6K1 and 4EBP1/eIF4E.* Genes Dev, 2002. **16**(12): p. 1472-87.

- 17. Allen, F.W., *The Biochemistry of the Nucleic Acids, Purines, and Pyrimidines.* Annual Review of Biochemistry, 1941. **10**(1): p. 221-244.
- 18. Shatkin, A.J., *Capping of eucaryotic mRNAs*. Cell, 1976. **9**(4 pt 2): p. 645-53.
- 19. Darnell, J.E., R. Wall, and R.J. Tushinski, *An adenylic acid-rich sequence in messenger RNA of HeLa cells and its possible relationship to reiterated sites in DNA*. Proc Natl Acad Sci U S A, 1971. **68**(6): p. 1321-5.
- 20. Edmonds, M., M.H. Vaughan, Jr., and H. Nakazato, *Polyadenylic acid sequences in the heterogeneous nuclear RNA and rapidly-labeled polyribosomal RNA of HeLa cells: possible evidence for a precursor relationship.* Proc Natl Acad Sci U S A, 1971. **68**(6): p. 1336-40.
- 21. Hinnebusch, A.G., I.P. Ivanov, and N. Sonenberg, *Translational control by 5'-untranslated regions of eukaryotic mRNAs.* Science, 2016. **352**(6292): p. 1413-6.
- 22. Buttgereit, F. and M.D. Brand, *A hierarchy of ATP-consuming processes in mammalian cells*. Biochem J, 1995. **312 (Pt 1)**(Pt 1): p. 163-7.
- 23. Sonenberg, N. and A.G. Hinnebusch, *Regulation of translation initiation in eukaryotes: mechanisms and biological targets.* Cell, 2009. **136**(4): p. 731-45.
- 24. Sonenberg, N. and A.G. Hinnebusch, *Regulation of Translation Initiation in Eukaryotes: Mechanisms and Biological Targets.* Cell, 2009. **136**(4): p. 731-745.
- 25. Pelletier, J. and N. Sonenberg, *The Organizing Principles of Eukaryotic Ribosome Recruitment*. Annual Review of Biochemistry, 2019. **88**(1): p. 307-335.
- 26. Marcotrigiano, J., et al., *Cap-dependent translation initiation in eukaryotes is regulated by a molecular mimic of eIF4G.* Mol Cell, 1999. **3**(6): p. 707-16.
- 27. Bennett, M.L., et al., *New tools for studying microglia in the mouse and human CNS.* Proceedings of the National Academy of Sciences, 2016. **113**(12): p. E1738-E1746.
- 28. Aguilar-Valles, A., et al., *Antidepressant actions of ketamine engage cell-specific translation via eIF4E.* Nature, 2021. **590**(7845): p. 315-319.
- 29. Gingras, A.C., et al., *Hierarchical phosphorylation of the translation inhibitor 4E-BP1*. Genes Dev, 2001. **15**(21): p. 2852-64.
- 30. Meyuhas, O., *Synthesis of the translational apparatus is regulated at the translational level.* European Journal of Biochemistry, 2000. **267**(21): p. 6321-6330.
- 31. Cockman, E., P. Anderson, and P. Ivanov, *TOP mRNPs: Molecular Mechanisms and Principles of Regulation.* Biomolecules, 2020. **10**(7).
- 32. Jia, J.-J., et al., mTORC1 promotes TOP mRNA translation through site-specific phosphorylation of LARP1. Nucleic Acids Research, 2021. **49**(6): p. 3461-3489.
- 33. Gandin, V., et al., nanoCAGE reveals 5' UTR features that define specific modes of translation of functionally related MTOR-sensitive mRNAs. Genome Res, 2016. **26**(5): p. 636-48.

- 34. Pelletier, J. and N. Sonenberg, *Internal initiation of translation of eukaryotic mRNA directed by a sequence derived from poliovirus RNA*. Nature, 1988. **334**(6180): p. 320-325.
- 35. Costa-Mattioli, M. and P. Walter, *The integrated stress response: From mechanism to disease.* Science, 2020. **368**(6489).
- 36. Jackson, R.J., C.U.T. Hellen, and T.V. Pestova, *The mechanism of eukaryotic translation initiation and principles of its regulation.* Nature Reviews Molecular Cell Biology, 2010. **11**(2): p. 113-127.
- 37. Costa-Mattioli, M., et al., *Translational Control of Long-Lasting Synaptic Plasticity and Memory.* Neuron, 2009. **61**(1): p. 10-26.
- 38. Warner, J.R., P.M. Knopf, and A. Rich, *A MULTIPLE RIBOSOMAL STRUCTURE IN PROTEIN SYNTHESIS*. Proceedings of the National Academy of Sciences, 1963. **49**(1): p. 122-129.
- 39. Halbeisen, R.E., T. Scherrer, and A.P. Gerber, *Affinity purification of ribosomes to access the translatome*. Methods, 2009. **48**(3): p. 306-310.
- 40. Larsson, O., N. Sonenberg, and R. Nadon, *Identification of differential translation in genome wide studies*. Proceedings of the National Academy of Sciences, 2010. **107**(50): p. 21487-21492.
- 41. Plotkin, J.B., *Transcriptional regulation is only half the story*. Molecular Systems Biology, 2010. **6**(1): p. 406.
- 42. Kusnadi, E.P., et al., *Regulation of gene expression via translational buffering*. Biochimica et Biophysica Acta (BBA) Molecular Cell Research, 2022. **1869**(1): p. 119140.
- 43. Duffy, E.E., et al., *Developmental dynamics of RNA translation in the human brain.* Nature Neuroscience, 2022. **25**(10): p. 1353-1365.
- 44. Glock, C., M. Heumüller, and E.M. Schuman, *mRNA transport & local translation in neurons*. Curr Opin Neurobiol, 2017. **45**: p. 169-177.
- 45. Ding, Q., et al., *Ribosome dysfunction is an early event in Alzheimer's disease.* Journal of Neuroscience, 2005. **25**(40): p. 9171-9175.
- 46. Association, A.s., 2019 Alzheimer's disease facts and figures. Alzheimer's & Dementia, 2019. **15**(3): p. 321-387.
- 47. (CDC)., C.f.D.C.a.P., From the Centers for Disease Control and Prevention. Public health and aging: trends in aging--United States and worldwide. 2003(0098-7484 (Print)).
- 48. Association, A.s., 2018 Alzheimer's disease facts and figures. Alzheimer's & Dementia, 2018. **14**(3): p. 367-429.
- 49. 2023 Alzheimer's disease facts and figures. Alzheimer's & Dementia. **n/a**(n/a).
- 50. Alzheimer A Fau Stelzmann, R.A., et al., *An English translation of Alzheimer's 1907 paper,* "Uber eine eigenartige Erkankung der Hirnrinde". Clin. Anat., 1995.
- 51. Serrano-Pozo, A., et al., *Neuropathological alterations in Alzheimer disease*. Cold Spring Harbor perspectives in medicine, 2011. **1**(1): p. a006189-a006189.

- 52. Heneka, M.T., et al., *Neuroinflammation in Alzheimer's disease*. The Lancet. Neurology, 2015. **14**(4): p. 388-405.
- 53. Long, J.M. and D.M. Holtzman, *Alzheimer Disease: An Update on Pathobiology and Treatment Strategies.* Cell, 2019. **179**(2): p. 312-339.
- 54. Hampel, H., et al., *The Amyloid-β Pathway in Alzheimer's Disease*. Molecular Psychiatry, 2021. **26**(10): p. 5481-5503.
- 55. Müller, U.C., T. Deller, and M. Korte, *Not just amyloid: physiological functions of the amyloid precursor protein family.* Nature Reviews Neuroscience, 2017. **18**(5): p. 281-298.
- 56. Heneka, M.T., D.T. Golenbock, and E. Latz, *Innate immunity in Alzheimer's disease.* Nature Immunology, 2015. **16**(3): p. 229-236.
- 57. Haass, C., et al., *Trafficking and Proteolytic Processing of APP.* Cold Spring Harbor Perspectives in Medicine, 2012. **2**(5).
- 58. Avila, J., et al., *Role of tau protein in both physiological and pathological conditions.* Physiol Rev, 2004. **84**(2): p. 361-84.
- 59. Mandelkow, E., et al., *Structural Principles of Tau and the Paired Helical Filaments of Alzheimer's Disease*. Brain Pathology, 2007. **17**(1): p. 83-90.
- 60. Biernat, J., et al., *Phosphorylation of Ser262 strongly reduces binding of tau to microtubules: Distinction between PHF-like immunoreactivity and microtubule binding.* Neuron, 1993. **11**(1): p. 153-163.
- 61. Dujardin, S. and B.T. Hyman, *Tau Prion-Like Propagation: State of the Art and Current Challenges*. Adv Exp Med Biol, 2019. **1184**: p. 305-325.
- 62. Hyman, B.T., et al., *National Institute on Aging-Alzheimer's Association guidelines for the neuropathologic assessment of Alzheimer's disease*. Alzheimers Dement, 2012. **8**(1): p. 1-13.
- 63. Hardy, J.A. and G.A. Higgins, *Alzheimer's disease: the amyloid cascade hypothesis.* Science, 1992. **256**(5054): p. 184-5.
- 64. Mawuenyega, K.G., et al., *Decreased Clearance of CNS β-Amyloid in Alzheimer's Disease.* Science, 2010. **330**(6012): p. 1774-1774.
- 65. Karch, C.M., C. Cruchaga, and A.M. Goate, *Alzheimer's disease genetics: from the bench to the clinic.* Neuron, 2014. **83**(1): p. 11-26.
- 66. Husain, M.A., B. Laurent, and M. Plourde, *APOE and Alzheimer's Disease: From Lipid Transport to Physiopathology and Therapeutics.* Frontiers in Neuroscience, 2021. **15**.
- 67. Prinz, M., S. Jung, and J. Priller, *Microglia Biology: One Century of Evolving Concepts.* Cell, 2019. **179**(2): p. 292-311.
- 68. Wolf, S.A., H.W.G.M. Boddeke, and H. Kettenmann, *Microglia in Physiology and Disease*. Annual Review of Physiology, 2017. **79**(1): p. 619-643.

- 69. Frost, J.L. and D.P. Schafer, *Microglia: Architects of the Developing Nervous System.* Trends in Cell Biology, 2016. **26**(8): p. 587-597.
- 70. Li, Q. and B.A. Barres, *Microglia and macrophages in brain homeostasis and disease.* Nature Reviews Immunology, 2018. **18**(4): p. 225-242.
- 71. Tremblay, M.-È., et al., *The Role of Microglia in the Healthy Brain.* The Journal of Neuroscience, 2011. **31**(45): p. 16064-16069.
- 72. Paolicelli, R.C., et al., *Microglia states and nomenclature: A field at its crossroads.* Neuron, 2022. **110**(21): p. 3458-3483.
- 73. Glass, C.K., et al., *Mechanisms underlying inflammation in neurodegeneration.* Cell, 2010. **140**(6): p. 918-34.
- 74. Wildsmith, K.R., et al., *Evidence for impaired amyloid beta clearance in Alzheimer's disease*. Alzheimers Res Ther, 2013. **5**(4): p. 33.
- 75. Shi, H., et al., Genetic variants influencing human aging from late-onset Alzheimer's disease (LOAD) genome-wide association studies (GWAS). Neurobiol Aging, 2012. **33**(8): p. 1849.e5-18.
- 76. Nott, A., et al., *Brain cell type–specific enhancer–promoter interactome maps and disease*<*strong>-*<*fstrong>risk association.* Science, 2019. **366**(6469): p. 1134-1139.
- 77. Felsky, D., et al., *Neuropathological correlates and genetic architecture of microglial activation in elderly human brain.* Nature Communications, 2019. **10**(1): p. 409.
- 78. Pascoal, T.A., et al., *Microglial activation and tau propagate jointly across Braak stages.*Nature Medicine, 2021. **27**(9): p. 1592-1599.
- 79. Hamelin, L., et al., *Early and protective microglial activation in Alzheimer's disease: a prospective study using 18F-DPA-714 PET imaging.* Brain, 2016. **139**(Pt 4): p. 1252-64.
- 80. Hansen, D.V., J.E. Hanson, and M. Sheng, *Microglia in Alzheimer's disease*. The Journal of Cell Biology, 2018. **217**(2): p. 459.
- 81. Shi, Y. and D.M. Holtzman, *Interplay between innate immunity and Alzheimer disease: APOE and TREM2 in the spotlight.* Nature Reviews Immunology, 2018. **18**(12): p. 759-772.
- 82. Yeh, F.L., et al., TREM2 Binds to Apolipoproteins, Including APOE and CLU/APOJ, and Thereby Facilitates Uptake of Amyloid-Beta by Microglia. Neuron, 2016. **91**(2): p. 328-40.
- 83. Kawabori, M., et al., *Triggering receptor expressed on myeloid cells 2 (TREM2) deficiency attenuates phagocytic activities of microglia and exacerbates ischemic damage in experimental stroke.* J Neurosci, 2015. **35**(8): p. 3384-96.
- 84. Atagi, Y., et al., *Apolipoprotein E Is a Ligand for Triggering Receptor Expressed on Myeloid Cells 2 (TREM2).* J Biol Chem, 2015. **290**(43): p. 26043-50.
- 85. Condello, C., et al., *Microglia constitute a barrier that prevents neurotoxic protofibrillar A842 hotspots around plaques.* Nature Communications, 2015. **6**(1): p. 6176.

- 86. Yuan, P., et al., TREM2 Haplodeficiency in Mice and Humans Impairs the Microglia Barrier Function Leading to Decreased Amyloid Compaction and Severe Axonal Dystrophy. Neuron, 2016. **90**(4): p. 724-739.
- 87. Bien-Ly, N., et al., Reducing human apolipoprotein E levels attenuates age-dependent Abeta accumulation in mutant human amyloid precursor protein transgenic mice. J Neurosci, 2012. **32**(14): p. 4803-11.
- 88. Huang, Y., et al., *Microglia use TAM receptors to detect and engulf amyloid β plaques.*Nature Immunology, 2021. **22**(5): p. 586-594.
- 89. Baik, S.H., et al., Microglia contributes to plaque growth by cell death due to uptake of amyloid θ in the brain of Alzheimer's disease mouse model. Glia, 2016. **64**(12): p. 2274-2290.
- 90. Duyckaerts, C., B. Delatour, and M.-C. Potier, *Classification and basic pathology of Alzheimer disease*. Acta Neuropathologica, 2009. **118**(1): p. 5-36.
- 91. Bisht, K., K. Sharma, and M.-È. Tremblay, *Chronic stress as a risk factor for Alzheimer's disease: Roles of microglia-mediated synaptic remodeling, inflammation, and oxidative stress.* Neurobiology of Stress, 2018. **9**: p. 9-21.
- 92. Brown, G.C. and J.J. Neher, *Microglial phagocytosis of live neurons*. Nature Reviews Neuroscience, 2014. **15**(4): p. 209-216.
- 93. Liddelow, S.A., et al., *Neurotoxic reactive astrocytes are induced by activated microglia*. Nature, 2017. **541**(7638): p. 481-487.
- 94. Jack, C.R., Jr., et al., *Hypothetical model of dynamic biomarkers of the Alzheimer's pathological cascade*. Lancet Neurol, 2010. **9**(1): p. 119-28.
- 95. Stevens, B., et al., *The Classical Complement Cascade Mediates CNS Synapse Elimination*. Cell, 2007. **131**(6): p. 1164-1178.
- 96. Zanjani, H., et al., *Complement Activation in Very Early Alzheimer Disease*. Alzheimer Disease & Associated Disorders, 2005. **19**(2): p. 55-66.
- 97. Spangenberg, E., et al., Sustained microglial depletion with CSF1R inhibitor impairs parenchymal plaque development in an Alzheimer's disease model. Nature Communications, 2019. **10**(1): p. 3758.
- 98. Ising, C., et al., *NLRP3 inflammasome activation drives tau pathology.* Nature, 2019. **575**(7784): p. 669-673.
- 99. Asai, H., et al., *Depletion of microglia and inhibition of exosome synthesis halt tau propagation.* Nat Neurosci, 2015. **18**(11): p. 1584-93.
- 100. Shi, Y., et al., *Microglia drive APOE-dependent neurodegeneration in a tauopathy mouse model.* The Journal of Experimental Medicine, 2019. **216**(11): p. 2546-2561.
- 101. Krasemann, S., et al., *The TREM2-APOE Pathway Drives the Transcriptional Phenotype of Dysfunctional Microglia in Neurodegenerative Diseases.* Immunity, 2017. **47**(3): p. 566-581.e9.

- 102. Butovsky, O. and H.L. Weiner, *Microglial signatures and their role in health and disease.* Nature Reviews Neuroscience, 2018. **19**(10): p. 622-635.
- 103. Keren-Shaul, H., et al., *A unique microglia type associated with restricting development of Alzheimer's disease.* Cell, 2017. **169**(7): p. 1276-1290. e17.
- 104. Guerreiro, R. and J. Hardy, *Genetics of Alzheimer's disease*. Neurotherapeutics, 2014. **11**(4): p. 732-7.
- 105. Guerreiro, R., et al., *TREM2 Variants in Alzheimer's Disease*. New England Journal of Medicine, 2012. **368**(2): p. 117-127.
- 106. Jonsson, T., et al., *Variant of TREM2 associated with the risk of Alzheimer's disease.* New England Journal of Medicine, 2013. **368**(2): p. 107-116.
- 107. Zhao, Y., et al., *TREM2 Is a Receptor for β-Amyloid that Mediates Microglial Function*. Neuron, 2018. **97**(5): p. 1023-1031.e7.
- 108. Hou, J., et al., *TREM2 dependent and independent functions of microglia in Alzheimer's disease.* Molecular Neurodegeneration, 2022. **17**(1): p. 84.
- 109. Sessa, G., et al., Distribution and signaling of TREM2/DAP12, the receptor system mutated in human polycystic lipomembraneous osteodysplasia with sclerosing leukoencephalopathy dementia. European Journal of Neuroscience, 2004. **20**(10): p. 2617-2628.
- 110. Peng, Q., et al., TREM2- and DAP12-Dependent Activation of PI3K Requires DAP10 and Is Inhibited by SHIP1. Science Signaling, 2010. **3**(122): p. ra38-ra38.
- 111. Ulland, T.K., et al., *TREM2 Maintains Microglial Metabolic Fitness in Alzheimer's Disease*. Cell, 2017. **170**(4): p. 649-663.e13.
- 112. Baik, S.H., et al., A Breakdown in Metabolic Reprogramming Causes Microglia Dysfunction in Alzheimer's Disease. Cell Metabolism, 2019. **30**(3): p. 493-507.e6.
- 113. Morita, M., et al., *mTORC1 Controls Mitochondrial Activity and Biogenesis through 4E-BP-Dependent Translational Regulation*. Cell Metabolism, 2013. **18**(5): p. 698-711.
- 114. Prokop, S., K.R. Miller, and F.L. Heppner, *Microglia actions in Alzheimer's disease*. Acta Neuropathologica, 2013. **126**(4): p. 461-477.
- 115. Lewcock, J.W., et al., *Emerging Microglia Biology Defines Novel Therapeutic Approaches* for Alzheimer's Disease. Neuron, 2020. **108**(5): p. 801-821.
- 116. Schafer, D.P. and J.M. Stillman, *Microglia are SYK of A6 and cell debris*. Cell, 2022. **185**(22): p. 4043-4045.
- 117. Bourgey, M., et al., *GenPipes: an open-source framework for distributed and scalable genomic analyses.* Gigascience, 2019. **8**(6).
- 118. Anders, S., P.T. Pyl, and W. Huber, *HTSeq--a Python framework to work with high-throughput sequencing data*. Bioinformatics, 2015. **31**(2): p. 166-9.

- 119. Shi, Q., et al., Microglial mTOR Activation Upregulates Trem2 and Enhances β-Amyloid Plaque Clearance in the 5XFAD Alzheimer's Disease Model. The Journal of Neuroscience, 2022. **42**(27): p. 5294.
- 120. Fairley, L.H., J.H. Wong, and A.M. Barron, *Mitochondrial Regulation of Microglial Immunometabolism in Alzheimer's Disease.* Frontiers in Immunology, 2021. **12**.
- 121. Réu, P., et al., *The Lifespan and Turnover of Microglia in the Human Brain*. Cell Rep, 2017. **20**(4): p. 779-784.
- 122. Prokop, S., et al., *Impact of TREM2 risk variants on brain region-specific immune activation and plaque microenvironment in Alzheimer's disease patient brain samples.* Acta Neuropathologica, 2019. **138**(4): p. 613-630.
- 123. Zhou, Y., T.K. Ulland, and M. Colonna, *TREM2-Dependent Effects on Microglia in Alzheimer's Disease*. Frontiers in Aging Neuroscience, 2018. **10**.
- 124. Jha, Abhishek K., et al., *Network Integration of Parallel Metabolic and Transcriptional Data Reveals Metabolic Modules that Regulate Macrophage Polarization.* Immunity, 2015. **42**(3): p. 419-430.
- 125. McQuade, A., et al., Gene expression and functional deficits underlie TREM2-knockout microglia responses in human models of Alzheimer's disease. Nature Communications, 2020. **11**(1): p. 5370.
- 126. Burguillos, M.A., et al., *Caspase signalling controls microglia activation and neurotoxicity.* Nature, 2011. **472**(7343): p. 319-24.
- 127. Ferreira, S., et al., Soluble amyloid-b oligomers as synaptotoxins leading to cognitive impairment in Alzheimer's disease. Frontiers in Cellular Neuroscience, 2015. **9**.
- 128. Batista, A.F., et al., Interleukin-16 mediates alterations in mitochondrial fusion/fission proteins and memory impairment induced by amyloid-β oligomers. Journal of Neuroinflammation, 2021. **18**(1): p. 54.
- 129. Lourenco, Mychael V., et al., *TNF-α Mediates PKR-Dependent Memory Impairment and Brain IRS-1 Inhibition Induced by Alzheimer's β-Amyloid Oligomers in Mice and Monkeys.* Cell Metabolism, 2013. **18**(6): p. 831-843.
- 130. Oliveira, M.M., et al., Correction of eIF2-dependent defects in brain protein synthesis, synaptic plasticity, and memory in mouse models of Alzheimer's disease. Science Signaling, 2021. **14**(668): p. eabc5429.
- 131. Fitz, N.F., et al., Phospholipids of APOE lipoproteins activate microglia in an isoform-specific manner in preclinical models of Alzheimer's disease. Nature Communications, 2021. **12**(1): p. 3416.
- 132. Meyer-Luehmann, M. and M. Prinz, *Myeloid Cells in Alzheimer's Disease: Culprits, Victims or Innocent Bystanders?* Trends in Neurosciences, 2015. **38**(10): p. 659-668.
- 133. Haimon, Z., et al., Re-evaluating microglia expression profiles using RiboTag and cell isolation strategies. Nature Immunology, 2018. **19**(6): p. 636-644.

- 134. Sanz, E., et al., *RiboTag: Ribosomal Tagging Strategy to Analyze Cell-Type-Specific mRNA Expression In Vivo.* Curr Protoc Neurosci, 2019. **88**(1): p. e77.
- 135. Schott, J., et al., *Translational regulation of specific mRNAs controls feedback inhibition and survival during macrophage activation.* PLoS Genet, 2014. **10**(6): p. e1004368.
- 136. Ennerfelt, H., et al., SYK coordinates neuroprotective microglial responses in neurodegenerative disease. Cell, 2022. **185**(22): p. 4135-4152.e22.
- 137. Wang, S., et al., *TREM2 drives microglia response to amyloid-β via SYK-dependent and independent pathways.* Cell, 2022. **185**(22): p. 4153-4169.e19.
- 138. Roux, P.P. and I. Topisirovic, *Signaling Pathways Involved in the Regulation of mRNA Translation.* Molecular and Cellular Biology, 2018. **38**(12): p. e00070-18.
- 139. Weichhart, T., M. Hengstschläger, and M. Linke, *Regulation of innate immune cell function by mTOR.* Nature reviews. Immunology, 2015. **15**(10): p. 599-614.
- 140. Heneka, M.T., et al., *Neuroinflammation in Alzheimer's disease*. The Lancet Neurology, 2015. **14**(4): p. 388-405.
- 141. Mela, V., et al., Exercise-induced re-programming of age-related metabolic changes in microglia is accompanied by a reduction in senescent cells. Brain, behavior, and immunity, 2020. **87**: p. 413-428.
- 142. Olah, M., et al., *A transcriptomic atlas of aged human microglia*. Nature communications, 2018. **9**(1): p. 539.
- 143. Minhas, P.S., et al., Restoring metabolism of myeloid cells reverses cognitive decline in ageing. Nature, 2021. **590**(7844): p. 122-128.
- 144. Kang, S.S., et al., *Microglial translational profiling reveals a convergent APOE pathway from aging, amyloid, and tau.* J Exp Med, 2018. **215**(9): p. 2235-2245.
- 145. Pereira, J.B., et al., *Microglial activation protects against accumulation of tau aggregates in nondemented individuals with underlying Alzheimer's disease pathology.* Nature Aging, 2022. **2**(12): p. 1138-1144.
- 146. Larsson, O., B. Tian, and N. Sonenberg, *Toward a genome-wide landscape of translational control.* Cold Spring Harb Perspect Biol, 2013. **5**(1): p. a012302.
- 147. Ingolia, N.T., et al., *The ribosome profiling strategy for monitoring translation in vivo by deep sequencing of ribosome-protected mRNA fragments*. Nature Protocols, 2012. **7**(8): p. 1534-1550.
- 148. Filipello, F., et al., *Soluble TREM2: Innocent bystander or active player in neurological diseases?* Neurobiology of Disease, 2022. **165**: p. 105630.
- 149. Leng, L., et al., Author Correction: Microglial hexokinase 2 deficiency increases ATP generation through lipid metabolism leading to β-amyloid clearance. Nature Metabolism, 2022. **4**(10): p. 1420-1420.